

2001

Phenomenology of the $SU(2)(L) \times SU(2)(I) \times U(1)(Y) \times U(1)(Y')$ model

Shuquan Nie

College of William & Mary - Arts & Sciences

Follow this and additional works at: <https://scholarworks.wm.edu/etd>



Part of the [Physics Commons](#)

Recommended Citation

Nie, Shuquan, "Phenomenology of the $SU(2)(L) \times SU(2)(I) \times U(1)(Y) \times U(1)(Y')$ model" (2001). *Dissertations, Theses, and Masters Projects*. Paper 1539623377.

<https://dx.doi.org/doi:10.21220/s2-60p4-0p26>

This Dissertation is brought to you for free and open access by the Theses, Dissertations, & Master Projects at W&M ScholarWorks. It has been accepted for inclusion in Dissertations, Theses, and Masters Projects by an authorized administrator of W&M ScholarWorks. For more information, please contact scholarworks@wm.edu.

NOTE TO USERS

This reproduction is the best copy available.

UMI[®]

Phenomenology of the $SU(2)_L \times SU(2)_I \times U(1)_Y \times U(1)_{Y'}$ model

Dissertation

Presented to

The faculty of the Department of Physics

The College of William and Mary in Virginia

In Partial Fulfillment

of the Requirements of the Degree of

Doctor of Philosophy

by

Shuquan Nie

2001

UMI Number: 3012231

UMI[®]

UMI Microform 3012231

Copyright 2001 by Bell & Howell Information and Learning Company.

All rights reserved. This microform edition is protected against
unauthorized copying under Title 17, United States Code.

Bell & Howell Information and Learning Company

300 North Zeeb Road

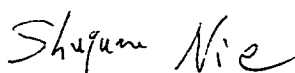
P.O. Box 1346

Ann Arbor, MI 48106-1346

APPROVAL SHEET

This dissertation is submitted in partial fulfillment of
the requirements for the degree of

Doctor of Philosophy




Shuquan Nie

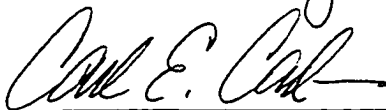
Approved, April 2001



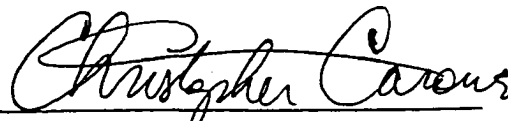
Marc Sher



David Armstrong



Carl Carlson



Christopher Carone



Winston Roberts
Old Dominion University

To my mom

Contents

Acknowledgements	vii
List of Tables	viii
List of Figures	ix
Abstract	xii
1 Introduction	1
1.1 Standard Model	1
1.1.1 Basic ingredients	1
1.1.2 The status of the SM	1
1.1.3 Beyond the SM	3
1.2 The E_6 model	5
1.2.1 A little history	5
1.2.2 E_6 group and its subgroups	5
1.2.3 Effective low-energy models	8
1.3 Outline	11
2 Higgs boson sector	14
2.1 Introduction	14
2.2 The SM Higgs boson	15
2.3 Higgs bosons in the two-Higgs doublets models	18
2.3.1 FCNC in the two-Higgs doublet models	19
2.3.2 Bound on Higgs boson masses	25

2.4	Higgs bosons in $SU(2)_L \times U(1)_Y \times SU(2)_I \times U(1)_{Y'}$	32
3	Gauge boson sector	41
3.1	Introduction	41
3.2	Gauge bosons in the SM	43
3.3	W_I boson	44
3.3.1	Production of W_I	44
3.3.2	Effects of W_I	45
3.4	Extra gauge bosons and mixing	48
3.5	Electroweak observables	58
3.5.1	Observables in Z-pole experiments	59
3.5.2	W boson mass	63
3.5.3	Observables in LENC experiments	63
3.5.3.1	Polarization asymmetries	66
3.5.3.2	The weak charge	68
3.5.3.3	Neutrino-quark scattering	71
3.5.3.4	Neutrino-electron scattering	72
3.6	Constraints on extra neutral gauge bosons	73
3.6.1	Constraints from Z-pole and m_W data	74
3.6.2	Constraints from Z-pole+ m_W +LENC data	76
3.6.3	Constraints from Z-pole+ m_W +LENC+ Q_W^P data	78
4	Fermion sector	80
4.1	Introduction	80

4.2	Lagrangian	80
4.3	Masses and mixing	82
4.3.1	d-h quark mixing	82
4.3.2	e-E lepton mixing	83
4.3.3	Constraints on masses and mixings	84
4.4	Pair production of heavy charged leptons	85
4.4.1	Cross section and asymmetries	85
4.4.2	Results	87
4.5	Pair production of h-quark	90
5	Conclusions	97
	Appendix	99
	References	104
	Vita	113

Acknowledgments

Here I want to express my thanks and gratitude to Professor Marc Sher, my supervisor, for his patient guidance. Also I would like to thank Professor Christopher D. Carone for his wonderful teaching of Quantum Field Theory and helpful discussions in my research. I am also indebted to Professor Carl E. Carlson for his patience and helpful criticism in my annual reports during these years. And last, not least, I want to thank the nuclear and particle theory group and the department for a good atmosphere and kind financial support and pleasant times I have spent in the College.

List of Tables

1.1	The fields of the Standard Model	1
1.2	Subgroups of E_6 with $U(1)_{em} \times SU(3)_C$ as subgroup	8
1.3	The quantum numbers of fermions in $\mathbf{27}$ of E_6	12
3.1	Summary of electroweak measurements	59
3.2	Numerical values of factors C_{f_V} and C_{f_V} for quarks and leptons	62
4.1	Coefficients appearing in Eq. (194)	87
4.2	Coefficients appearing in Eq. (194) for calculating σ_L	88
4.3	Coefficients appearing in Eq. (194) for calculating σ_R	89

List of Figures

1	An illustration of unification based on a larger group, <i>motivated by</i> Ref. [15]	4
2	Dynkin diagram and extended Dynkin diagram for E_6 algebra	7
3	Bounds on the SM Higgs boson mass by requiring that the vacuum is stable and the perturbation is valid up to a large scale Λ , assuming $M_t = 175$ GeV and $\alpha_s(m_Z) = 0.118$	17
4	χ^2 variation as a function of the Higgs mass from the global fit of the electroweak measurements	18
5	Contribution to the anomalous magnetic moment of the muon from the exchange of flavor-changing scalars	22
6	The contribution of the diagram of Fig. 5 to the anomalous magnetic moment of the muon	23
7	The allowed region in the neutral scalar mass plane, with $m_{\chi^\pm} = m_{\chi^0} = 100$ GeV and $\tan \beta = 2$	28
8	The allowed region in the neutral scalar mass plane for various values of the charged Higgs mass (in GeV), with the χ^0 mass chosen to be 100 GeV and $\tan \beta = 2$	29
9	The allowed region in the neutral scalar mass plane for various values of $\tan \beta$, with the χ^0 and χ^\pm masses chosen to be 100 GeV	30
10	The allowed region in the neutral scalar mass plane for various values of the pseudoscalar Higgs mass (in GeV), with the χ^\pm mass chosen to be 100 GeV and $\tan \beta = 2$	31
11	Parton-level process responsible for $p\bar{p} \rightarrow W_I + h + X$	44
12	Feynman diagram responsible for $e^+e^- \rightarrow W_I W_I^\dagger$	44
13	Diagrams for the process $\gamma e \rightarrow W_I E$	45

14	Diagrams for the process $ed \rightarrow Eh$	45
15	Tree-level flavor-changing neutral current processes present if all six quarks d, s, b and $h_i(i=1,2,3)$ mix with each other	46
16	Box diagrams contributing to $\bar{d}s \rightarrow \bar{s}d$ mixing	46
17	Loop diagrams involving exotic fermions and W_I contributing to $\mu \rightarrow e\gamma$	46
18	Contribution to the anomalous magnetic moment of the muon from the exchange of W_I	47
19	The contribution of the diagram of Fig. 18 to the anomalous magnetic moment of the muon	47
20	The decoupling limit of mass-squared matrix for the neutral gauge bosons	54
21	(a) Parity-violating electron-fermion amplitude generated by Z^0 -exchange, (b) Effective four-fermion electron-fermion PV interaction	68
22	The contours of $\Delta\chi^2 = \chi^2 - \chi_{SM}^2 = 1.0$ for extra neutral gauge bosons. The constraints are obtained by use of Z-pole experiments [74] and m_W measurement [74]	75
23	The contours of $\Delta\chi^2 = \chi^2 - \chi_{SM}^2 = 1.0$ for extra neutral gauge bosons. The constraints are obtained by use of Z-pole experiments [74], m_W mea- surement [74] and LENC experiments [75]	76
24	The contours of $\Delta\chi^2 = \chi^2 - \chi_{SM}^2 = 1.0$ for extra neutral gauge bosons. The constraints are obtained by use of Z-pole experiments [74], m_W mea- surement [74], LENC experiments [75] and a proposed measurement of Q_W^P	78
25	Constraints on the lightest extra neutral gauge boson, Z_2	79
26	Feynman diagram responsible for $e^+e^- \rightarrow E^+E^-$	86
27	Feynman diagrams at the parton level for pair production of h quark in $pp(\bar{p})$ collisions	90

28	Total cross section for the process $e^+e^- \rightarrow L^+L^-$ as a function of \sqrt{s} , for a heavy lepton of 200 GeV in the rank-5 model	91
29	A_{FB} , the forward-backward asymmetry, for the process $e^+e^- \rightarrow L^+L^-$ as a function of \sqrt{s} , for a heavy lepton of 200 GeV in the rank-5 model	92
30	A_{LR} , the left-right asymmetry, for the process $e^+e^- \rightarrow L^+L^-$ as a function of \sqrt{s} , for a heavy lepton of 200 GeV in the rank-5 model	93
31	Total cross section for the process $e^+e^- \rightarrow L^+L^-$ as a function of \sqrt{s} , for a heavy lepton of 200 GeV in the rank-6 model	94
32	A_{FB} , the forward-backward asymmetry, for the process $e^+e^- \rightarrow L^+L^-$ as a function of \sqrt{s} , for a heavy lepton of 200 GeV in the rank-6 model	95
33	A_{LR} , the left-right asymmetry, for the process $e^+e^- \rightarrow L^+L^-$ as a function of \sqrt{s} , for a heavy lepton of 200 GeV in the rank-6 model	96

Abstract

We consider the effective low-energy $SU(2)_L \times SU(2)_I \times U(1)_Y \times U(1)_{Y'}$ model, which is based on the E_6 grand unification theory. $SU(2)_I$ is a subgroup of $SU(3)_R$ and commutes with the electric charge operator.

Higgs bosons in the Standard Model and two-Higgs doublet models are reviewed and studied first. The flavor-changing neutral currents and their effects on the anomalous magnetic moment of the muon are discussed. Bounds on masses of Higgs bosons are obtained by requiring that the vacuum is stable and perturbation theory is valid up to a large scale. We introduce Higgs multiplets including two neutral doublets to break down $SU(2)_L \times SU(2)_I \times U(1)_Y \times U(1)_{Y'}$ to $U(1)_{em}$. An upper bound of about 150 GeV to the lightest neutral Higgs scalar mass is found.

The gauge bosons corresponding to $SU(2)_I$ are charge-neutral. Production and effects of W_I bosons are reviewed first. Mixings among neutral gauge bosons appear naturally. Electroweak precision experiments, including Z-pole experiments, m_W measurements and low-energy neutral current experiments are used to put indirect constraints on masses of the extra neutral gauge bosons and the mixings between them and the ordinary Z boson. We also consider the possible constraint from a proposed measurement at Jefferson Lab of the proton's weak charge. It is found that the mixing angles are very small, namely $|\theta| \leq 0.005$. The lower bound for the mass of the lightest extra neutral gauge boson is found to be about 560 – 800 GeV, which is comparable with the current direct search limit. Low-energy neutral current experiments give the strongest bounds on the lightest extra neutral gauge boson.

Fermions reside in the **27** fundamental representation of E_6 . We study the pair production of heavy charged exotic leptons at e^+e^- colliders in this model. In addition to the standard γ and Z boson contributions, a t-channel contribution due to W_I -boson exchange, which is unsuppressed by mixing angles, is quite important. We calculate

the cross section, the left-right and forward-backward asymmetries, and discuss how to differentiate different models.

Phenomenology of the $SU(2)_L \times SU(2)_I \times U(1)_Y \times U(1)_{Y'}$ model

Chapter 1 Introduction

1.1 Standard Model

1.1.1 Basic ingredients

The Standard Model (SM) is a gauge field theory describing the electromagnetic interaction, weak interaction and strong interaction [1]. Its gauge group is $SU(3)_C \times SU(2)_L \times U(1)_Y$, which spontaneously breaks down to $SU(3)_C \times U(1)_{em}$ through the Higgs mechanism.

The particle spectrum of the SM includes three sectors: Gauge bosons, Fermions and Higgs scalars. It is summarized in Table 1.1. The first two numbers in the brackets of the second column indicate the dimensions of representations to which particles are arranged, and the third component is the $U(1)_Y$ quantum numbers of particles.

Table 1.1 The Fields of the Standard Model

Particle	$SU(3)_C \times SU(2)_L \times U(1)_Y$
G_μ^a	(8, 1, 0)
W_μ^a	(1, 3, 0)
B_μ	(1, 1, 0)
$q_L^i = \begin{pmatrix} u^i \\ d^i \end{pmatrix}_L$	(3, 2, 1/6)
u_R^i	(3, 1, 2/3)
d_R^i	(3, 1, -1/3)
$l_L^i = \begin{pmatrix} \nu^i \\ e^i \end{pmatrix}_L$	(1, 2, -1/2)
e_R^i	(1, 1, -1)
$\phi = \begin{pmatrix} \phi^+ \\ \phi^0 \end{pmatrix}$	(1, 2, 1/2)

Excellent and detailed reviews of the SM can be found in Ref. [2].

1.1.2 The status of the SM

The SM is theoretically beautiful and phenomenologically successful. All interactions in the model are determined by gauge invariance. Spontaneous symmetry breaking(SSB)

gives masses to all massive particles observed so far. Almost all observables can be calculated, in the sense that the SM is renormalizable, except in the strong interaction region. With the discovery of the top quark [3] and direct observation of the τ neutrino [4], there is only one particle, the Higgs boson, remaining to be observed. Recently there are reports indicating the observation of signals in the search for the SM Higgs boson at the detectors of LEP [5-8]. Precision measurements also fit the SM very well so far and this can give strong constraints on possible new physics. More reviews on the status of the SM can be found in Ref. [9].

But the SM also leaves too much unsaid or just put in by hand. Why do we have three-generation leptons and quarks? Why are the left-handed fields treated as $SU(2)_L$ doublets while the right-handed fields are singlets? There is no way to determine the structure of Higgs fields, the minimal Higgs doublet is introduced for reasons of economy. Gravity is neglected in the SM. In addition, there are too many free parameters in the SM, including three gauge coupling constants, nine Yukawa couplings constants, three mixing angles and one phase from the CKM matrix, and so on. And the hierarchy problem is an intrinsic ailment of the SM. Radiative corrections to the mass of Higgs boson are quadratically divergent, so when extrapolating the SM to a large scale, fine tuning is required to obtain the mass of Higgs boson at the order of the electroweak scale. At the same time, the fine tuning should be maintained to higher orders of perturbation theory. One major deviation from the SM may be the recent strong experimental evidence [10] that neutrinos are massive, although the masses are very small. All of these lead many people to think that the SM can not be a complete and final theory, it can only be an effective theory of a more complete theory. This gives incentives to explore physics beyond the SM.

1.1.3 Beyond the SM

There are many ways to go beyond the SM [11].

The simplest generalization of the SM is to add a fourth sequential family. An immediate phenomenological difficulty with a fourth light neutrino is with the data on the invisible Z decay width [12] which leads to the number of families $n = 2.984 \pm 0.008$. A similar limit on the number of light neutrinos, $N_\nu = 3.00 \pm 0.08$, was obtained by measuring the cross section of the process $e^+e^- \rightarrow \nu\bar{\nu}\gamma$ [13]. So the fourth neutrino should not be light, this can be resolved by the addition of a massive right-handed neutrino. A good review on the quarks and leptons beyond the third generation can be found in Ref. [14].

In the SM there is only one scalar doublet in the Higgs sector. A direct extension of the SM is to change the Higgs structure. The most popular model is the two-Higgs doublet model. As is well known, at least two doublets are needed to produce masses for all quarks in supersymmetric models which prevent conjugates of fields from appearing in the Lagrangian. Additional doublets can also provide sources of CP violation through complex vacuum expectation values.

To account for parity violation in low-energy physics, the SM treats left-handed fields and right-handed fields differently by hand. A straightforward extension of the SM, the left-right symmetric model, assumes that the original theory is intrinsically left-right symmetric, and the asymmetry observed in nature arises from spontaneous breaking of the left-right symmetry.

The most popular extension of the SM is supersymmetry. The primary motivation for supersymmetry is that it solves the gauge hierarchy problem, since contributions to the Higgs boson mass corrections from supersymmetric partners can cancel each other. At the same time, supersymmetric transformations are very closely related to spacetime

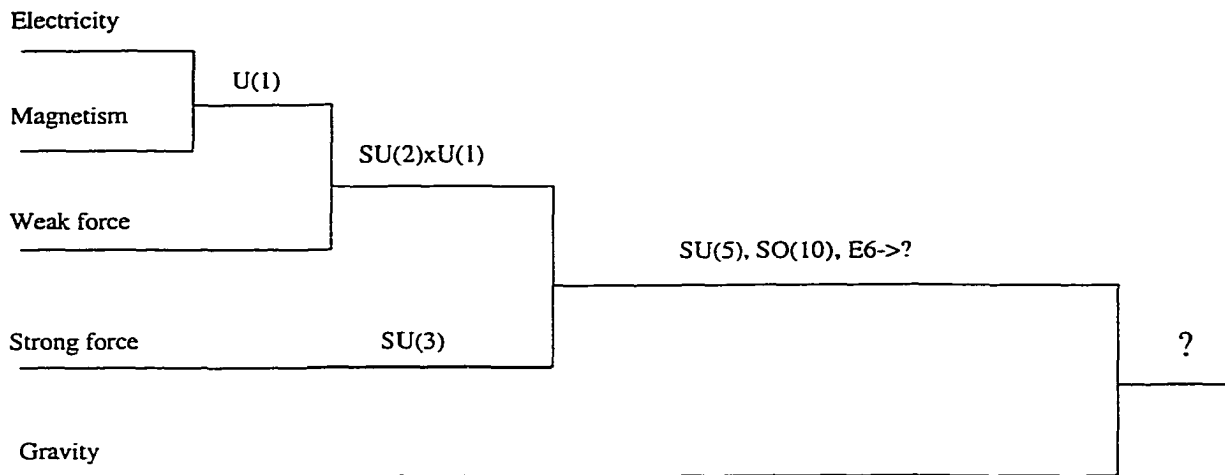


Figure 1: An illustration of unification based on a larger group, *motivated by* Ref. [15]

transformations. There is a possibility that supersymmetric theories might unify gravity with the other three fundamental interactions described by gauge field theories.

The description of nature from the Abelian $U(1)$ gauge theory describing the electromagnetic interaction, to the non-Abelian $SU(2)_L \times U(1)_Y$ gauge theory describing the electroweak interaction, further to $SU(3)_C \times SU(2)_L \times U(1)_Y$ describing all fundamental interactions except gravity, is a great triumph of the gauge revolution and one of the most important achievements in the recent history of physics. It is noted that the gauge group becomes bigger and bigger when more interactions are included. One is tempted to suggest a bigger simple or semisimple group to describe all interactions in the principle of gauge invariance. This brought the development of grand unification theories (GUT). This is illustrated in Fig. 1.

Although there are many proposed extensions of the SM, there is no experimental evidence for any of them yet. Agreement of the SM and current experiments can put constraints on possible new physics.

1.2 The E_6 Model

1.2.1 A little history

Early attempts to find a unified theory based on a larger simple or semisimple group were made by Pati and Salam [16]. Shortly after, Georgi and Glashow [17] found that the SM can be embedded into the simple Lie group $SU(5)$. Failures of the ordinary $SU(5)$ model to account for the proton lifetime and the electroweak mixing angle [18] led later to a larger group, the $SO(10)$ model [19]. As in the SM, the three(or more) copies of the generation structure are still put in by hand. Great interest in the E_6 unification model was sparked in the late 1970's when it was noted that (i) E_6 was the next natural anomaly-free choice for a GUT group after $SO(10)$, (ii) E_6 could have several intermediate mass breaking scales, and, more importantly, (iii) each generation of fermions was placed in the 27 dimensional representation. The last feature allowed the possibility to arrange for the then newly-discovered τ lepton and b quark to fit into a 27 representation and there was no need to include a third generation, but later data ruled out this possibility because both τ and b belong to a new generation.

The second surge of interest in E_6 came during the first revolution of superstring theories in the middle 1980's. The heterotic, anomaly-free, $E_8 \times E_8$, ten-dimensional superstring theory [20] can result in E_6 grand unified theories as the low-energy limit [21]. This superstring-inspired E_6 model has been discussed greatly in literature. A good summary can be found in Ref. [22].

1.2.2 E_6 group and its subgroups

E_6 is an exceptional algebra [23]. It has 78 generators and rank 6(the maximum number of simultaneously diagonalizable generators). It is the only exceptional group having non-self conjugate irreducible representations, so it is the only exceptional group from which a flavor-chiral theory is possible.

In the standard Cartan-Weyl analysis, the generators of a simple group can be divided into two sets. The first set consists of all simultaneously diagonalizable generators H_i ,

$$[H_i, H_j] = 0, \quad i, j = 1, 2, \dots, \text{rank}(G); \quad (1)$$

while the other generators can be chosen to satisfy eigenvalue equations of the form

$$[H_i, E_\alpha] = \alpha_i E_\alpha, \quad i = 1, 2, \dots, \text{rank}(G), \quad (2)$$

where the numbers α_i are structure constants of the algebra in the Cartan-Weyl basis. For each operator E_α , there are $\text{rank}(G)$ numbers α_i , called root α , that can be used to designate a point in a $\text{rank}(G)$ -dimensional euclidean space called the root space.

Written in a basis, a positive root is defined by the requirement that the first nonzero component of the root is positive, and a simple root is a positive root that cannot be written as a linear combination with positive coefficients of the other positive roots. There are only $\text{rank}(G)$ simple roots for a simple group G . The relative length and angle relations among the simple roots completely characterize a simple Lie algebra. This can be represented graphically by a two-dimensional diagram called the Dynkin diagram. It is possible to add only one root, the negative of the root of the highest weight, to the set of simple roots that satisfies the requirement that the difference of the two roots is not a root. The Dynkin diagram for the extended root set is called the extended Dynkin diagram with the new root marked by x .

From Fig. 2, the lengths of simple roots of E_6 are equal and the angles between connected simple roots are all 120° .

A fundamental problem of unification model building is to find all the ways that the currently known interactions can be embedded in a unified group G . This is to find all subgroups of G having the form,

$$G \supset G^{flavor} \times SU(3)_C \quad (3)$$

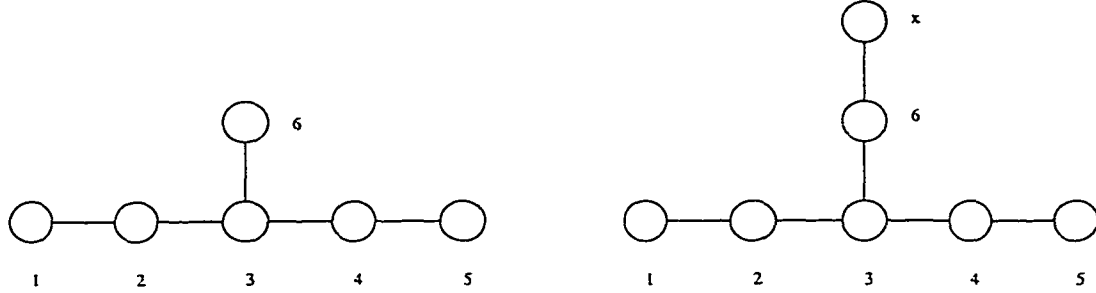


Figure 2: Dynkin diagram and extended Dynkin diagram for E_6 algebra

with G^{flavor} generated by the color singlet generators of G , including $SU(2)_L \times U(1)_Y$.

A proper subalgebra G' of G is denoted by $G \supset G'$, and G' is a maximal subalgebra of G if there is no algebra G'' such that $G \supset G'' \supset G'$. Maximal subalgebras of a simple algebra can be classified as regular and special subalgebras. A subalgebra G' is regular if there exists a basis of G such that $\{H_i\} \supset \{H'_i\}$ and $\{E_\alpha\} \supset \{E'_\alpha\}$ where $\{H'_i\}$ and $\{E'_\alpha\}$ are Cartan subalgebra and ladder operators of G' written in a Cartan-Weyl basis. A regular subalgebra can be semisimple or nonsemisimple. Each maximal nonsemisimple subgroup is a $U(1)$ factor times a semisimple factor obtained by removing one dot from the Dynkin diagram for G . The maximal regular semisimple subalgebra can be obtained similarly by removing a dot from the extended Dynkin diagram for G . All subgroups of E_6 with $U(1)_{em} \times SU(3)_C$ as subgroup are listed in Table 1.2. Here F_4 has rank 4 and has 52 generators. Its irreducible representations are all self-conjugate, so all theories based on F_4 are vector-like. $SO(10)$ may be classified as E_5 and $SU(5)$ may be classified as E_4 , so the chain of subgroups $E_6 \supset SO(10) \times U(1) \supset SU(5) \times U(1) \times U(1)$ may contain many of the interesting flavor-chiral theories and is studied most in the literature. $SU(3) \times SU(3) \times SU(3)$ is the only maximal subgroup decomposition of E_6 including QCD as an explicit factor. A more detailed summary of the E_6 group can be found in Ref. [24].

Table 1.2 Subgroups of E_6 with $U(1)_{em} \times SU(3)_C$ as subgroup.

Group	Maximal subgroups
E_6	$F_4, SO(10) \times U(1), SU(2) \times SU(6), SU(3) \times SU(3) \times SU(3)$
F_4	$SO(9), SU(3) \times SU(3)$
$SO(9)$	$SO(8), SU(2) \times SU(4)$
$SO(8)$	$SO(7), SU(4) \times U(1)$
$SO(7)$	$SU(4)$
$SU(4)$	$SU(3) \times U(1)$
$SO(10)$	$SU(5) \times U(1), SU(2) \times SU(2) \times SU(4), SO(9), SU(2) \times SO(7), SO(8) \times U(1)$
$SU(6)$	$SU(5) \times U(1), SU(4) \times SU(2) \times U(1), SU(3) \times SU(3) \times U(1)$
$SU(5)$	$SU(4) \times U(1), SU(3) \times SU(2) \times U(1)$

1.2.3 Effective low-energy models

Models based on subgroups of E_6 can be rank 5 or rank 6. Choosing the color group to be $SU(3)$ at these E_6 symmetry breaking scales, the rank-5 model can be determined uniquely to be

$$SU(3)_C \times SU(2)_L \times U(1)_Y \times U(1)_\eta. \quad (4)$$

where $U(1)_\eta$ is the only additional factor and its couplings are essentially fixed. In the rank-6 case, there are two kinds of relevant models

$$(a). \quad SU(3)_C \times SU(2)_L \times U(1)_Y \times U(1)' \times U(1)'', \quad (5)$$

$$(b). \quad SU(3)_C \times SU(2)_L \times SU(2)' \times U(1)' \times U(1)'' \quad (6)$$

where the product $U(1)' \times U(1)''$ can be taken, without loss of generality, to be $U(1)_\psi \times U(1)_\chi$ via the decomposition

$$E_6 \rightarrow SO(10) \times U(1)_\psi \rightarrow SO(10) \times SU(5) \times U(1)_\chi \times U(1)_\psi, \quad (7)$$

and the most frequently discussed $SU(2)'$ can be $SU(2)_R$ or $SU(2)_I$ (which will be introduced in the following). In most cases a rank-6 model can be reduced further to an effective rank-5 model through

$$U(1)_\psi \times U(1)_\chi \rightarrow U(1)_\theta, \quad (8)$$

or

$$U(1)_L \times U(1)_R \rightarrow U(1)_{V=L+R}, \quad SU(2)_I \times U(1)' \rightarrow SU(2)_I \quad (9)$$

where the mixing angle between $U(1)_\psi$ and $U(1)_\chi$, θ , can have different values corresponding to specific models which will be discussed later when we study gauge boson mixings. These effective rank-5 models and the rank-5 model($U(1)_\eta$) are discussed most often in the literature.

Each generation of fermions in the SM has 15 degrees of freedom, so the most economical way is to put all of them into a fundamental representation of E_6 . Then some new particles, which sometimes are called exotic particles compared with the ordinary SM particles, will be introduced. In term of the subgroups $SO(10)$ and $SU(5)$, the fundamental representation **27** decomposes as

$$\mathbf{27} = (\mathbf{16}, \bar{\mathbf{5}}) + (\mathbf{16}, \mathbf{10}) + (\mathbf{16}, \mathbf{1}) + (\mathbf{10}, \bar{\mathbf{5}}) + (\mathbf{10}, \mathbf{5}) + (\mathbf{1}, \mathbf{1}) \quad (10)$$

which gives the classification of particles in the $SU(5)$ and $SO(10)$ unification model. Under the $SU(3)_C \times SU(3)_L \times SU(3)_R$ subgroup, the **27** has the branching rule

$$\mathbf{27} = \underbrace{(\mathbf{3}^c, \mathbf{3}, \mathbf{1})}_q + \underbrace{(\bar{\mathbf{3}}^c, \mathbf{1}, \bar{\mathbf{3}})}_{\bar{q}} + \underbrace{(\mathbf{1}^c, \bar{\mathbf{3}}, \mathbf{3})}_l \quad (11)$$

and the particles of the first family are assigned as

$$\begin{pmatrix} u \\ d \\ h \end{pmatrix} + \begin{pmatrix} u^c & d^c & h^c \end{pmatrix} + \begin{pmatrix} E^c & \nu & N \\ N^c & e & E \\ e^c & \nu^c & S^c \end{pmatrix}.$$

where the superscript c represents charge conjugate and all fields are given in left-handed fields. It is noted that an isosinglet charge $-\frac{1}{3}$ quark h and its antiparticle h^c , a right-handed neutrino are introduced. (Different symbols for these particles have been used in the literature.)

Because the antiquarks are in an $SU(3)_L$ singlet, the electromagnetic charge operator cannot be $Q^{em} = T_{3L} + \frac{Y_L}{2}$, with Y_L coming from $SU(3)_L$, otherwise all antiquarks will

have same electric charge $\frac{Y_L}{2}$. The fact is that the anti-u quark and the anti-d quark have different electric charges. Therefore at least one extra U(1) factor, Y_R , coming from the last $SU(3)_R$ must contribute to the electric charge operator.

There are three possible ways to break the **3** of the $SU(3)_R$ into $2 + 1$. Consider the above representation. Firstly, (u^c, d^c) forms an SU(2) doublet and h^c forms a singlet with $Q^{em} = T_{3L} + T_{3R} + \frac{Y_L}{2} + \frac{Y_R}{2}$, which leads to the well-known and well-studied left-right symmetric model; and this model has the attractive feature that it can be embedded in the SO(10) unification model. Secondly, (u^c, h^c) forms an SU(2) doublet and d^c forms a singlet with $Q^{em} = T_{3L} - T_{3R} + \frac{Y_L}{2} + \frac{Y_R}{2}$, this is not a physically interesting case because it is similar to the left-right symmetric model with d^c replaced by h^c , and it has received little attention in the literature. Thirdly, (d^c, h^c) forms an SU(2) doublet and u^c forms a singlet with $Q^{em} = T_{3L} + \frac{Y_L}{2} - Y_R$. In the third choice the SU(2) doesn't contribute to the electromagnetic charge operator and it is called $SU(2)_I$ (I stands for Inert). So the vector gauge bosons corresponding to $SU(2)_I$ are electrically neutral.

The two U(1) factors, Y_L and Y_R , can be combined linearly to produce two other U(1) factors in order that only one of them contributes to the electric charge operator, which is called $U(1)_Y$ here, and the other one has no contribution to the electric charge operator, which is called $U(1)_{Y'}$. So we have $Q^{em} = T_{3L} + \frac{Y}{2}$ and Y' can be determined correspondingly. In the third case above, it is easy to find $Y = Y_L - 2Y_R$ and $Y' = 2Y_L + Y_R$. Then we get our desired group structure as $SU(2)_L \times SU(2)_I \times U(1)_Y \times U(1)_{Y'}$.

The most extensive work on the phenomenology of this model was performed by Rizzo [25] and Godfrey [26], who looked at the production of the neutral W's in hadron-hadron, positron-electron, and electron-proton colliders. There has been very little work done since then, in spite of the fact that there is much more information obtained from precision electroweak studies, flavor-changing neutral current processes, the discovery of the top quark, etc. We find it is remarkable that so little is known about the phenomenology of

one of the main possible subgroups of E_6 , and propose to study this phenomenology in detail in this project.

At the $SU(2)_L \times SU(2)_I \times U(1)_Y \times U(1)_{Y'}$ level, a single generation of fermions can be represented as

$$\left(\begin{array}{cc} \nu & N \\ e^- & E^- \end{array} \right)_L, \left(\begin{array}{c} u \\ d \end{array} \right)_L, \left(\begin{array}{cc} d^c & h^c \end{array} \right)_L, \left(\begin{array}{c} E^c \\ N^c \end{array} \right)_L, \left(\begin{array}{cc} \nu^c & S^c \end{array} \right)_L, h_L, e_L^c, u_L^c$$

where $SU(2)_{L(I)}$ acts vertically(horizontally). For example, additional heavy leptons (N, E) and their conjugates (E^c, N^c) form two new isodoublets under $SU(2)_L$; a right-handed neutrino and an additional neutral lepton forms an $SU(2)_I$ doublet (ν^c, S^c). The quantum numbers are listed in Table 1.3.

1.3 Outline

After a brief introduction of the background and the model we will work on, the thesis is organized as below. The Higgs boson sector, gauge boson sector and fermion sector of this model will each be explored separately.

Chapter 2 deals with the Higgs boson sector. The main aim is to find bounds on the masses of the (lightest) Higgs scalars. The SM and two-Higgs doublet model are studied first as an introduction and comparison. Experimental searches for Higgs boson(s) are reviewed briefly, and constraints on the masses of Higgs bosons in the SM and two-Higgs doublet models are derived, by the requirement that the vacuum is stable and the perturbation theory is valid up to a large scale. The flavor-changing neutral currents and their effect on the anomalous magnetic moment of the muon are also discussed. Then a specific assignment of Higgs multiplets for $SU(2)_L \times SU(2)_I \times U(1)_Y \times U(1)_{Y'}$ is introduced, and the mass-squared matrices for various scalars are derived. An upper bound of about 150 GeV to the lightest neutral Higgs scalar in the model is found. Other Higgs mass relationships are also discussed.

Table 1.3 The quantum numbers of fermions in $\mathbf{27}$ of E_6

State	T_{3L}	Y_L	T_{3I}	Y_R	$Y(Y_L - 2Y_R)$	$Y'(2Y_L + Y_R)$	Q^{em}	Exotic(?)
u	1/2	1/3	0	0	1/3	2/3	2/3	
d	-1/2	1/3	0	0	1/3	2/3	-1/3	
u^c	0	0	0	2/3	-4/3	2/3	-2/3	
d^c	0	0	1/2	-1/3	2/3	-1/3	1/3	
h	0	-2/3	0	0	-2/3	-4/3	-1/3	✓
h^c	0	0	-1/2	-1/3	2/3	-1/3	1/3	✓
e^-	-1/2	-1/3	1/2	1/3	-1	-1/3	-1	
e^+	0	2/3	0	-2/3	2	2/3	1	
E^-	-1/2	-1/3	-1/2	1/3	-1	-1/3	-1	✓
E^+	1/2	-1/3	0	-2/3	1	-4/3	1	✓
ν_e	1/2	-1/3	1/2	1/3	-1	-1/3	0	
ν_e^c	0	2/3	1/2	1/3	0	5/3	0	✓
N	1/2	-1/3	-1/2	1/3	-1	-1/3	0	✓
N^c	-1/2	-1/3	0	-2/3	1	-4/3	0	✓
S^c	0	2/3	-1/2	1/3	0	5/3	0	✓

In Chapter 3 the gauge boson sector of the model is studied. Mixing and mass relationships of gauge bosons in the SM are introduced first. Then a general discussion of gauge boson mixings is given. A remarkable feature of our model is that the gauge bosons corresponding to $SU(2)_I$ are neutral. Special attention is paid to the W_I boson. Its production, effects in rare processes and contribution to the anomalous magnetic moment of the muon is presented. The mass-squared matrix of neutral gauge bosons for our model is given. Mixing appears naturally. Results from electroweak precision experiments, including Z-pole experiments, m_W measurements and low-energy neutral current experiments are used to put indirect constraints on masses of the extra neutral gauge bosons and the mixings between them and the ordinary Z boson. We also consider the possible constraint from a proposed measurement at Jefferson Lab of the proton's weak charge. It is found that the mixing angles are very small, namely $|\theta| \leq 0.005$. The lower bound of the mass of the lightest extra neutral gauge boson is found to be about 560–800 GeV, which is comparable to the current direct search limit. low-energy neutral current

experiments give the strongest bounds on the lightest extra neutral gauge boson.

In Chapter 4 the fermion sector of the model is explored. The mixing between exotic fermions and the SM fermions are briefly reviewed first. The pair production of heavy charged exotic leptons at e^+e^- colliders is studied. In addition to the standard γ and Z boson contributions, we also include the contributions from extra neutral gauge bosons. A t-channel contribution due to the W_I -boson exchange, which is unsuppressed by mixing angles, is quite important. We calculate the cross section, the left-right and forward-backward asymmetries, and discuss how to differentiate different models. Pair production of the h-quark is also discussed briefly.

Chapter 5 includes our conclusions and an outlook for future work. The mass-squared matrices for Higgs bosons are listed in the Appendix.

Chapter 2 Higgs boson sector

2.1 Introduction

Although the SM is very successful phenomenologically, the experimental information of the scalar sector of the SM is very weak. The most important piece comes from the ρ -parameter, defined through the relation

$$\mathcal{L}_Z^{eff} = \frac{4G_F}{\sqrt{2}} \rho J_Z^\mu J_{Z\mu}, \quad (12)$$

where G_F is the Fermi constant, \mathcal{L}_Z^{eff} is the effective low-energy neutral current Lagrangian and $J_{Z\mu}$ is the standard weak neutral current. ρ is a measure of the ratio of the neutral current to the charged current strength in the effective low-energy Lagrangian. It can be expressed [27]

$$\rho = \frac{\sum_{i=1}^N [I_i(I_i + 1) - \frac{1}{4}Y_i^2] \sigma_i}{\sum_{i=1}^N \frac{1}{2}Y_i^2 \sigma_i}, \quad (13)$$

where N is the number of the scalar multiplets, ϕ_i , with vacuum expectation values σ_i , isospin I_i and hypercharge Y_i . In the SM $\rho = 1$ at the tree level. In our model, scalar multiplets (introduced later) N and N' are $SU(2)_L \times U(1)_Y$ singlets, and scalar multiplets \mathcal{H} and H_2 are doublets with $Y = \pm 1$, therefore ρ is also equal to 1 at the tree level automatically. The deviation from the unity, less than 1%, is assumed to be due to electroweak radiative corrections which are sensitive to new particles in loops.

The discovery of the Higgs boson remains one of the main challenges for today's particle physicists. The most important thing is to determine the mass(es) of the Higgs boson(s). In this section, we present studies on the Higgs structure of the SM first, then the two-Higgs-doublet models, and finally the $SU(2)_L \times U(1)_Y \times SU(2)_I \times U(1)_{Y'}$ model. Some constraints on the model from the Higgs-boson mass bounds are obtained.

2.2 The SM Higgs boson

In the minimal version of the SM, only one complex Higgs doublet is introduced as

$$\phi = \begin{pmatrix} \phi^+ \\ \phi^0 \end{pmatrix}, \quad (14)$$

where $Y(\phi) = +1$. The most general gauge-invariant renormalizable scalar potential is

$$V(\phi) = -\frac{1}{2}\mu^2\phi^\dagger\phi + \frac{1}{4}\lambda(\phi^\dagger\phi)^2, \quad (15)$$

where μ^2 is mass-squared parameter and λ is the self-interaction coupling constant.

It is most easily to find the mass matrix in the real basis where

$$\phi = \begin{pmatrix} \phi_1 + i\phi_2 \\ \phi_3 + i\phi_4 \end{pmatrix}, \quad (16)$$

and the potential becomes

$$V(\phi) = -\frac{1}{2}\mu^2(\phi_1^2 + \phi_2^2 + \phi_3^2 + \phi_4^2) + \frac{1}{4}\lambda(\phi_1^2 + \phi_2^2 + \phi_3^2 + \phi_4^2)^2, \quad (17)$$

The minimum conditions of the potential are

$$\frac{\partial V}{\partial \phi_i} \Big|_{\phi(x)=\phi_0} = 0, \quad (18)$$

which yields

$$-\mu^2\phi_i + \lambda(\phi_1^2 + \phi_2^2 + \phi_3^2 + \phi_4^2)\phi_i = 0. \quad (19)$$

The coefficients of the quadratic terms are

$$m_{ij}^2 = \frac{\partial^2 V}{\partial \phi_i \partial \phi_j} \Big|_{\phi(x)=\phi_0}, \quad (20)$$

which yield

$$m_{ij}^2 = -\mu^2\delta_{ij} + \lambda(\phi_1^2 + \phi_2^2 + \phi_3^2 + \phi_4^2)\delta_{ij} + 2\lambda\phi_i\phi_j. \quad (21)$$

As is well known, in the SM ϕ_0 can be chosen to be

$$\phi_0 = \frac{1}{\sqrt{2}} \begin{pmatrix} 0 \\ v \end{pmatrix}, \quad v = (2\mu^2/\lambda)^{1/2}, \quad (22)$$

and the mass of the only physical Higgs boson is

$$m_h = \sqrt{2}\mu = \sqrt{\lambda}v. \quad (23)$$

The other field components are massless and "eaten" by gauge bosons in order to give them masses.

The mass of the Higgs boson in the SM is, at first sight, completely arbitrary. It depends on the scalar self-coupling, λ , which is a free parameter. However, rather stringent bounds on the mass of the Higgs boson can be obtained [28, 29] by requiring that (a) λ remains perturbative up to a large scale (generally taken to be the unification scale of approximately 10^{16} GeV—the precise value doesn't much matter here), and (b) the vacuum of the standard model remains stable up to that large scale. The first condition gives an upper bound to the Higgs mass of approximately 180 GeV. The second condition is virtually identical to requiring that λ remain positive up to the large scale, and that gives a lower bound to the Higgs mass of approximately 130 GeV. Thus, these two conditions strongly constrain the mass of the Higgs boson to be between 130 and 180 GeV.

It is easy to see where these constraints arise. The renormalization group equation for the scalar self-coupling is of the form

$$\frac{d\lambda}{dt} = \beta_\lambda \quad (24)$$

with

$$\beta_\lambda = 4\lambda\gamma + (12\lambda^2 + B)/8\pi^2, \quad (25)$$

where the anomalous dimension $\gamma = (-9g_L^2 - 3g_Y^2 + 12g_{Y_t}^2)/64\pi^2$ and $B = (3/64\pi^2)[\frac{1}{16}(3g_L^4 + 2g_L^2g_Y^2 + g_Y^4) - g_{Y_t}^4]$. Only the top quark Yukawa coupling g_{Y_t} is considered. Qualitatively the renormalization group equation for the scalar self-coupling can be written as $\frac{d\lambda}{dt} = a\lambda^2 - bg_{Y_t}^4$. If λ is large, the first term dominates, and λ blows up; if it is small, the second term dominates, and λ becomes negative, leading to a vacuum instability. Only

for λ near the fixed point of this equation does λ remain positive and finite from the electroweak scale to the unification scale. The bounds on the mass of the SM Higgs boson are illustrated in Fig. 3. A more detailed review on how severe bounds on Higgs boson and fermion masses arise from the requirements of vacuum stability and the validity of perturbation theory up to a large scale can be found in a report by Sher [28].

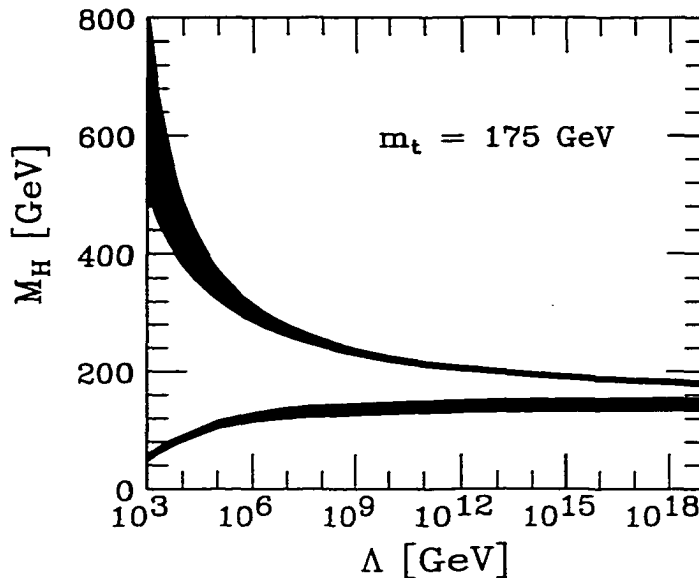


Figure 3: Bounds on the SM Higgs boson mass by requiring that the vacuum is stable and the perturbation is valid up to a large scale Λ , assuming $M_t = 175$ GeV and $\alpha_s(m_Z) = 0.118$. The shaded areas above reflect the theoretical uncertainties in the calculations of the Higgs mass bounds. This figure is taken from Ref. [30].

From Ref. [31], indirect experimental bounds for the Higgs boson mass are obtained from fits to precision measurements of electroweak observables, primarily from Z decay data, and to the measured top and W^\pm masses. These measurements are sensitive to $\log(m_H)$ through radiative corrections via top quark and Higgs boson loops. Currently the best fit value is $m_H = 77^{+69}_{-39}$ GeV and $m_H < 215$ GeV is obtained at the 95% confidence level(CL), still consistent with the SM being valid up to the grand unification scale. This is illustrated in Fig. 4.

Direct search results by the LEP collaborations, CDF and D0, give the value 102.6

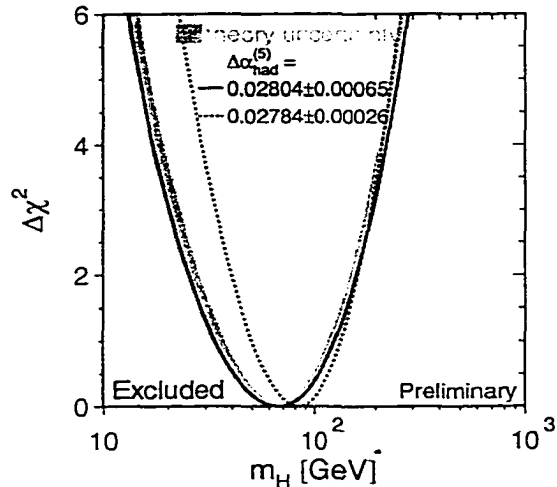


Figure 4: χ^2 variation as a function of the Higgs mass from the global fit of the electroweak measurements. This figure is taken from Ref. [32].

GeV as the 95% CL lower bound for the SM Higgs mass. Recent reports [5-8] on the observation of an excess in the search for the SM Higgs boson with a mass near 114 GeV need to be confirmed in the future.

2.3 Higgs bosons in the two-Higgs-doublet models

The most straightforward extension of the SM is the two-Higgs-doublet model (2HDM). It includes two complex scalar doublets (see Ref. [28] for a review),

$$\Phi_1 = \begin{pmatrix} \chi_1^+ \\ (\phi_1 + i\chi_1)/\sqrt{2} \end{pmatrix}, \quad \Phi_2 = \begin{pmatrix} \chi_2^+ \\ (\phi_2 + i\chi_2)/\sqrt{2} \end{pmatrix}. \quad (26)$$

Of the eight real fields, three must become the longitudinal components of the W^\pm and Z bosons after the spontaneous symmetry breaking. Linear combinations of χ_1^\pm and χ_2^\pm are absorbed into the longitudinal parts of the W^\pm bosons and a linear combination of χ_1 and χ_2 gives mass to the Z boson. Five physical Higgs scalars will remain: a charged scalar χ^\pm and three neutral scalars ϕ_1 , ϕ_2 and the other linear combination of χ_1 and χ_2 , called χ^0 .

2.3.1 FCNC in the two-Higgs-doublet models

A potential danger with additional Higgs doublets is the possibility of flavor-changing neutral currents (FCNC). The Higgs doublet of the standard model does not generate tree level FCNC because the mass matrix is directly proportional to the Yukawa coupling matrix, so diagonalization of the former automatically diagonalizes the latter. However, in a two-Higgs-doublet model, the mass matrix is the sum of two Yukawa coupling matrices (each times the appropriate vacuum expectation value), for example, the Yukawa couplings of the $Q = -1/3$ quarks are given by

$$\mathcal{L}_Y = h_{ij}^1 \bar{\psi}_i \psi_j \Phi_1 + h_{ij}^2 \bar{\psi}_i \psi_j \Phi_2, \quad (27)$$

where i and j are generation indices. The mass matrix is then

$$M_{ij} = h_{ij}^1 v_1 + h_{ij}^2 v_2. \quad (28)$$

Since the Yukawa coupling matrices are generally not simultaneously diagonalizable, diagonalization of the mass matrix will *not*, in general, diagonalize the Yukawa coupling matrices, thereby leading to tree-level FCNC.

These tree-level FCNC are dangerous, leading to potentially large contributions to processes such as $K^0 - \bar{K}^0$ mixing. It is well known that FCNC are highly suppressed relative to the charged current processes, so it would be desirable to “naturally” suppress them in these models. If all quarks with the same quantum numbers couple to the same scalar multiplet, then FCNC will be absent. This led Glashow and Weinberg [33] to propose a discrete symmetry which forces all the quarks of a given charge to couple to only one doublet. There are two such possible discrete symmetries in the 2HDM,

$$(I) \phi_2 \rightarrow -\phi_2 \quad (II) \phi_2 \rightarrow -\phi_2, \quad d_R^i \rightarrow -d_R^i \quad (29)$$

In model I, all quarks couple to the same doublet, and no quarks couple to the other

doublet. In model II, the $Q=2/3$ quarks couple to one doublet and the $Q=-1/3$ quarks couple to the other doublet.

However, it was pointed out by Cheng and Sher [35] that, for many models, the coupling is the geometric mean of the Yukawa couplings of the two fermions. As a result, FCNC involving the first generation fields are very small, and the bounds are not as severe. Thus, one can also consider Model III, in which no discrete symmetry is imposed, and the flavor-changing neutral couplings are simply constrained by experiments.

This had led to a number of calculations involving Model III [36-45]. The most extensive analyses were those of Refs. [43, 45]. In Ref. [43], the implications of tree-level FCNC for many processes were considered, including $K^0 - \bar{K}^0$, $D^0 - \bar{D}^0$, $B^0 - \bar{B}^0$ and $B_s^0 - \bar{B}_s^0$ mixing, $e^+e^-(\mu^+\mu^-) \rightarrow t\bar{c} + c\bar{t}$, $Z \rightarrow b\bar{b}$, $t \rightarrow c\gamma$ and the ρ parameter. In Ref. [45], the effects on $\tau \rightarrow \mu\gamma$, $\tau \rightarrow e\gamma$ and $\mu \rightarrow e\gamma$, other lepton-flavor violating decays of the τ and μ , and a number of rare B-decays were determined. In all of these papers, the results were given as upper bounds on the neutral flavor-changing scalar couplings. In most of these calculations, the results were given in terms of the product of various Yukawa couplings. For example, the bound from $\tau^- \rightarrow \mu^- \mu^+ \mu^-$ is dependent on $h_{\tau\mu}h_{\mu\mu}$, where h_{ij} is the coupling of the scalar to fermions i and j .

Here we point out [46] that a bound on leptonic flavor changing couplings can be obtained from the anomalous magnetic moment of the muon (AMMM). This bound has several advantages over previous bounds: it depends only on a single Yukawa coupling, rather than a product; it is stronger than previous bounds, using reasonable assumptions about the ratio of couplings; it could be improved significantly in the near future at the upcoming experiment E821 [47] at Brookhaven National Lab. By the time this dissertation is finished, they have published their new result [48], its implications is also discussed in the following.

For a spin- $\frac{1}{2}$ particle f , the form-factor decomposition of the matrix element of the

electromagnetic current j_μ is

$$\langle f(p') | j_\mu(0) | f(p) \rangle = \bar{u}(p') \Gamma_\mu(q) u(p), \quad (30)$$

where

$$\Gamma_\mu(q) = F_1(q^2) \gamma_\mu + F_2(q^2) \frac{i\sigma_{\mu\nu} q^\nu}{2m} + F_A(q^2) (\gamma_\mu q^2 - 2mq_\mu) \gamma_5 + F_3(q^2) \frac{\sigma_{\mu\nu} \gamma_5 q^\nu}{2m}, \quad (31)$$

with $q = p' - p$, and m denotes the mass of f .

The anomalous magnetic moment of f is then given by

$$a_f = \left(\frac{g-2}{2} \right)_f = F_2(0). \quad (32)$$

As shown in the above references, one can choose a basis for the two Higgs doublets such that only one doublet, H , obtains a vacuum expectation value. That doublet will then have flavor-diagonal couplings, while the couplings of the other, ϕ , will be unconstrained. The relevant terms in the Lagrangian contributing to the AMMM is

$$m_e \bar{e}_L e_R (\sqrt{2}H/v) + m_\mu \bar{\mu}_L \mu_R (\sqrt{2}H/v) + m_\tau \bar{\tau}_L \tau_R (\sqrt{2}H/v) + h_{ij} \bar{l}_i l_j \phi + \text{H.c.} \quad (33)$$

The ϕ field is composed of a scalar ϕ_s and a pseudoscalar ϕ_p . Since one expects [35] the heavier generations to have larger flavor-changing couplings, we will look at the bound on the $h_{\mu\tau}$ arising from the AMMM.

The diagram is given in Fig. 5. The diagrams in which the photon couples to the external lines do not give a contribution to the magnetic moment of the muon. The calculation is straightforward, and we find that the contribution to $a_\mu \equiv \frac{g_\mu-2}{2}$ is given by

$$a_\mu = \frac{h_{\mu\tau}^2}{16\pi^2} \int_0^1 \frac{z^2(1-z) \pm z^2 \frac{m_\tau}{m_\mu}}{z(z-1) + z \frac{m_\tau^2}{m_\mu^2} + (1-z) \frac{m_\phi^2}{m_\mu^2}} dz, \quad (34)$$

where m_ϕ is the mass of the scalar or pseudoscalar, and the $+(-)$ sign is chosen for the scalar (pseudoscalar). In the expected limit $m_\mu \ll m_\tau \ll m_\phi$, the integral becomes

$$\mp \frac{m_\mu m_\tau}{m_\phi^2} \left(\log \frac{m_\tau^2}{m_\phi^2} + \frac{3}{2} \right), \quad (35)$$

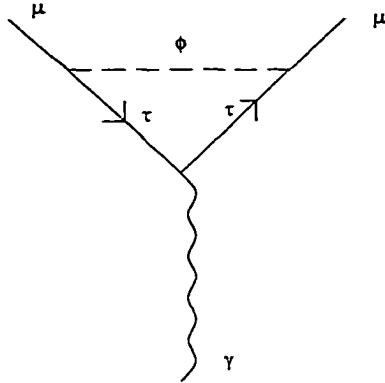


Figure 5: Contribution to the anomalous magnetic moment of the muon from the exchange of flavor-changing scalars. The scalar can be either a scalar or a pseudoscalar.

It is noted that a_μ is proportional to the product of the masses of fermions involved.

The resulting contribution is given in Fig. 6. The scalar and pseudoscalar have contributions which are almost identical (within a few percent), but of opposite sign; the scalar contribution is shown. Since there is no reason that the masses should be similar, and since the result is so sharply dependent on the mass, we expect the lighter of the two to make the dominant contribution.

Consider the case in which the lighter scalar is 80 GeV (current LEP bounds apply to a standard model Higgs, and are generally weaker for two doublet models). We see that this gives a value of a_μ which is $1.14 \times 10^{-6} h_{\mu\tau}^2$. The current value of a_μ is in agreement with expectations, and the uncertainty [44] is 7.4×10^{-9} . Thus, the contribution of the flavor-changing coupling must be less than this uncertainty, or $h_{\mu\tau}$ must be less than 0.11. More importantly, the experimental uncertainty in the anomalous magnetic moment will shortly decrease by up to a factor of 20, so that a bound on $h_{\mu\tau}$ of 0.027 can be obtained.

How does this bound compare with other bounds? As noted above, all other bounds depend on the product of $h_{\mu\tau}$ times other unknown Yukawa couplings. Thus, the bound is unique. However, one can make reasonable assumptions about these other couplings. For example, in Ref. [45], it was argued that grand unified theories will give a relationship

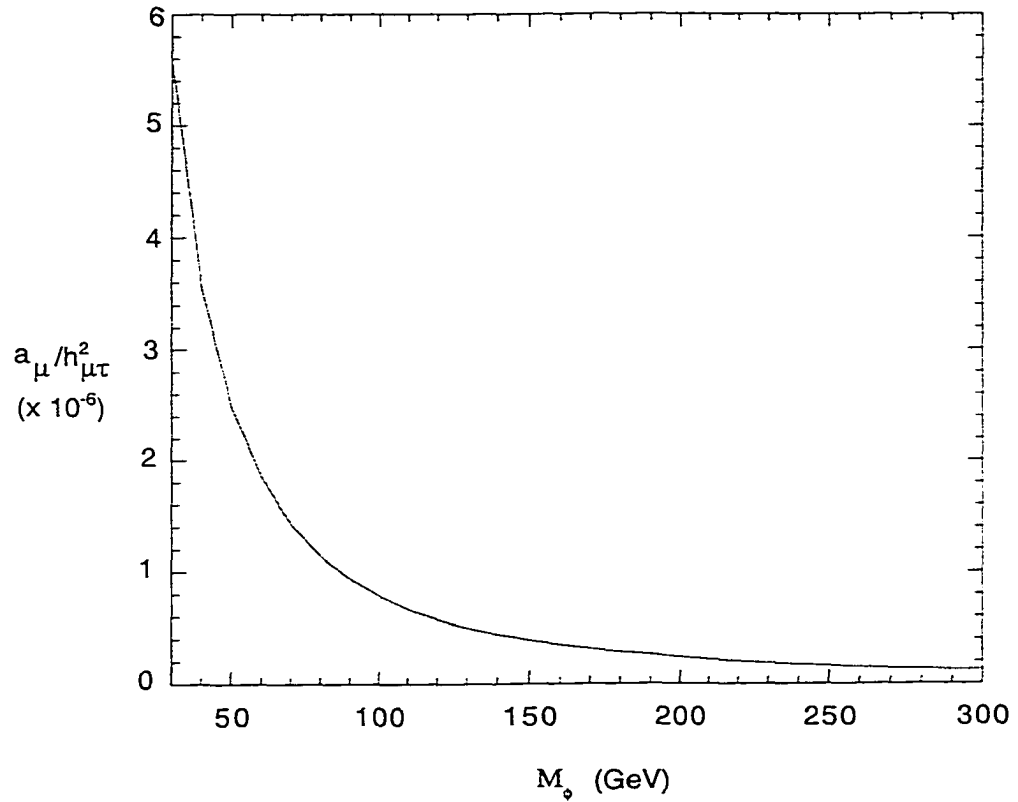


Figure 6: The contribution of the diagram of Fig. 5 to the anomalous magnetic moment of the muon. The contribution of the scalar is shown; that of the pseudoscalar is within a few percent of that of the scalar, but of opposite sign.

between h_{bs} and $h_{\mu\tau}$; from this, they looked at the process $B \rightarrow K\mu\tau$ to get the bound $h_{\mu\tau} < 0.024$. Unfortunately, there are no experimental limits listed for $B \rightarrow K\mu\tau$; their bound was obtained by noting that 17% of τ 's decay into μ 's, and using the bound on $B \rightarrow \mu^+\mu^-X$. Since the experimental cuts would be quite different, this result is very uncertain, and thus the bound on $h_{\mu\tau}$ could be considerably higher (and also requires the assumption of grand unification). In addition, one can assume that the ratio of $h_{\tau\tau}$ to $h_{\mu\tau}$ is $\sqrt{\frac{m_\tau}{m_\mu}}$, in which case the bound on $h_{\mu\tau}$ from $\tau \rightarrow 3\mu$ gives 0.2, which is also much weaker. It was argued by Cheng and Sher [35] that the most natural value for $h_{\mu\tau}$ is the geometric mean of the Yukawa couplings of the muon and tau, or 0.0025. Our bound is still above that value. However, the symmetry arguments in that work apply only to the ratio of the couplings, not their overall scale, and thus higher couplings are certainly possible.

It should be pointed out that a similar diagram could bound the flavor-changing $h_{\mu e}$ coupling, but much stronger bounds on that can be obtained from bounds on radiative muon decays such as $\mu \rightarrow e\gamma$ and $\mu \rightarrow 3e$.

In the absence of any solid theoretical understandings of Yukawa couplings, one must rely on experiments to put bounds on such couplings. In the simplest extension of the standard model, a flavor-changing coupling of the μ and τ to a neutral scalar can, in general, exist. In the above, we have shown that the strongest bound on such a coupling (independent of assumptions about other couplings) arises from the contribution to the AMMM.

As for the recent report from Muon g-2 Collaboration [48], a precise measurement of a_μ for the positive muon had been made. The difference between the weighted mean of experimental results, $a_\mu(\text{exp}) = 11\,659\,203(15) \times 10^{-10}$ (1.3 ppm), and the theoretical

value from the standard model is

$$a_\mu(\text{exp}) - a_\mu(\text{SM}) = 43(16) \times 10^{-10}. \quad (36)$$

The difference is 2.6 times the stated error and may be due to new physics beyond the SM.

Were it due to the contribution from the scalar in the model, choosing the mass of the lighter scalar as 115 GeV, this gives a value of a_μ which is $6.13 \times 10^{-7} h_{\mu\tau}^2$. So $h_{\mu\tau}$ would be 0.08 ± 0.05 , which is consistent with the result discussed above.

2.3.2 Bound on Higgs boson masses

Given how stringently the Higgs mass in the SM is constrained, one might ask how stringently the masses of the scalars in the 2HDM are constrained. There are many more self-couplings (which could potentially diverge by the unification scale) and more directions in the field space where an instability could arise. In this section, we examine these constraints in the 2HDM [49]. Similar constraints have been examined before [28, 34], but the top quark mass was unknown at the time (and only values up to about 130 GeV for the top quark mass were considered).

The most general potential subject to one of the discrete symmetries, for two doublets of hypercharge +1 (if one of the doublets has hypercharge -1 our arguments will be unaffected), is

$$\begin{aligned} V = & \mu_1^2 \Phi_1^+ \Phi_1 + \mu_2^2 \Phi_2^+ \Phi_2 + \lambda_1 (\Phi_1^+ \Phi_1)^2 + \lambda_2 (\Phi_2^+ \Phi_2)^2 \\ & + \lambda_3 (\Phi_1^+ \Phi_1) (\Phi_2^+ \Phi_2) + \lambda_4 (\Phi_1^+ \Phi_2)^2 + \frac{1}{2} \lambda_5 [(\Phi_1^+ \Phi_2)^2 + (\Phi_2^+ \Phi_1)^2] \end{aligned} \quad (37)$$

where the vacuum expectation values of Φ_1 and Φ_2 can be written as

$$\Phi_1 = 1/\sqrt{2} \begin{pmatrix} 0 \\ v_1 \end{pmatrix}, \quad \Phi_2 = 1/\sqrt{2} \begin{pmatrix} 0 \\ v_2 \end{pmatrix} \quad (38)$$

with $v_1^2 + v_2^2 = \sqrt{2}G_F = (247 \text{ GeV})^2$. The masses of the physical scalars are given by

$$m_{\chi^\pm}^2 = -\frac{1}{2}(\lambda_4 + \lambda_5)(v_1^2 + v_2^2), \quad m_{\chi^0}^2 = -\lambda_5(v_1^2 + v_2^2), \quad (39)$$

$$m_\phi^2 = \frac{1}{2}(A + B + \sqrt{(A - B)^2 + 4C^2}), \quad m_\eta^2 = \frac{1}{2}(A + B - \sqrt{(A - B)^2 + 4C^2}), \quad (40)$$

where $A = 2\lambda_1 v_1^2$, $B = 2\lambda_2 v_2^2$ and $C = (\lambda_3 + \lambda_4 + \lambda_5)v_1 v_2$.

It is required that all scalar boson masses-squared must be positive. This implies that

$$\begin{aligned} (i) \quad & \lambda_5 < 0 \\ (ii) \quad & \lambda_4 + \lambda_5 < 0 \\ (iii) \quad & \lambda_1 > 0 \\ (iv) \quad & \lambda_2 > 0 \\ (v) \quad & 2\sqrt{\lambda_1 \lambda_2} > \lambda_3 + \lambda_4 + \lambda_5 \end{aligned} \quad (41)$$

In the SM the positivity of the scalar boson masses-squared implies that $\lambda > 0$. To ensure vacuum stability for all scales up to M_X , one must have $\lambda(q^2) > 0$ for all q^2 from M_Z^2 to M_X^2 . Similarly, to ensure vacuum stability in the 2HDM up to M_X^2 , one must require that all of the five constraints be valid up to M_X^2 . If the condition λ_1 or $\lambda_2 > 0$ is violated, the potential will be unstable in the ϕ_1 or ϕ_2 direction. If the condition (v) is violated, the potential will be unstable in some direction in the $\phi_1 - \phi_2$ plane. If the condition $\lambda_4 + \lambda_5 < 0$ is violated, the mass of the charged Higgs bosons will be negative. If λ_5 become positive, a new minimum which violates CP will be formed. Thus it is required that all of the constraints should be valid up to M_X . At the same time it is physically reasonable to demand that all λ 's be finite (or perturbative) up to M_X .

Starting with $\lambda_1, \lambda_2, \lambda_3, \lambda_4, \lambda_5$ and $\tan \beta$ at the electroweak scale, the renormalization group equations are integrated numerically to check whether one of the five constraints is violated or whether any of the couplings becomes nonperturbative before reaching M_X . The results give an allowed region in the six-dimensional parameter space. To explore this region, we choose the six parameters to be the four physical scalar masses, $\tan \beta$ and λ_3 . For a point in this parameter-space to be acceptable, all of the above constraints, as

well as perturbativity, must be satisfied at all scales up to M_χ . In practice, since λ_3 is unmeasurable, we consider the other five parameters as starting points, and see if any initial values of λ_3 give acceptable values. In this way, we determine if a given point in the five-dimensional space of the scalar masses and $\tan\beta$ is acceptable.

It is, of course, difficult to plot a region in five-dimensional space. However, the basic features can easily be seen with a few examples. Let us first consider the case in which $m_{\chi^\pm} = m_{\chi^0} = 100$ GeV. We choose $\tan\beta = 2$, and plot the allowed region in the neutral scalar mass plane. The region is shown in Fig. 7. For m_η between 40 and 88 GeV, one sees that the value of m_ϕ must lie below 180 GeV and above a value which ranges from 130 GeV to 100 GeV; this bound is very similar to the result in the SM. However, there are no solutions in which m_η is greater than 88 GeV or below 40 GeV. Below the region, λ_1 becomes negative, above the region λ_1 becomes non-perturbative, to the left and to the right of the region, the constraint (v) is violated.

One can now vary some of the three input parameters to see how this region changes. As the charged Higgs mass increases, the region shrinks dramatically, disappearing when it reaches 140 GeV, as shown in Fig. 8. As $\tan\beta$ increases, the region shifts to smaller values of m_η , as shown in Fig. 9. This is not surprising since m_η becomes small as $\tan\beta \rightarrow \infty$. As $\tan\beta$ decreases, the size of the allowed region shrinks, since the top quark Yukawa coupling is getting larger, leading to an instability. Finally, varying m_{χ^0} gives the result in Fig. 10. As in the charged Higgs case, the allowed region disappears when the pseudoscalar mass exceeds 140 GeV.

The most important result is seen from Fig. 8, where this is a stringent upper bound on the charged Higgs mass. By optimizing $\tan\beta$ and m_{χ^0} , we find that the maximum allowed value for the charged Higgs mass is 150 GeV .

What are the experimental constraints? As discussed in Ref. [50], there are very few constraints on the neutral scalar masses. If one takes the χ^0 mass to be 100 GeV, the

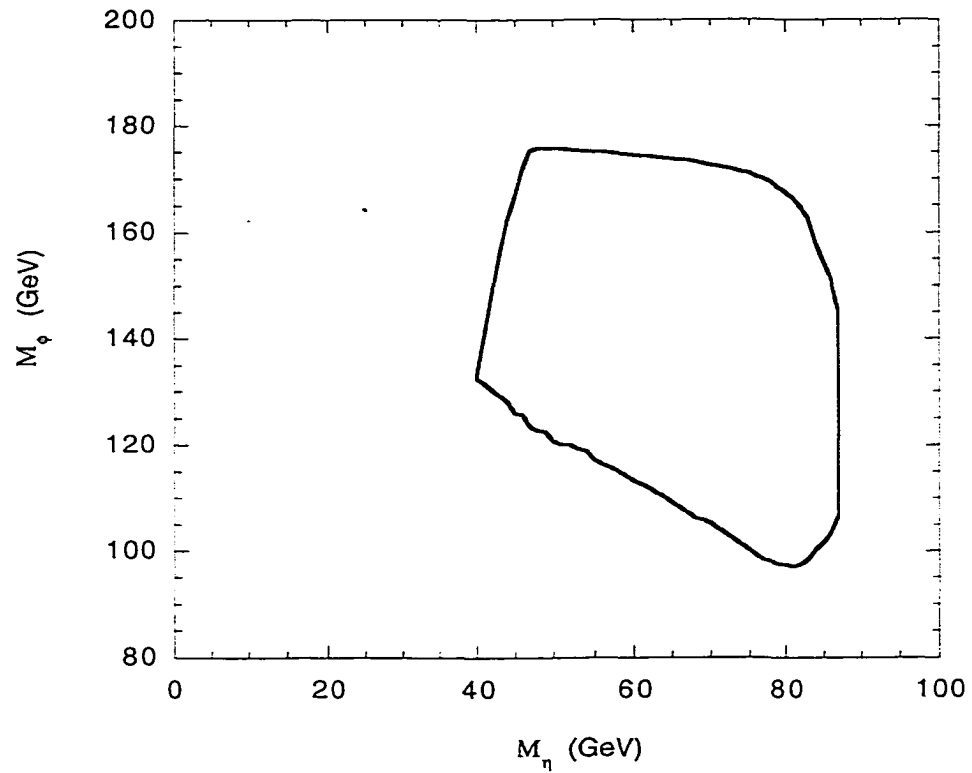


Figure 7: The allowed region in the neutral scalar mass plane, with $m_{\chi^\pm} = m_{\chi^0} = 100$ GeV and $\tan \beta = 2$

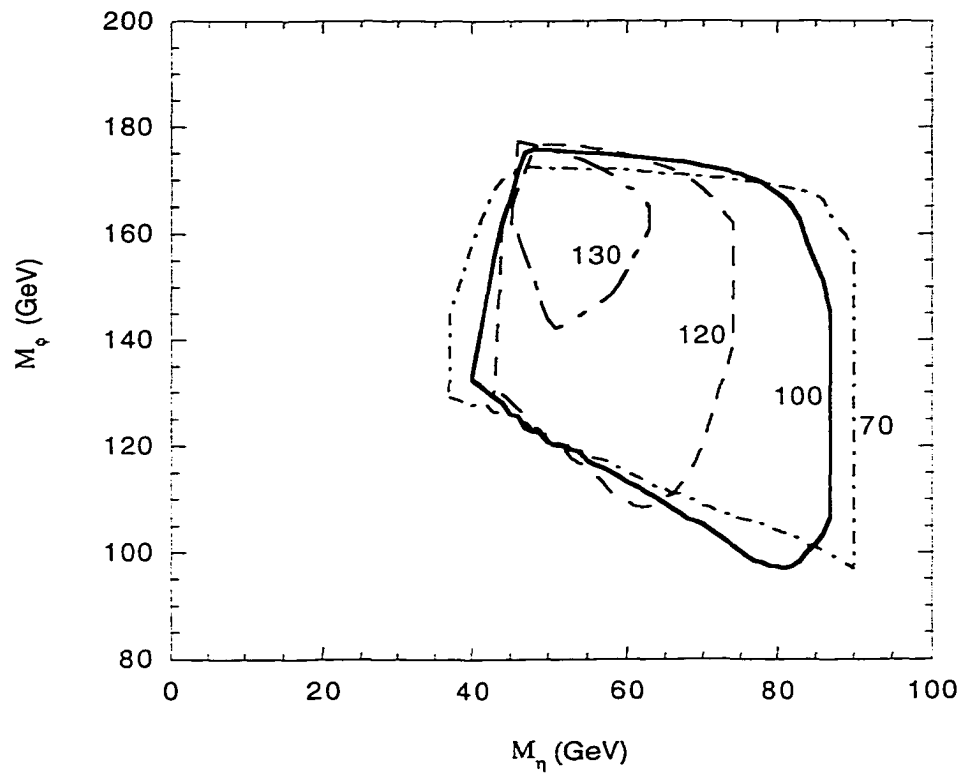


Figure 8: The allowed region in the neutral scalar mass plane for various values of the charged Higgs mass (in GeV), with the χ^0 mass chosen to be 100 GeV and $\tan\beta = 2$

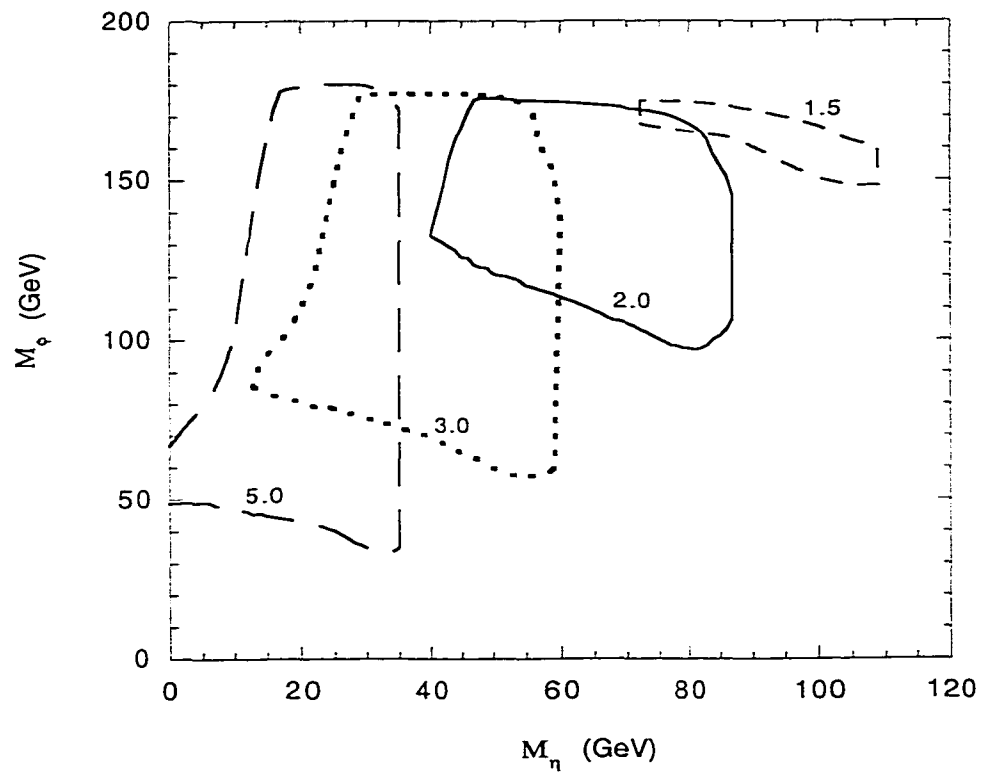


Figure 9: The allowed region in the neutral scalar mass plane for various values of $\tan\beta$, with the χ^0 and χ^\pm masses chosen to be 100 GeV

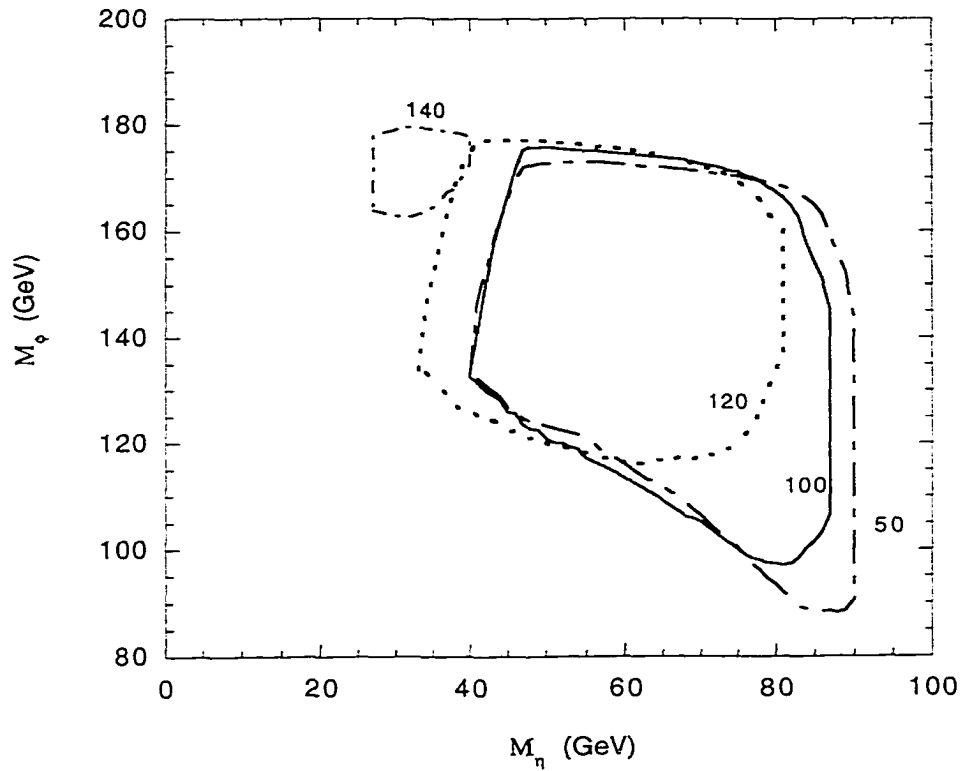


Figure 10: The allowed region in the neutral scalar mass plane for various values of the pseudoscalar Higgs mass (in GeV), with the χ^\pm mass chosen to be 100 GeV and $\tan \beta = 2$

only constraints come from the Bjorken process, $e^+e^- \rightarrow Z^* \rightarrow Z\eta$, and the rate can be significantly reduced by judicious choice of the mixing angle. So no bounds on m_η are relevant. There is, however, a strong bound [50, 51] on m_χ^\pm coming from $B \rightarrow X_s\gamma$, where X_s is a hadronic recoil system containing an s quark. In Model II, this process forces the charged Higgs mass to be greater than 165 GeV. This is inconsistent with our upper bound. Model I, however, has no such constraint, and the charged Higgs mass could be as light as 45 GeV.

We conclude that the popular two-Higgs doublet model, Model II, can not be valid up to the unification scale. Model I is not excluded, however we do find that the charged Higgs mass must be lighter than 150 GeV, the lightest neutral scalar must be lighter than 110 GeV and the pseudoscalar must be lighter than 140 GeV for the model to be valid up to the unification scale.

As mentioned before, LEP has found possible signals of the SM Higgs boson, and put a lower constraint of about 114 GeV on the mass of the SM Higgs boson. But the analysis is model-dependent. The constraint does not apply here because the ZZH coupling is different in the 2HDM from that in the SM, so the constraint should be weaker.

2.4 Higgs bosons in $SU(2)_L \times U(1)_Y \times SU(2)_I \times U(1)_{Y'}$ model

We now consider the Higgs multiplets for the model as below

$$H_2 \equiv \begin{pmatrix} H_2^+ & H_2^0 \end{pmatrix}, \quad \mathcal{H} \equiv \begin{pmatrix} H_1^0 & H_1^- \\ \tilde{\nu} & \tilde{e}^- \end{pmatrix}, \quad N \equiv \begin{pmatrix} N_2 \\ N_1 \end{pmatrix}, \quad N' \equiv \begin{pmatrix} N'_2 \\ N'_1 \end{pmatrix}$$

with $SU(2)_L$ acting in the horizontal direction and $SU(2)_I$ acting in the vertical direction. The quantum numbers of hypercharges are assigned as: $Y(H_2) = 1, Y(\mathcal{H}) = -1, Y(N) = Y(N') = 0$, and $Y'(H_2) = 4/3, Y'(\mathcal{H}) = 1/3, Y'(N) = Y'(N') = -5/3$. The doublets N and N' are also neutral. Note that two neutral doublets are needed. The reason can be seen in the limit where the model is broken down to the SM at a scale much

greater than the electroweak scale. A single N doublet can only break $SU(2)_I \times U(1)_{\mathcal{Y}}$ down to $U(1)$, leaving an extra unbroken $U(1)$ factor.

There are a large number of Higgs bosons in the model: 6 scalar, 3 pseudoscalar and 4 charged Higgs bosons. In general, the scalar potential will have too many parameters to make any meaningful statement about masses of Higgs bosons. However, in the supersymmetric version of the model, the scalar potential is highly constrained.

The most general potential satisfying the gauge invariance can be written as

$$W = \lambda H_2 \mathcal{H} N + \lambda' H_2 \mathcal{H} N' \quad (42)$$

Here by $H_2 \mathcal{H} N$, we mean that $\varepsilon_{ij} H_2^i \mathcal{H}^{\alpha j} \varepsilon_{\alpha\beta} N^\beta$, i, j are $SU(2)_L$ indices and α, β are $SU(2)_I$ indices.

The scalar potential is given by

$$V = V_F + V_D + V_{soft} \quad (43)$$

where

$$V_F = \sum_i |\partial W / \partial \phi_i|^2 \quad (44)$$

is the F-term, and the sum runs over all complex scalar ϕ_i 's appearing in the theory, and

$$V_D = 1/2 \sum_a \left| \sum_i (g_a \phi_i^\dagger T^a \phi_i) + \xi_a \right|^2 \quad (45)$$

is the D-term, where T^a represent generators of the corresponding gauge groups and g_a are coupling constants. The ξ terms only exist if a labels a $U(1)$ generator, and in our consideration they are set to zero as they will not arise if the theory is embedded in a grand unified or string theory. Here

$$\begin{aligned} V_{soft} = & m_{\mathcal{H}}^2 \text{Tr}(\mathcal{H}^\dagger \mathcal{H}) + m_{H_2}^2 H_2^\dagger H_2 + m_N^2 N^\dagger N + m_{N'}^2 N'^\dagger N' \\ & - \lambda A (H_2 \mathcal{H} N + h.c.) - \lambda' A' (H_2 \mathcal{H} N' + h.c.) - m_3^2 (N^\dagger N' + h.c.) \end{aligned} \quad (46)$$

are soft supersymmetry breaking terms. The soft supersymmetry breaking parameters will be considered as completely arbitrary, therefore we only study the tree-level potential. The radiative corrections to the potential will not significantly affect the results because the primary effects of the radiative corrections are to change the effective soft supersymmetry breaking terms. The exception is due to the top quark contribution, proportional to m_{top}^4 , which will increase some mass limits by up to 20 GeV.

The computation of the Higgs boson mass matrices is most easily done in a real basis where

$$\begin{aligned}
H_2 &= \begin{pmatrix} \phi_5 + i\phi_6 \\ \phi_7 + i\phi_8 \end{pmatrix}, \\
\mathcal{H} &= \begin{pmatrix} \phi_3 - i\phi_4 & -\phi_1 + i\phi_2 \\ \phi_{11} - i\phi_{12} & -\phi_9 + i\phi_{10} \end{pmatrix}, \\
N &= \begin{pmatrix} n_2 + im_2 \\ n_1 + im_1 \end{pmatrix}, \\
N' &= \begin{pmatrix} n'_2 + im'_2 \\ n'_1 + im'_1 \end{pmatrix}.
\end{aligned} \tag{47}$$

The multiplets can get vacuum expectation values in the following way,

$$\langle H_2 \rangle = \frac{1}{\sqrt{2}} \begin{pmatrix} 0 & v_2 \end{pmatrix}, \quad \langle \mathcal{H} \rangle = \frac{1}{\sqrt{2}} \begin{pmatrix} v_1 & 0 \\ v_3 & 0 \end{pmatrix}, \quad \langle N \rangle = \frac{1}{\sqrt{2}} \begin{pmatrix} n_2 \\ n_1 \end{pmatrix}, \quad \langle N' \rangle = \frac{1}{\sqrt{2}} \begin{pmatrix} n'_2 \\ n'_1 \end{pmatrix}$$

All of vacuum expectation values are chosen to be real. It appears that there are seven vacuum expectation values in the model, but one of them can be set to zero by performing an $SU(2)_I$ rotation. So there are only six physically relevant vacuum expectation values.

The scalar potential can be written in the component fields as

$$\begin{aligned}
V_F &= |\phi_9(\lambda n_2 + \lambda' n'_2) + \phi_{10}(\lambda m_2 + \lambda' m'_2) - \phi_1(\lambda n_1 + \lambda' n'_1) - \phi_2(\lambda m_1 + \lambda' m'_1)|^2 \\
&\quad + |\phi_2(\lambda n_1 + \lambda' n'_1) - \phi_1(\lambda m_1 + \lambda' m'_1) + \phi_9(\lambda n_2 + \lambda' n'_2) - \phi_{10}(\lambda m_2 + \lambda' m'_2)|^2 \\
&\quad + |\phi_{11}(\lambda n_2 + \lambda' n'_2) + \phi_{12}(\lambda m_2 + \lambda' m'_2) - \phi_3(\lambda n_1 + \lambda' n'_1) - \phi_4(\lambda m_1 + \lambda' m'_1)|^2 \\
&\quad + |\phi_{11}(\lambda m_2 + \lambda' m'_2) - \phi_{12}(\lambda n_2 + \lambda' n'_2) - \phi_3(\lambda m_1 + \lambda' m'_1) + \phi_4(\lambda n_1 + \lambda' n'_1)|^2
\end{aligned}$$

$$\begin{aligned}
& +|\phi_7(\lambda n_1 + \lambda' n'_1) - \phi_8(\lambda m_1 + \lambda' m'_1)|^2 + |\phi_7(\lambda m_1 + \lambda' m'_1) + \phi_8(\lambda n_1 + \lambda' n'_1)|^2 \\
& +|\phi_7(\lambda n_2 + \lambda' n'_2) - \phi_8(\lambda m_2 + \lambda' m'_2)|^2 + |\phi_7(\lambda m_2 + \lambda' m'_2) + \phi_8(\lambda n_2 + \lambda' n'_2)|^2 \\
& +|\phi_5(\lambda n_1 + \lambda' n'_1) - \phi_6(\lambda m_1 + \lambda' m'_1)|^2 + |\phi_5(\lambda m_1 + \lambda' m'_1) + \phi_6(\lambda n_1 + \lambda' n'_1)|^2 \\
& +|\phi_5(\lambda n_2 + \lambda' n'_2) - \phi_6(\lambda m_2 + \lambda' m'_2)|^2 + |\phi_5(\lambda m_2 + \lambda' m'_2) + \phi_6(\lambda n_2 + \lambda' n'_2)|^2 \\
& +(\lambda^2 + \lambda'^2)((\phi_7\phi_{11} + \phi_8\phi_{12} + \phi_5\phi_9 + \phi_6\phi_{10})^2 + (\phi_8\phi_{11} - \phi_7\phi_{12} - \phi_5\phi_{10} + \phi_6\phi_9)^2) \\
& +(\lambda^2 + \lambda'^2)((\phi_1\phi_5 + \phi_2\phi_6 + \phi_3\phi_7 + \phi_4\phi_8)^2 + (\phi_2\phi_5 - \phi_1\phi_6 - \phi_3\phi_8 + \phi_4\phi_7)^2). \quad (48)
\end{aligned}$$

There are four parts in V_D corresponding to the subgroups respectively.

For $SU(2)_L$:

$$\begin{aligned}
\frac{1}{8}g_L^2 \{ & (\phi_1^2 + \phi_2^2 + \phi_3^2 + \phi_4^2)^2 + (\phi_5^2 + \phi_6^2 + \phi_7^2 + \phi_8^2)^2 + (\phi_9^2 + \phi_{10}^2 + \phi_{11}^2 + \phi_{12}^2)^2 \\
& +4[(\phi_3\phi_5 - \phi_4\phi_6 - \phi_1\phi_7 + \phi_2\phi_8)^2 + (\phi_3\phi_6 + \phi_4\phi_5 - \phi_1\phi_8 - \phi_2\phi_7)^2] \\
& +4[(\phi_5\phi_{11} - \phi_6\phi_{12} - \phi_7\phi_9 + \phi_8\phi_{10})^2 + (\phi_7\phi_{10} + \phi_8\phi_9 - \phi_5\phi_{12} - \phi_6\phi_{11})^2] \\
& +4[(\phi_3\phi_{11} + \phi_4\phi_{12} + \phi_1\phi_9 + \phi_2\phi_{10})^2 + (\phi_4\phi_{11} - \phi_3\phi_{12} - \phi_1\phi_{10} + \phi_2\phi_9)^2] \\
& -2(\phi_1^2 + \phi_2^2 + \phi_3^2 + \phi_4^2)^2(\phi_5^2 + \phi_6^2 + \phi_7^2 + \phi_8^2)^2 \\
& -2(\phi_1^2 + \phi_2^2 + \phi_3^2 + \phi_4^2)^2(\phi_9^2 + \phi_{10}^2 + \phi_{11}^2 + \phi_{12}^2)^2 \\
& -2(\phi_5^2 + \phi_6^2 + \phi_7^2 + \phi_8^2)^2(\phi_9^2 + \phi_{10}^2 + \phi_{11}^2 + \phi_{12}^2)^2 \}, \quad (49)
\end{aligned}$$

For $SU(2)_I$:

$$\begin{aligned}
\frac{1}{8}g_I^2 \{ & (\phi_3^2 + \phi_4^2 + \phi_{11}^2 + \phi_{12}^2)^2 + (\phi_1^2 + \phi_2^2 + \phi_9^2 + \phi_{10}^2)^2 \\
& +(n_1^2 + n_2^2 + m_1^2 + m_2^2)^2 + (n_1'^2 + n_2'^2 + m_1'^2 + m_2'^2)^2 \\
& +4[(\phi_1\phi_3 + \phi_2\phi_4 + \phi_9\phi_{11} + \phi_{10}\phi_{12})^2 + (\phi_2\phi_3 - \phi_1\phi_4 + \phi_{10}\phi_{11} - \phi_9\phi_{12})^2] \\
& +4[(\phi_3n_2 - \phi_4m_2 + \phi_{11}n_1 - \phi_{12}m_1)^2 + (\phi_3m_2 + \phi_4n_2 + \phi_{11}m_1 + \phi_{12}n_1)^2] \\
& +4[(\phi_3n_2' - \phi_4m_2' + \phi_{11}n_1' - \phi_{12}m_1')^2 + (\phi_3m_2' + \phi_4n_2' + \phi_{11}m_1' + \phi_{12}n_1')^2] \\
& +4[(\phi_1n_2 - \phi_2m_2 + \phi_9n_1 - \phi_{10}m_1)^2 + (\phi_1m_2 + \phi_2n_2 + \phi_9m_1 + \phi_{10}n_1)^2]
\end{aligned}$$

$$\begin{aligned}
& +4[(\phi_1 n'_2 - \phi_2 m'_2 + \phi_9 n'_1 - \phi_{10} m'_1)^2 + (\phi_1 m'_2 + \phi_2 n'_2 + \phi_9 m'_1 + \phi_{10} n'_1)^2] \\
& +4[(n_2 n'_2 + m_2 m'_2 + n_1 n'_1 + m_1 m'_1)^2 + (n_2 m'_2 - m_2 n'_2 + n_1 m'_1 - m_1 n'_1)^2] \\
& -2(\phi_3^2 + \phi_4^2 + \phi_{11}^2 + \phi_{12}^2)(\phi_1^2 + \phi_2^2 + \phi_9^2 + \phi_{10}^2) \\
& -2(\phi_3^2 + \phi_4^2 + \phi_{11}^2 + \phi_{12}^2)(n_1^2 + n_2^2 + m_1^2 + m_2^2) \\
& -2(\phi_3^2 + \phi_4^2 + \phi_{11}^2 + \phi_{12}^2)(n_1'^2 + n_2'^2 + m_1'^2 + m_2'^2) \\
& -2(\phi_1^2 + \phi_2^2 + \phi_9^2 + \phi_{10}^2)(n_1^2 + n_2^2 + m_1^2 + m_2^2) \\
& -2(\phi_1^2 + \phi_2^2 + \phi_9^2 + \phi_{10}^2)(n_1'^2 + n_2'^2 + m_1'^2 + m_2'^2) \\
& -2(n_1^2 + n_2^2 + m_1^2 + m_2^2)(n_1'^2 + n_2'^2 + m_1'^2 + m_2'^2)\}, \tag{50}
\end{aligned}$$

For $U(1)_Y$:

$$\frac{1}{8} g_Y^2 |\phi_1^2 + \phi_2^2 + \phi_3^2 + \phi_4^2 + \phi_9^2 + \phi_{10}^2 + \phi_{11}^2 + \phi_{12}^2 - \phi_5^2 - \phi_6^2 - \phi_7^2 - \phi_8^2|^2, \tag{51}$$

For $U(1)_{Y'}$:

$$\begin{aligned}
& \frac{1}{72} g_{Y'}^2 | \phi_1^2 + \phi_2^2 + \phi_3^2 + \phi_4^2 + \phi_9^2 + \phi_{10}^2 + \phi_{11}^2 + \phi_{12}^2 + 4(\phi_5^2 + \phi_6^2 + \phi_7^2 + \phi_8^2) \\
& -5(n_1^2 + n_2^2 + m_1^2 + m_2^2 + n_1'^2 + n_2'^2 + m_1'^2 + m_2'^2) |^2, \tag{52}
\end{aligned}$$

$$\begin{aligned}
V_{soft} = & m_{\mathcal{H}}^2 (\phi_1^2 + \phi_2^2 + \phi_3^2 + \phi_4^2 + \phi_9^2 + \phi_{10}^2 + \phi_{11}^2 + \phi_{12}^2) + m_{\mathcal{H}_2}^2 (\phi_5^2 + \phi_6^2 + \phi_7^2 + \phi_8^2) \\
& + m_{\mathcal{N}}^2 (n_1^2 + n_2^2 + m_1^2 + m_2^2) + m_{\mathcal{N}'}^2 (n_1'^2 + n_2'^2 + m_1'^2 + m_2'^2) \\
& + 2\lambda A (\phi_2 \phi_5 m_1 - \phi_1 \phi_6 m_1 + \phi_1 \phi_5 n_1 + \phi_2 \phi_6 n_1) \\
& + 2\lambda A (\phi_6 \phi_9 m_2 - \phi_5 \phi_{10} m_2 - \phi_5 \phi_9 n_2 - \phi_6 \phi_{10} n_2) \\
& + 2\lambda A (\phi_3 \phi_7 n_1 + \phi_4 \phi_8 n_1 + \phi_4 \phi_7 m_1 - \phi_3 \phi_8 m_1) \\
& + 2\lambda A (\phi_8 \phi_{11} m_2 - \phi_7 \phi_{12} m_2 - \phi_7 \phi_{11} n_2 - \phi_8 \phi_{12} n_2) \\
& + 2\lambda' A' (\phi_2 \phi_5 m_1' - \phi_1 \phi_6 m_1' + \phi_1 \phi_5 n_1' + \phi_2 \phi_6 n_1') \\
& + 2\lambda' A' (\phi_6 \phi_9 m_2' - \phi_5 \phi_{10} m_2' - \phi_5 \phi_9 n_2' - \phi_6 \phi_{10} n_2')
\end{aligned}$$

$$\begin{aligned}
& +2\lambda' A'(\phi_3\phi_7n'_1 + \phi_4\phi_8n'_1 + \phi_4\phi_7m'_1 - \phi_3\phi_8m'_1) \\
& +2\lambda' A'(\phi_8\phi_{11}m'_2 - \phi_7\phi_{12}m'_2 - \phi_7\phi_{11}n'_2 - \phi_8\phi_{12}n'_2) \\
& -2m_3^2(n_1n'_1 + m_1m'_1 + n_2n'_2 + m_2m'_2). \tag{53}
\end{aligned}$$

The vacuum minimum conditions are

$$\begin{aligned}
& (\lambda n_1 + \lambda' n'_1)^2 v_1 - (\lambda n_1 + \lambda' n'_1)(\lambda n_2 + \lambda' n'_2) v_3 + (\lambda^2 + \lambda'^2) v_1 v_2^2 + \frac{1}{4} g_L^2 (v_1^2 + v_3^2 - v_2^2) v_1 \\
& + \frac{1}{4} g_I^2 \{v_1(v_1^2 + v_3^2) + 2(v_1 n_2 + v_3 n_1) n_2 + 2(v_1 n'_2 + v_3 n'_1) n'_2 - v_1(n_1^2 + n_2^2 + n_1'^2 + n_2'^2)\} \\
& + \frac{1}{4} g_Y^2 (v_1^2 + v_3^2 - v_2^2) v_1 + \frac{1}{36} g_{Y'} (v_1^2 + v_3^2 + 4v_2^2 - 5n_1^2 - 5n_2^2 - 5n_1'^2 - n_2'^2) v_1 \\
& + m_{H_1}^2 v_1 + \lambda A v_2 n_1 + \lambda' A' v_2 n'_1 = 0, \tag{54}
\end{aligned}$$

$$\begin{aligned}
& (\lambda n_1 + \lambda' n'_1)^2 v_2 + (\lambda n_2 + \lambda' n'_2)^2 v_2 + (\lambda^2 + \lambda'^2) v_2 (v_1^2 + v_3^2) \\
& - \frac{1}{4} g_L^2 (v_1^2 + v_3^2 - v_2^2) v_2 - \frac{1}{4} g_Y^2 (v_1^2 + v_3^2 - v_2^2) v_2 \\
& + \frac{1}{9} g_{Y'} (v_1^2 + v_3^2 + 4v_2^2 - 5n_1^2 - 5n_2^2 - 5n_1'^2 - n_2'^2) v_2 \\
& + m_{H_2}^2 v_2 + \lambda A (v_1 n_1 - v_3 n_2) + \lambda' A' (v_1 n'_1 - v_3 n'_2) = 0, \tag{55}
\end{aligned}$$

$$\begin{aligned}
& (\lambda n_2 + \lambda' n'_2)^2 v_3 - (\lambda n_1 + \lambda' n'_1)(\lambda n_2 + \lambda' n'_2) v_1 + (\lambda^2 + \lambda'^2) v_3 v_2^2 + \frac{1}{4} g_L^2 (v_1^2 + v_3^2 - v_2^2) v_3 \\
& + \frac{1}{4} g_I^2 \{v_3(v_1^2 + v_3^2) + 2(v_1 n_2 + v_3 n_1) n_1 + 2(v_1 n'_2 + v_3 n'_1) n'_1 - v_3(n_1^2 + n_2^2 + n_1'^2 + n_2'^2)\} \\
& + \frac{1}{4} g_Y^2 (v_1^2 + v_3^2 - v_2^2) v_3 + \frac{1}{36} g_{Y'} (v_1^2 + v_3^2 + 4v_2^2 - 5n_1^2 - 5n_2^2 - 5n_1'^2 - n_2'^2) v_3 \\
& + m_{H_3}^2 v_3 + \lambda A v_2 n_2 + \lambda' A' v_2 n'_2 = 0, \tag{56}
\end{aligned}$$

$$\begin{aligned}
& \lambda v_3 [(\lambda n_2 + \lambda' n'_2) v_3 - (\lambda n_1 + \lambda' n'_1) v_1] + \lambda v_2^2 (\lambda n_2 + \lambda' n'_2) \\
& + \frac{1}{4} g_I^2 \{n_2(n_1^2 + n_2^2) + 2(v_1 n_2 + v_3 n_1) v_1 + 2(n_2 n'_2 + n_1 n'_1) n'_2 - n_2(v_1^2 + v_3^2 + n_1'^2 + n_2'^2)\} \\
& - \frac{5}{36} g_{Y'} (v_1^2 + v_3^2 + 4v_2^2 - 5n_1^2 - 5n_2^2 - 5n_1'^2 - n_2'^2) n_2
\end{aligned}$$

$$+m_N^2 n_2 + \lambda A v_2 v_3 - m_3^2 n_2' = 0, \quad (57)$$

$$\begin{aligned} & \lambda v_1 [(\lambda n_1 + \lambda' n_1') v_1 - (\lambda n_2 + \lambda' n_2') v_3] + \lambda v_2^2 (\lambda n_1 + \lambda' n_1') \\ & + \frac{1}{4} g_I^2 \{ n_1 (n_1^2 + n_2^2) + 2(v_1 n_2 + v_3 n_1) v_3 + 2(n_2 n_2' + n_1 n_1') n_1' - n_1 (v_1^2 + v_3^2 + n_1'^2 + n_2'^2) \} \\ & - \frac{5}{36} g_{Y'} (v_1^2 + v_3^2 + 4v_2^2 - 5n_1^2 - 5n_2^2 - 5n_1'^2 - n_2'^2) n_1 \\ & + m_N^2 n_1 + \lambda A v_1 v_2 - m_3^2 n_1' = 0, \end{aligned} \quad (58)$$

$$\begin{aligned} & \lambda' v_3 [(\lambda n_2 + \lambda' n_2') v_3 - (\lambda n_1 + \lambda' n_1') v_1] + \lambda' v_2^2 (\lambda n_2 + \lambda' n_2') \\ & + \frac{1}{4} g_I^2 \{ n_2' (n_1'^2 + n_2'^2) + 2(v_1 n_2' + v_3 n_1') v_1 + 2(n_2 n_2' + n_1 n_1') n_2 - n_2' (v_1^2 + v_3^2 + n_1^2 + n_2 r) \} \\ & - \frac{5}{36} g_{Y'} (v_1^2 + v_3^2 + 4v_2^2 - 5n_1^2 - 5n_2^2 - 5n_1'^2 - n_2'^2) n_2' \\ & + m_N^2 n_2' - \lambda' A' v_2 v_3 - m_3^2 n_2 = 0, \end{aligned} \quad (59)$$

$$\begin{aligned} & \lambda' v_1 [(\lambda n_1 + \lambda' n_1') v_1 - (\lambda n_2 + \lambda' n_2') v_3] + \lambda' v_2^2 (\lambda n_1 + \lambda' n_1') \\ & + \frac{1}{4} g_I^2 \{ n_1' (n_1'^2 + n_2'^2) + 2(v_1 n_2' + v_3 n_1') v_3 + 2(n_2 n_2' + n_1 n_1') n_1 - n_1' (v_1^2 + v_3^2 + n_1^2 + n_2 r) \} \\ & - \frac{5}{36} g_{Y'} (v_1^2 + v_3^2 + 4v_2^2 - 5n_1^2 - 5n_2^2 - 5n_1'^2 - n_2'^2) n_1' \\ & + m_N^2 n_1' - \lambda' A' v_1 v_2 - m_3^2 n_1 = 0. \end{aligned} \quad (60)$$

The complete potential has nine parameters: λ , λ' , the coefficients of the two trilinear terms A and A' , the four mass-squared parameters $m_{\mathcal{H}}^2$, $m_{H_2}^2$, m_N^2 and $m_{N'}^2$, and m_3^2 . Six of them can be transferred to vacuum expectation values, thus three undetermined parameters remain, which we take to be λ , λ' and m_3^2 .

It is straightforward but tedious to work out the mass-squared matrices for various Higgs bosons, which are given in the appendices. The mass-squared matrices for the neutral scalars and pseudoscalars are 7×7 matrices. The former must have one zero eigenvalue

and the latter must have four zero eigenvalues, corresponding to the five Goldstone bosons eaten by the five massive neutral vector gauge bosons [the zero eigenvalue of the scalar mass-squared matrix corresponds to the freedom to perform an $SU(2)_I$ rotation in order to set one of neutral vacuum expectation values to zero]. The mass-squared matrices for charged Higgs scalars turn out to be 3×3 matrices. The positive states and negative states decouple, and they share the same mass squared matrix. There should have one zero eigenvalue for each of them in order to produce masses for the two charged vector bosons of $SU(2)_L$. As we must resort to numerical techniques to find the eigenvalues of the Higgs bosons, the presence of the required number of zero eigenvalues provides an excellent check on our numerical calculation. As another check, we found that there exists a relationship

$$\text{Tr}M_\phi^2 = \text{Tr}M_Z^2 + \text{Tr}M_{H_3^0}^2 \quad (61)$$

where M_Z^2 is the neutral-vector mass squared matrix, M_ϕ^2 is the neutral-scalar mass squared matrix, and $M_{H_3^0}^2$ represents the pseudoscalar mass-squared matrix. This is a very general relation. It holds in any supersymmetric model based on an extended gauge group in which there are no gauge-singlet fields. Interestingly, in this model, the trace of the neutral-vector mass-squared matrix must include the W_I fields, which are the neutral nondiagonal bosons of the $SU(2)_I$ group.

We choose λ and λ' to be up to 1 and m_3 to be up to 1000 GeV. If the value of λ or λ' is too large, it will blow up at the unification scale. We don't consider the radiative corrections in our numerical analysis. For every set of values λ , λ' and m_3^2 , we search numerically for the minimum of the scalar potential. Adjusting the various vacuum expectation values until the eigenvalues of the Higgs-boson mass matrices are positive or zero, we read off the value of the smallest nonzero eigenvalue of the neutral scalar mass-squared matrix. Then we vary the values of λ , λ' and m_3^2 to find the largest

possible value of this smallest nonzero eigenvalue. We find that its value is about 150 GeV, It therefore means that in this model there must have a Higgs scalar lighter than 150 GeV.

The current limits on the SM Higgs boson and Higgs bosons in the general two-Higgs doublet models have been discussed in the previous sections. The minimal supersymmetric Standard Model (MSSM) is an example of a 2HDM. Higgs bosons in the MSSM have also been discussed widely in the literature. The current 95% CL bounds are $m_{h^0} > 84.3$ GeV and $m_{A^0} > 84.5$ GeV [31], which is below the bound we get here.

In conclusion we found an upper mass bound of about 150 GeV for the lightest neutral scalar Higgs boson in the $SU(2)_L \times SU(2)_I \times U(1)_Y \times U(1)_{Y'}$ model, which is based on the E_6 grand unification theory. It is found that our upper mass bound is greater than all experimental results available now. Therefore it is too early to make a final judgment about the model at this point.

Chapter 3 Gauge boson sector

3.1 Introduction

A gauge field theory based on a local symmetry G is a field theory with the symmetry currents coupled minimally to the vector-boson fields (called gauge bosons). The space integrals of the time components of the symmetry currents define formally the generators of the gauge group G . The number of gauge bosons is equal to the number of the generators of the gauge group G . The self-interactions of gauge bosons and their couplings to matter are completely determined by the gauge symmetry. Gauge symmetry also forbids the presence of mass terms for gauge bosons in the Lagrangian. Fortunately, gauge bosons can gain masses through spontaneous symmetry breaking, which doesn't break the gauge invariance of the Lagrangian. But mixings among gauge bosons generally appear when they form the physical massive states in extensions of the SM, even in the SM. These mixings can be constrained by experiments.

In many extensions of the SM, such as grand unification theories and left-right symmetric models, there are additional gauge bosons. Mixings between the W or Z boson and these additional gauge bosons naturally appear in these extensions. Generally the masses of extra gauge bosons remain unpredicted and may or may not be of the order of the electroweak scale. The closeness of the observed W and Z boson properties with the predictions of the SM does not yield any direct information about the masses of extra gauge bosons, but seems to imply that the mixings of W or Z with extra gauge bosons should be very small.

An old direct search¹ for new neutral gauge bosons were performed by UA1 and UA2 [54, 55]. Analysis from Barger *et al.* [56] and Ellis *et al.* [57] gave then lower mass

¹Direct searches have also been done for light neutral gauge bosons, but it will not be discussed here.

limit on the new neutral gauge boson to be in the range of 100-200 GeV. It should be pointed out that the bounds were very model dependent. In Ref. [58], a direct search for extra gauge bosons was reported and lower mass limits of approximately 500 ~ 700 GeV were set, depending on the Z' couplings. The discovery potential and diagnostic abilities of proposed future colliders for new neutral or charged gauge bosons were summarized in Ref. [59]. Even though there is as yet no direct experimental evidence of extra gauge bosons, stringent indirect constraints can be put on the mixings and the masses of extra gauge bosons by electroweak precision data. In Ref. [60-63], such constraints were derived in the $SU(2)_L \times U(1)_Y \times U(1)_{Y'}$ model. The lower mass limits are generally several hundreds of GeV and are competitive with experimental bounds from direct searches. A good summary of Z' searches can be found in Ref. [64] and references therein.

Compared with the $SU(2)_L \times U(1)_Y \times U(1)_{Y'}$ model, there are several extra neutral gauge bosons in our model. Generally they will mix with each other and also with the ordinary Z boson. Electroweak experiments for Z-pole measurements, m_W measurement and low-energy neutral current (LENC) experiments are used to put indirect constraints on the masses of the extra neutral gauge bosons and the mixings. We also consider the possible constraint arising from a proposed measurement at Jefferson Lab of the proton's weak charge. In the following, it is assumed that none of all the superpartners of the SM particles and the exotic particles affect the radiative corrections to the electroweak observables significantly, *i.e.*, they are supposed to be heavy enough to decouple from the weak boson mass scale.

In this chapter, after a brief review of the gauge boson sector of the SM, we will study a special feature of the $SU(2)_L \times U(1)_Y \times SU(2)_I \times U(1)_{Y'}$ model: the neutral gauge boson W_I . Its production and effects in various processes will be reviewed, with special attention being paid to its contribution to $(g-2)_\mu$. Then the full mass-squared matrix of neutral gauge bosons and mixings will be discussed. The phenomenology of the mixings

will also be explored. Both the effects of the mixings and the direct contributions due to exchanges of extra neutral gauge bosons are included. Constraints on the masses and mixings will be found.

3.2 Gauge bosons in the SM

We have introduced gauge bosons and spontaneous symmetry breaking in the SM in the first and second Chapter. The relevant terms to give masses to gauge bosons are

$$\frac{1}{2} \begin{pmatrix} 0 & v \end{pmatrix} \left(g_L W_\mu^a \tau^a + \frac{1}{2} g_Y B_\mu \right) \left(g_L W_\mu^b \tau^b + \frac{1}{2} g_Y B_\mu \right) \begin{pmatrix} 0 \\ v \end{pmatrix}, \quad (62)$$

It is easy to find the three massive vector bosons noted as below

$$\begin{aligned} W^\pm &= \frac{1}{\sqrt{2}}(W^1 \mp iW^2), & m_W &= g_L \frac{v}{2}; \\ Z &= \frac{1}{\sqrt{g_L^2 + g_Y^2}}(g_L W^3 - g_Y B), & m_Z &= \sqrt{g_L^2 + g_Y^2} \frac{v}{2}. \end{aligned} \quad (63)$$

The fourth vector field, identified as the photon, which is orthogonal to Z , remains massless,

$$A = \frac{1}{\sqrt{g_L^2 + g_Y^2}}(g_Y W^3 + g_L B) \quad (64)$$

If we define the weak mixing angle as

$$\cos \theta_W = \frac{g_L}{\sqrt{g_L^2 + g_Y^2}}, \quad \sin \theta_W = \frac{g_Y}{\sqrt{g_L^2 + g_Y^2}}, \quad (65)$$

We can write the mixing in an elegant form

$$\begin{pmatrix} Z \\ A \end{pmatrix} = \begin{pmatrix} \cos \theta_W & -\sin \theta_W \\ \sin \theta_W & \cos \theta_W \end{pmatrix} \begin{pmatrix} W^3 \\ B \end{pmatrix}. \quad (66)$$

Here we see that there is mixing among gauge bosons even in the SM. The best fit value of the electroweak mixing angle is $\sin^2 \theta_W = 0.23117 \pm 0.00016$ [31].

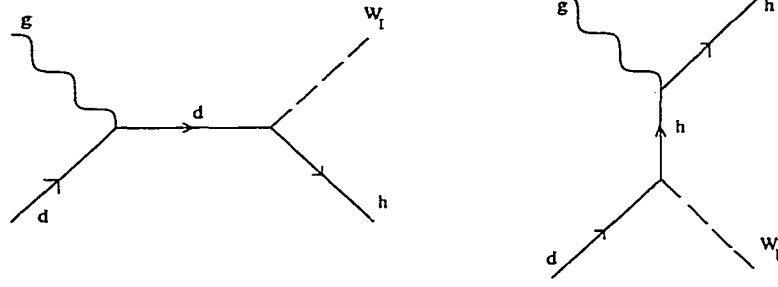


Figure 11: Parton-level process responsible for $p\bar{p} \rightarrow W_T + h + X$

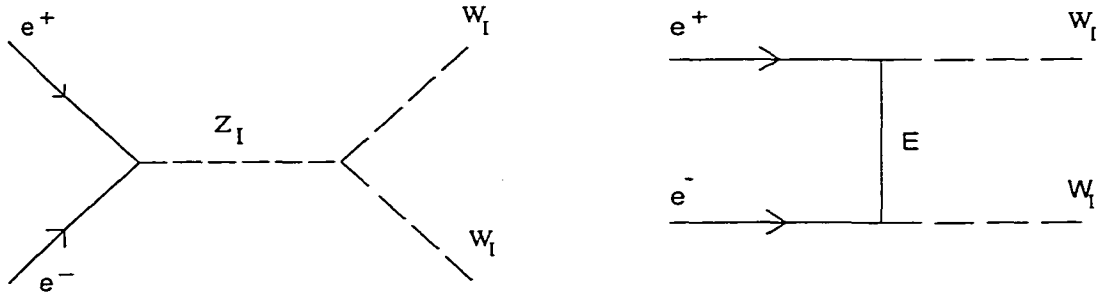


Figure 12: Feynman diagram responsible for $e^+e^- \rightarrow W_T W_T^\dagger$

3.3 W_T boson

3.3.1 Production of W_T boson

Theoretical studies of production of neutral W 's in hadron-hadron, positron-electron, electron-proton colliders were carried out in Ref. [25, 26], later Ref. [65] also considered the production of W_T at LHC and SSC.

At a hadron collider, single W_T production can proceed via associated production $g + d \rightarrow h + W_T$ (see Fig. 11).

At an e^+e^- collider, pair production of W_T can occur via s-channel Z_T exchange as well as t-channel E-lepton exchange (see Fig. 12). Single production can also proceed through $e^+e^- \rightarrow W_T E^- e^+ (W_T E^+ e^-)$ (see Fig. 13).

In ep collisions, W_T exchange in the t-channel can produce exotic fermions via the sub-process $ed \rightarrow Eh$ with a very clean signature (see Fig. 14), but the cross section for such a process is not large because the two exotic particles are heavy.

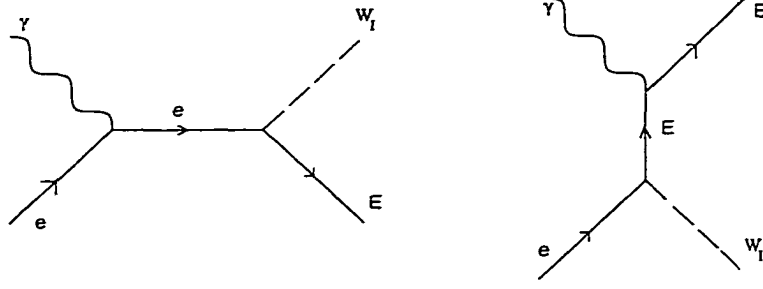


Figure 13: Diagrams for the process $\gamma e \rightarrow W_I E$

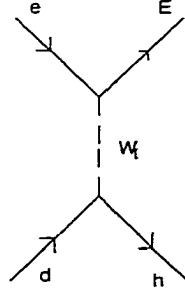


Figure 14: Diagrams for the process $ed \rightarrow Eh$

3.3.2 Effect of W_I

W_I can participate in the production of exotic particles (t-channel pair production of heavy charged leptons will be discussed in the next chapter) and rare processes, especially flavor-changing neutral currents, for instance, $K^0 - \bar{K}^0$ mixing and $\mu \rightarrow e\gamma$ (see Fig. 15, 16 and 17). Mixings between generations are usually needed in these cases. This was considered in Ref. [66].

Because of the high precision of the measurement of the AMMM, it has played a great role in precision tests of the SM and probing new physics such as supersymmetry and lepton substructure. Here we will consider the contribution of W_I to the AMMM and a bound on the mass of W_I bosons will be obtained.

The relevant terms in the Lagrangian are

$$\mathcal{L} = e\bar{\mu}\gamma^\mu\mu A_\mu + e\bar{M}\gamma^\mu M A_\mu + \frac{g_I}{4}\bar{\mu}\gamma^\mu(1 - \gamma_5)MW_{I\mu} + \text{H.c.} \quad (67)$$

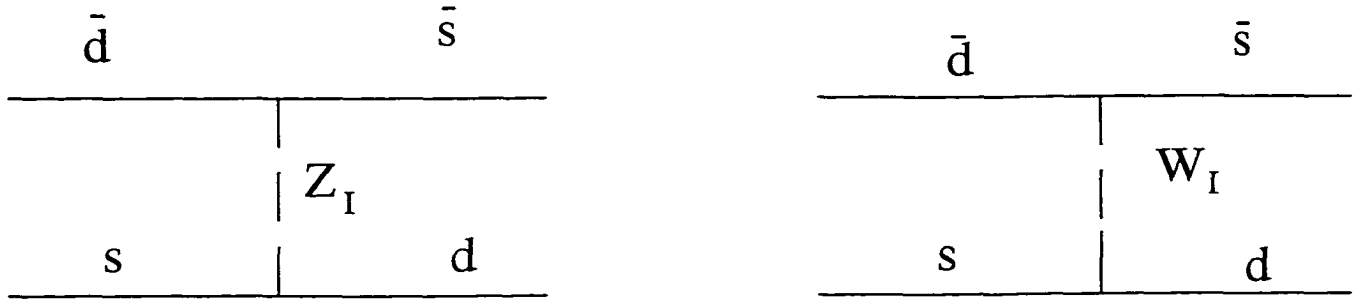


Figure 15: Tree-level flavor-changing neutral current processes present if all six quarks d, s, b and $h_i(i=1,2,3)$ mix with each other



Figure 16: Box diagrams contributing to $\bar{d}s \rightarrow \bar{s}d$ mixing

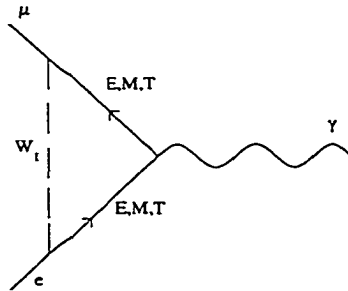


Figure 17: Loop diagrams involving exotic fermions and W_I contributing to $\mu \rightarrow e\gamma$

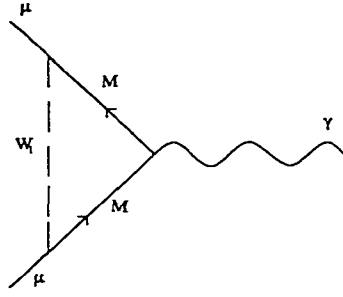


Figure 18: Contribution to the anomalous magnetic moment of the muon from the exchange of W_I

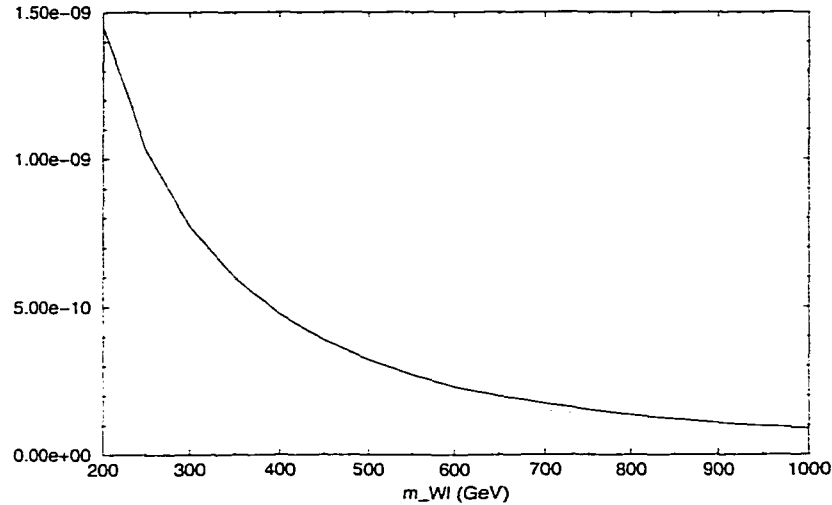


Figure 19: The contribution of the diagram of Fig. 18 to the anomalous magnetic moment of the muon, assuming that $m_M = 100$ GeV (solid line) and 200 GeV (dotted line)

The Feynman diagram is given in Fig. 18. The calculation is straightforward, and we find that the contribution to $a_\mu \equiv \frac{g_\mu - 2}{2}$ is given by

$$a_\mu = -\frac{g_I^2}{8\pi^2} \int_0^1 \frac{z(1-z^2)}{z(z-1) + z\frac{m_{W_I}^2}{m_\mu^2} + (1-z)\frac{m_M^2}{m_\mu^2}} dz \quad (68)$$

where m_{W_I} and m_M are the masses of the W_I boson and the M-lepton, the second generation exotic lepton corresponding to the muon. The result is given in Fig. 19.

Consider the case in which the mass of the exotic heavy lepton $m_M = 200$ GeV and $m_{W_I} = 650$ GeV. We see that this gives a value of a_μ which is $1.7 \times 10^{-10} g_I^2$. If we take $g_I = g_L$, it is about 0.7×10^{-10} . This is much less than the current experimental limit

from the AMMM.

In the absence of any solid theoretical understandings of masses of exotic fermion and extra neutral gauge bosons, one must rely on experiments to provide bounds on such parameters. It is found that the constraint from AMMM is very weak. Stronger constraints can be obtained by electroweak precision data in the following.

3.4 Extra neutral gauge bosons and mixings

The first part of the Lagrangian concerns itself with the gauge fields. It contains the kinetic and self-interaction terms for the vector fields

$$\mathcal{L}_{gauge} = -\frac{1}{4}W_{\mu\nu}^{La}W^{La\mu\nu} - \frac{1}{4}W_{\mu\nu}^{Ia}W^{Ia\mu\nu} - \frac{1}{4}A_{\mu\nu}A^{\mu\nu} - \frac{1}{4}B_{\mu\nu}B^{\mu\nu}$$

where

$$W_{\mu\nu}^{La} = \partial_\mu W_\nu^{La} - \partial_\nu W_\mu^{La} - g_L f_L^{abc} W_\mu^{Lb} W_\nu^{Lc}$$

with $[T_L^a, T_L^b] = i\varepsilon^{abc}T_L^c$, $T_L^a = \frac{\sigma^a}{2}$, where σ^a are Pauli matrices and $f_L^{abc} = \varepsilon^{abc}$.

$$W_{\mu\nu}^{Ia} = \partial_\mu W_\nu^{Ia} - \partial_\nu W_\mu^{Ia} - g_I f_I^{abc} W_\mu^{Ib} W_\nu^{Ic}$$

with $[T_I^a, T_I^b] = i\varepsilon^{abc}T_I^c$, $T_I^a = \frac{\tau^a}{2}$, where τ^a are also Pauli matrices and $f_I^{abc} = \varepsilon^{abc}$, and

where

$$A_{\mu\nu} = \partial_\mu A_\nu - \partial_\nu A_\mu,$$

$$B_{\mu\nu} = \partial_\mu B_\nu - \partial_\nu B_\mu.$$

The relevant part of the Lagrangian which gives masses for gauge bosons after the spontaneous symmetry breaking is

$$\begin{aligned} \sim & \left| \left(-\frac{i}{2}g_L \vec{\sigma} \cdot W_\mu^L - \frac{i}{2}g_Y(+1)A_\mu - \frac{i}{2}g_{Y'}\left(-\frac{4}{3}\right)B_\mu \right) H_2 \right|^2 \\ & + \left| \left(-\frac{i}{2}g_I \vec{\tau} \cdot W_\mu^I - \frac{i}{2}g_{Y'}\left(\frac{5}{3}\right)B_\mu \right) N \right|^2 \end{aligned}$$

$$\begin{aligned}
& + \left| \left(-\frac{i}{2} g_I \vec{\tau} \cdot W_\mu^I - \frac{i}{2} g_{Y'} \left(\frac{5}{3} \right) B_\mu \right) N' \right|^2 \\
& + \left| \left(-\frac{i}{2} g_L \vec{\sigma} \cdot W_\mu^L - \frac{i}{2} g_Y (-1) A_\mu - \frac{i}{2} g_{Y'} \left(-\frac{1}{3} \right) B_\mu \right) \mathcal{H} - \frac{i}{2} \mathcal{H} \vec{\tau} \cdot \vec{W}_\mu^I \right|^2. \quad (69)
\end{aligned}$$

It is easy to find that there are mixings among various gauge fields in order to get physical mass eigenstates. Before we discuss the gauge boson mixings in our specific model in detail, we will first discuss the mixings among gauge bosons in the general case.

In Ref. [67], bounds on mixings between light and heavy gauge bosons were considered. For simplicity, first consider the case of two gauge bosons Z and Z' . Assume that in the absence of the mixing the masses would be m_Z and $m'_{Z'} \geq m_Z$ respectively. Including mixing, the Hermitian mass-squared matrix becomes

$$\mathcal{M}^2 = \begin{pmatrix} m_Z^2 & m_{ZZ'}^2 \\ m_{ZZ'}^2 & m_{Z'}^2 \end{pmatrix}, \quad (70)$$

where $m_{ZZ'}^2$ is an arbitrary mixing term, which can be chosen to be real for neutral gauge bosons. It is well-known that the physical states are

$$\begin{aligned}
Z_1 &= Z \cos \theta + Z' \sin \theta, \\
Z_2 &= -Z \sin \theta + Z' \cos \theta
\end{aligned} \quad (71)$$

with physical masses

$$\begin{aligned}
m_{Z_1}^2 &= m_Z^2 \cos^2 \theta + m_{Z'}^2 \sin^2 \theta + 2m_{ZZ'}^2 \sin \theta \cos \theta, \\
m_{Z_2}^2 &= m_Z^2 \sin^2 \theta + m_{Z'}^2 \cos^2 \theta - 2m_{ZZ'}^2 \sin \theta \cos \theta
\end{aligned} \quad (72)$$

and the mixing angle θ is given

$$\tan 2\theta = \frac{-2m_{ZZ'}^2}{m_{Z'}^2 - m_Z^2}, \quad (73)$$

or written in terms of physical observables $m_{Z_1}^2$ and $m_{Z_2}^2$ as

$$\tan^2 \theta = \frac{m_Z^2 - m_{Z_1}^2}{m_{Z_2}^2 - m_Z^2}. \quad (74)$$

Since $\tan^2 \theta$ cannot be negative, the mixing always lowers the mass of the ordinary Z boson. The lighter mass state, Z_1 , should be identified with the observed Z in experiments at LEP or SLC. The observed value is very close to the value predicted by the $SU(2)_L \times U(1)_Y$ model. This means that the mixing angle should be very small, or the mass of the extra gauge boson should be very large (e.g. $M_{Z_2} \sim 1$ TeV). In Ref. [62, 69] Z - Z' mixing was considered with a mixing term in the kinetic terms [70] between the Z' and the hypercharge gauge boson in $SU(2)_L \times U(1)_Y \times U(1)_{Y'}$ model. The phenomenology of gauge kinetic mixing has been reviewed in Ref. [71]. In our model and analysis zero kinetic mixing at the electroweak scale will be assumed.

In many extensions of the SM, there are several $U(1)$ factors. Another simple case is the mixing between two extra Z bosons. The Z' - Z'' mixing is generally discussed in the basis of $U(1)_\psi$ and $U(1)_\chi$ in E_6 models. The mass eigenstates are defined to be Z' and Z'' given by

$$\begin{aligned} Z'(\theta) &\equiv Z_\psi \cos \theta - Z_\chi \sin \theta, \\ Z''(\theta) &\equiv Z_\chi \cos \theta + Z_\psi \sin \theta. \end{aligned} \tag{75}$$

It is found that the Z_η , the extra $U(1)$ factor in rank-5 model described in the first part of this thesis, is just a special case of $Z'(\theta)$ with $\theta = \sin^{-1} \sqrt{3/8}$, and the Z_I is also a special case corresponding to $\theta = -\sin^{-1} \sqrt{5/8}$. It is interesting that Z_η is orthogonal to Z_I . It is generally assumed that $Z''(\theta)$ is too heavy to mix with the SM Z . Then there is only one extra neutral gauge boson in the model which could have effects on the electroweak section. The $Z_{\psi,\chi,\eta,I}$ models are the ones most frequently discussed as being representatives of those which can arise from the E_6 models. In Ref. [68] the phenomenology of the E_6 electroweak model with two extra Z bosons was discussed. Mixings of the full three neutral gauge bosons were considered there in several limiting cases.

Now consider the case of n charged or neutral gauge bosons B_i^0 (the notation of Ref. [67] will be used.), with an $n \times n$ Hermitian mass-squared matrix

$$\mathcal{M}^2 = \begin{pmatrix} m_0^2 & b_2 & b_3 & \cdots & b_n \\ b_2^* & & & & \\ \vdots & & \mathcal{M}_H^2 & & \\ b_n^* & & & & \end{pmatrix}, \quad (76)$$

where m_0 is m_{W_0} or m_{Z_0} , \mathcal{M}_H^2 is the $(n-1) \times (n-1)$ mass-squared matrix for the $n-1$ heavy bosons, and b_i , $i = 2, \dots, n$ are arbitrary mixing parameters. Assume \mathcal{M}_H^2 is diagonal with elements $a_2 < a_3 < \dots < a_n$. The physical states are

$$B_i = \sum_{j=1}^n (u_i)_j^* B_j^0, \quad (77)$$

where u_i is the i -th normalized eigenvector of \mathcal{M}^2 with eigenvalues m_i^2 , $i = 1, \dots, n$. The major results of Ref. [67] are

$$\frac{|(u_1)_i|}{|(u_1)_1|} \leq \left(\frac{m_0^2 - m_1^2}{m_i^2 - m_0^2} \right)^{1/2}, \quad i = 2, \dots, n \quad (78)$$

and

$$|(u_i)_1| < \left(\frac{m_0^2 - m_1^2}{m_i^2 - m_0^2} \right)^{1/2}, \quad i = 2, \dots, n. \quad (79)$$

The proof can be found in Ref. [67]. Therefore if the mixings are very small, we can take $\left(\frac{m_0^2 - m_1^2}{m_i^2 - m_0^2} \right)^{1/2}$ as the upper bounds of mixing angles between B_1^0 and B_i^0 , $i = 2, \dots, n$. We will use these results in our analysis and calculate the upper bounds of mixings between the ordinary Z and extra neutral gauge bosons in the following.

In the $SU(2)_L \times U(1)_Y \times SU(2)_I \times U(1)_{Y'}$ model, the neutral gauge fields include the ordinary Z coming from the $SU(2)_L \times U(1)_Y$, W_I^1 , W_I^2 and W_I^3 for the $SU(2)_I$ group and B for $U(1)_{Y'}$ (we will use linear combinations $W_I^\pm = (W_I^1 \mp iW_I^2)/\sqrt{2}$ instead of W_I^1 and W_I^2 , here \pm is just a convention, as they are neutral). After the spontaneous symmetry breaking mechanism described in the previous section, the mass-squared matrix for the

neutral gauge bosons generally has the form

$$\frac{1}{2}V^T \mathcal{M}^2 V \quad (80)$$

where $V^T = (Z, W_I^3, B, W_I^+, W_I^-)$. The matrix \mathcal{M}^2 is a symmetric 5×5 matrix

$$\mathcal{M}^2 = \begin{pmatrix} m_Z^2 & m_{12} & m_{13} & m_{14} & m_{15} \\ m_{12} & m_{W_I^3}^2 & m_{23} & m_{24} & m_{25} \\ m_{13} & m_{23} & m_B^2 & m_{34} & m_{35} \\ m_{14} & m_{24} & m_{34} & 0 & m_{W_I^\pm}^2 \\ m_{15} & m_{25} & m_{35} & m_{W_I^\pm}^2 & 0 \end{pmatrix} \quad (81)$$

The specific expressions for the matrix elements in our model are

$$\begin{aligned} m_Z^2 &= \frac{1}{4}(g_L^2 + g_Y^2)(v_1^2 + v_2^2 + v_3^2) \\ m_{12} &= \frac{1}{4}\sqrt{g_L^2 + g_Y^2}g_I(v_1^2 - v_3^2) \\ m_{13} &= \frac{1}{12}\sqrt{g_L^2 + g_Y^2}g_{Y'}(-v_1^2 + 4v_2^2 - v_3^2) \\ m_{14} &= m_{15} = \frac{1}{4}\sqrt{g_L^2 + g_Y^2}g_I v_1 v_3 \\ m_{W_I^3}^2 &= \frac{1}{4}g_I^2(v_1^2 + v_3^2 + n_1^2 + n_2^2 + n_1'^2 + n_2'^2) \\ m_{23} &= \frac{1}{12}g_I g_{Y'}[-v_1^2 + v_3^2 - 5(n_1^2 - n_2^2 + n_1'^2 - n_2'^2)] \\ m_{24} &= m_{25} = 0 \\ m_B^2 &= \frac{1}{36}g_{Y'}^2[v_1^2 + 16v_2^2 + v_3^2 + 25(n_1^2 + n_2^2 + n_1'^2 + n_2'^2)] \\ m_{34} &= m_{35} = \frac{1}{12\sqrt{2}}g_I g_{Y'}[-v_1 v_3 + 5(n_1 n_2 + n_1' n_2')] \\ m_{W_I^\pm}^2 &= \frac{1}{4}g_I^2(v_1^2 + v_3^2 + n_1^2 + n_2^2 + n_1'^2 + n_2'^2) \end{aligned} \quad (82)$$

where $v_1, v_2, v_3, n_1, n_2, n_1'$ and n_2' are vacuum expectation values for Higgs fields introduced in our model. It should be pointed out that $m_{W^\pm}^2 = \frac{1}{4}g_L^2(v_1^2 + v_2^2 + v_3^2)$, so the relationship $m_W = m_Z \cos \theta_W$ still holds. It is apparent that there are mixings among the neutral gauge bosons. Before we go further to diagonalize the matrix to get the mass

eigenstates, we will consider a limiting case in order that we have some confidence that the mass-squared matrix makes sense physically.

It is noted that the elements in the first row and column are independent of the vacuum expectation values n_i and n'_i ($i=1,2$). Therefore when they are very large, the mixing should be small. In this decoupling limit, the only observable neutral gauge boson is the ordinary Z and its mass is the exact value measured experimentally. The extra neutral gauge bosons are not accessible experimentally at least in the facilities available currently or in the near future. To see how this limiting case happens, assume that $n_i = c_i M$, $n'_i = c'_i M$, where c_i and c'_i are order of 1 and M represents a large mass scale. Thus $1/M$ is small and it can be treated as a perturbation parameter. We write the mass-squared matrix in the form

$$\mathcal{M}^2 = M^2 \begin{pmatrix} m_Z^2/M^2 & m'_{12} & m'_{13} & m'_{14} & m'_{15} \\ m'_{12} & m_{W_3}^{\prime 2} & m'_{23} & m'_{24} & m'_{25} \\ m'_{13} & m'_{23} & m_B^{\prime 2} & m'_{34} & m'_{35} \\ m'_{14} & m'_{24} & m'_{34} & 0 & m_{W_I^\pm}^{\prime 2} \\ m'_{15} & m'_{25} & m'_{35} & m_{W_I^\pm}^{\prime 2} & 0 \end{pmatrix}, \quad (83)$$

where the prime on the elements means the factor of M^2 has been pulled out. It can be split into two parts

$$\mathcal{M}^2 = \mathcal{M}_0^2 + \mathcal{M}_I^2 \quad (84)$$

where

$$\mathcal{M}_0^2 = M^2 \begin{pmatrix} 0 & 0 & 0 & 0 & 0 \\ 0 & m_{W_3}^{\prime 2} & m'_{23} & m'_{24} & m'_{25} \\ 0 & m'_{23} & m_B^{\prime 2} & m'_{34} & m'_{35} \\ 0 & m'_{24} & m'_{34} & 0 & m_{W_I^\pm}^{\prime 2} \\ 0 & m'_{25} & m'_{35} & m_{W_I^\pm}^{\prime 2} & 0 \end{pmatrix} \quad (85)$$

and

$$\mathcal{M}_I^2 = M^2 \begin{pmatrix} m_Z^2/M^2 & m'_{12} & m'_{13} & m'_{14} & m'_{15} \\ m'_{12} & 0 & 0 & 0 & 0 \\ m'_{13} & 0 & 0 & 0 & 0 \\ m'_{14} & 0 & 0 & 0 & 0 \\ m'_{15} & 0 & 0 & 0 & 0 \end{pmatrix} \quad (86)$$

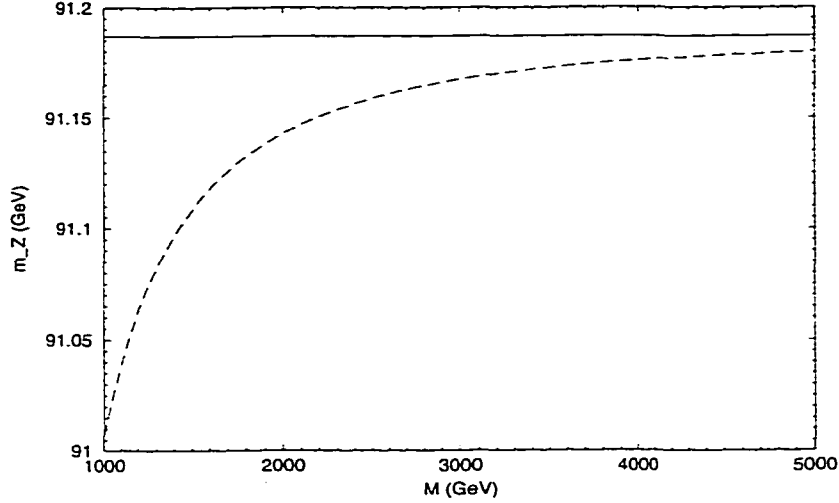


Figure 20: The decoupling limit of mass-squared matrix for the neutral gauge bosons, no mixing (solid line) and perturbation (dashed line).

We can treat \mathcal{M}_I^2 as a perturbation around \mathcal{M}_0^2 , and the mass of the mass eigenstate, Z_1 , identified as the ordinary Z should have the form

$$m_{Z_1}^2 = M^2 \left(a_0 + \frac{a_1}{M^2} + \frac{a_2}{M^4} + \dots \right) \quad (87)$$

It is straightforward to find that $a_0 = 0$ and $a_1 = M_Z^2 = \frac{1}{4}(g_L^2 + g_Y^2)(v_1^2 + v_2^2 + v_3^2)$, and that the second order correction, a_2 , will give mixing which is dependent on M . The result is illustrated in Fig. 20. It is found that when $M = 5$ TeV, the curve becomes almost flat.

After discussing the limiting case above, now we turn to diagonalize the mass-squared matrix. It is reasonably difficult to diagonalize the matrix analytically. Numerical calculations are needed to get the eigenstates and corresponding eigenvalues. The matrix \mathcal{M}^2 can be split into two parts

$$\begin{aligned} \mathcal{M}^2 &= \mathcal{M}_1^2 + \mathcal{M}_2^2 \\ &= \begin{pmatrix} m_Z^2 & 0 & 0 & 0 & 0 \\ 0 & m_{W_I^3}^2 & m_{23} & m_{24} & m_{25} \\ 0 & m_{23} & m_B^2 & m_{34} & m_{35} \\ 0 & m_{24} & m_{34} & 0 & m_{W_I^\pm}^2 \\ 0 & m_{25} & m_{35} & m_{W_I^\pm}^2 & 0 \end{pmatrix} + \begin{pmatrix} 0 & m_{12} & m_{13} & m_{14} & m_{15} \\ m_{12} & 0 & 0 & 0 & 0 \\ m_{13} & 0 & 0 & 0 & 0 \\ m_{14} & 0 & 0 & 0 & 0 \\ m_{15} & 0 & 0 & 0 & 0 \end{pmatrix} \quad (88) \end{aligned}$$

First we can find a 5×5 unitary matrix \mathbf{U}_1 to diagonalize \mathcal{M}_1^2 as

$$\mathbf{U}_1^\dagger \mathcal{M}_1^2 \mathbf{U}_1 = \mathcal{M}_1'^2 = \begin{pmatrix} m_Z^2 & & & & \\ & m_{Z_2}^2 & & & \\ & & m_{Z_3}^2 & & \\ & & & m_{Z_4}^2 & \\ & & & & m_{Z_5}^2 \end{pmatrix} \quad (89)$$

where \mathbf{U}_1 has the form

$$\mathbf{U}_1 = \begin{pmatrix} 1 & 0 \\ 0 & \mathbf{u}_1 \end{pmatrix} \quad (90)$$

with \mathbf{u}_1 is a 4×4 unitary matrix, and the corresponding eigenstates are

$$\begin{pmatrix} Z \\ Z_2 \\ Z_3 \\ Z_4 \\ Z_5 \end{pmatrix} = \mathbf{U}_1^\dagger \begin{pmatrix} Z \\ W_I^3 \\ B \\ W_I^+ \\ W_I^- \end{pmatrix} \quad (91)$$

We will call this transformation the first transformation for convenience in this paper. It gives linear combinations of extra neutral gauge fields. There is no mixing of the ordinary Z boson with extra neutral gauge bosons at this stage. The matrix \mathcal{M}_2^2 should also be transformed correspondingly as

$$\mathbf{U}_1^\dagger \mathcal{M}_2^2 \mathbf{U}_1 = \mathcal{M}_2'^2 = \begin{pmatrix} 0 & m'_{12} & m'_{13} & m'_{14} & m'_{15} \\ m'_{12} & & & & \\ m'_{13} & & 0 & & \\ m'_{14} & & & & \\ m'_{15} & & & & \end{pmatrix} \quad (92)$$

Then the total mass squared matrix for the neutral gauge bosons under the new basis has the form

$$\begin{aligned} \mathcal{M}^{\prime 2} &= \mathcal{M}_1^{\prime 2} + \mathcal{M}_2^{\prime 2} \\ &= \begin{pmatrix} m_Z^2 & m'_{12} & m'_{13} & m'_{14} & m'_{15} \\ m'_{12} & m_{Z_2}^2 & & & \\ m'_{13} & & m_{Z_3}^2 & & \\ m'_{14} & & & m_{Z_4}^2 & \\ m'_{15} & & & & m_{Z_5}^2 \end{pmatrix} \end{aligned} \quad (93)$$

\mathcal{M}^2 can be principally diagonalized by another unitary matrix U_2 as described at the beginning of this section, then we can get a unitary matrix $U = U_2 \times U_1$ which can be used to diagonalize the original matrix \mathcal{M}^2

$$U_2^\dagger \mathcal{M}^2 U_2 = \mathcal{M}'^2 = \begin{pmatrix} m_{Z_1}^2 & & & & \\ & m_{Z_2'}^2 & & & \\ & & m_{Z_3'}^2 & & \\ & & & m_{Z_4'}^2 & \\ & & & & m_{Z_5'}^2 \end{pmatrix}, \quad (94)$$

and the final physical eigenstates are

$$\begin{pmatrix} Z_1 \\ Z_2' \\ Z_3' \\ Z_4' \\ Z_5' \end{pmatrix} = U_2^\dagger \begin{pmatrix} Z \\ Z_2 \\ Z_3 \\ Z_4 \\ Z_5 \end{pmatrix}. \quad (95)$$

Compared with the U_1 -transformation, we will call this transformation the second transformation. The mixings of the ordinary Z boson with extra neutral gauge bosons occur in this transformation. The elements of U_2 satisfy the constraints given by Eq. (78) and Eq. (79) at the beginning of this section.

The couplings between neutral gauge bosons and fermions, which will give neutral current processes, are

$$\begin{aligned} \mathcal{L}_{NC} = & - \sum_{f,\alpha} \{ g_Z \bar{f}_\alpha \gamma^\mu (I_{fL}^3 - Q_{f\alpha} \sin^2 \theta_W) f_\alpha Z_\mu + g_{Y'} Y'_{f\alpha} / 2 \bar{f}_\alpha \gamma^\mu f_\alpha B_\mu \\ & + g_I T_{3f}^{f\alpha} \bar{f}_\alpha \gamma^\mu f_\alpha W_{I\mu}^3 \}, \end{aligned} \quad (96)$$

where the first term in the brackets represents the SM neutral currents, the second and third terms represent additional neutral currents introduced by extra neutral gauge bosons and $g_Z = g_L / \cos \theta_W = g_Y / \sin \theta_W$. The symbol f_α denotes the leptons or quarks with the chirality α ($\alpha = L$ or R). The quantum numbers I_{fL}^3 , $Q_{f\alpha}$, $Y'_{f\alpha}$ and $T_{3f}^{f\alpha}$ can be read from Table 1.3. The flavor-changing neutral currents caused by W_I^\pm involve heavy fermions and will not be discussed here.

Considering the first transformation, the interaction Lagrangian changes to

$$\begin{aligned}
\mathcal{L}_{NC} = & - \sum_{f,\alpha} \{g_Z \bar{f}_\alpha \gamma^\mu (I_{fL}^3 - Q_{f_\alpha} \sin^2 \theta_W) f_\alpha Z_\mu \\
& + g_{Y'} Y'_{f_\alpha} / 2 \bar{f}_\alpha \gamma^\mu f_\alpha \sum_{j \neq 1} (\mathbf{U}_1)_{3j} Z_{j\mu} \\
& + g_I T_{3I}^{f_\alpha} \bar{f}_\alpha \gamma^\mu f_\alpha \sum_{j \neq 1} (\mathbf{U}_1)_{2j} Z_{j\mu}\}. \tag{97}
\end{aligned}$$

where the first term is unchanged because there is no mixing of the ordinary Z boson with extra neutral gauge bosons. Including the second mixing, the final interaction Lagrangian is given as

$$\begin{aligned}
\mathcal{L}_{NC} = & - \sum_{f,\alpha} \{g_Z \bar{f}_\alpha \gamma^\mu (I_{fL}^3 - Q_{f_\alpha} \sin^2 \theta_W) f_\alpha [(\mathbf{U}_2)_{11} Z_{1\mu} + \sum_{j \neq 1} (\mathbf{U}_2)_{1j} Z'_{j\mu}] \\
& + g_{Y'} Y'_{f_\alpha} / 2 \bar{f}_\alpha \gamma^\mu f_\alpha \sum_{j \neq 1} (\mathbf{U}_1)_{3j} [(\mathbf{U}_2)_{j1} Z_{1\mu} + \sum_{k \neq 1} (\mathbf{U}_2)_{jk} Z'_{k\mu}] \\
& + g_I T_{3I}^{f_\alpha} \bar{f}_\alpha \gamma^\mu f_\alpha \sum_{j \neq 1} (\mathbf{U}_1)_{2j} [(\mathbf{U}_2)_{j1} Z_{1\mu} + \sum_{k \neq 1} (\mathbf{U}_2)_{jk} Z'_{k\mu}]\}, \tag{98}
\end{aligned}$$

where $(\mathbf{U}_2)_{11}$ is almost equal to 1.0 as the mixing should be very small; we will set it to equal to 1.0 and it represents the contributions from the SM. For small mixings the $(\mathbf{U}_2)_{j1}$ are also very close to $\left(\frac{m_Z^2 - m_{Z_j}^2}{m_{Z_j}^2 - m_Z^2}\right)^{1/2}$. They represent the mixings between the ordinary Z boson and the extra neutral gauge bosons. We will treat them as approximations of the mixing angles in our analysis (From Ref. [67] we know they are just upper limits of the mixing angles). Then it is easier to understand the physical meaning of the mixing angles when compared with the most conventional 2×2 Z - Z' mixing in $SU(2)_L \times U(1)_Y \times U(1)_{Y'}$ model. The second terms in the brackets of the second and third line, the $(\mathbf{U}_2)_{jk}, j \neq k$ terms, should be very small as they characterize the mixings among the Z_j 's themselves. We will omit these mixings in our analysis. The contributions from the term $\sum_{j \neq 1} (\mathbf{U}_2)_{1j} Z'_{j\mu}$ are also omitted in our analysis because they are combinations of mixings and exchanges of extra neutral gauge bosons and should be very small. Henceforth we will omit the prime on the Z_j .

Due to the mixings, the mass, m_{Z_1} of the observed Z boson is shifted from the SM prediction m_Z :

$$\Delta m^2 \equiv m_{Z_1}^2 - m_Z^2 \leq 0. \quad (99)$$

The presence of this mass shift will affect the T-parameter [72] at tree level. The oblique parameter S gets nonzero Z-Z' contribution only in the presence of kinetic mixing, and U will not get contributions from Z-Z' mixings. Following the notation of [73], the T-parameter is expressed in terms of the effective form factors $\bar{g}_Z^2(0)$, $\bar{g}_W^2(0)$ and the fine structure constant α as

$$\begin{aligned} \alpha T &\equiv 1 - \frac{\bar{g}_W^2(0)}{m_W^2} \frac{m_{Z_1}^2}{\bar{g}_Z^2(0)} \\ &= \alpha(T_{SM} + T_{new}), \end{aligned} \quad (100)$$

where T_{SM} and the new physics contribution T_{new} are given by

$$\begin{aligned} \alpha T_{SM} &= 1 - \frac{\bar{g}_W^2(0)}{m_W^2} \frac{m_Z^2}{\bar{g}_Z^2(0)}, \\ \alpha T_{new} &= -\frac{\Delta m^2}{m_{Z_1}^2} \geq 0. \end{aligned} \quad (101)$$

It is noted that the positiveness of T_{new} is attributed to the mixings which lower the mass of the ordinary Z boson. The effects of Z-Z' mixings in the electroweak experiments can be described by the effective mixing angles and the positive T_{new} .

3.5 Electroweak observables

In this section, we give the theoretical predictions for the electroweak observables which will be used in our analysis. Similar consideration for the $SU(2)_L \times U(1)_Y \times U(1)_{Y'}$ model can be found in Ref. [62]. The experimental data are summarized in Table 3.1. The experimental data from the Z-pole experiments and the W boson mass measurement are taken from Ref. [74], and LENC experiments are taken from Ref. [75]. Some of data used here are out-of-date, but are convenient in comparing with results existing in the

Table 3.1 Summary of electroweak measurements

Z-pole experiments	
m_Z (GeV)	91.1867 ± 0.0020
Γ_Z (GeV)	2.4948 ± 0.0025
σ_h^0 (nb)	41.486 ± 0.053
R_l	20.775 ± 0.027
$A_{FB}^{0,l}$	0.0171 ± 0.0010
A_τ	0.1411 ± 0.0064
A_e	0.1399 ± 0.0073
R_b	0.2170 ± 0.0009
R_c	0.1734 ± 0.0048
$A_{FB}^{0,b}$	0.0984 ± 0.0024
$A_{FB}^{0,c}$	0.0741 ± 0.0048
A_{LR}^0	0.1547 ± 0.0032
A_b	0.900 ± 0.050
A_c	0.650 ± 0.058
W-mass measurement	
m_W (GeV)	80.43 ± 0.084
LENC experiments	
A_{SLAC}	0.80 ± 0.058
A_{CERN}	-1.57 ± 0.38
A_{Bates}	-0.137 ± 0.033
A_{Mainz}	-0.94 ± 0.19
$Q_W(^{133}_{55}Cs)$	-72.08 ± 0.92
K_{FH}	0.3247 ± 0.0040
K_{CCFR}	0.5820 ± 0.0049
$g_{LL}^{\nu_\mu e}$	-0.269 ± 0.011
$g_{LR}^{\nu_\mu e}$	0.234 ± 0.011

literature. It will subsequently be found that slightly stronger constraints will be expected if updated data are used.

3.5.1 Observables in Z-pole experiments

The decay amplitude for the process $Z_1 \rightarrow f_\alpha \bar{f}_\alpha$ can be expressed in the form as

$$T(Z_1 \rightarrow f_\alpha \bar{f}_\alpha) = M_\alpha^f \epsilon_{Z_1} \cdot J_{f_\alpha}, \quad (102)$$

where $\epsilon_{Z_1}^\mu$ is the polarization vector of the Z_1 boson and $J_{f_\alpha}^\mu = \bar{f}_\alpha \gamma^\mu f_\alpha$ is the fermion current without the coupling constants. The pseudo-observables of the Z -pole experiments are related to the real scalar amplitude M_α^f with the following normalization [62]

$$g_\alpha^f = \frac{M_\alpha^f}{\sqrt{4\sqrt{2}G_F m_{Z_1}^2}} \approx \frac{M_\alpha^f}{0.74070}. \quad (103)$$

The effective coupling g_α^f can be written as the sum of two parts

$$g_\alpha^f = (g_\alpha^f)_{SM} + (g_\alpha^f)_{new}. \quad (104)$$

The $(g_\alpha^f)_{new}$ at tree level can be read off from the expression for the neutral current interaction including the mixings, see Eq. (98).

$$(g_\alpha^f)_{new} = g_{Y'} Y'_{f_\alpha} / 2 \sum_{j \neq 1} (\mathbf{U}_1)_{3j} (\mathbf{U}_2)_{j1} + g_I T_{3I}^{f_\alpha} \sum_{j \neq 1} (\mathbf{U}_1)_{2j} (\mathbf{U}_2)_{j1} \quad (105)$$

The SM predictions [73, 76] for the effective couplings $(g_\alpha^f)_{SM}$ can be parameterized as

$$(g_L^{\nu'})_{SM} = 0.50214 + 0.453 \Delta \bar{g}_Z^2, \quad (106)$$

$$(g_L^e)_{SM} = -0.26941 - 0.244 \Delta \bar{g}_Z^2 + 1.001 \Delta \bar{s}^2, \quad (107)$$

$$(g_R^e)_{SM} = 0.23201 + 0.208 \Delta \bar{g}_Z^2 + 1.001 \Delta \bar{s}^2, \quad (108)$$

$$(g_L^u)_{SM} = 0.34694 + 0.314 \Delta \bar{g}_Z^2 - 0.668 \Delta \bar{s}^2, \quad (109)$$

$$(g_R^u)_{SM} = -0.15466 - 0.139 \Delta \bar{g}_Z^2 - 0.668 \Delta \bar{s}^2, \quad (110)$$

$$(g_L^d)_{SM} = -0.42451 - 0.383 \Delta \bar{g}_Z^2 + 0.334 \Delta \bar{s}^2, \quad (111)$$

$$(g_R^d)_{SM} = 0.07732 + 0.069 \Delta \bar{g}_Z^2 + 0.334 \Delta \bar{s}^2, \quad (112)$$

$$(g_L^b)_{SM} = -0.42109 - 0.383 \Delta \bar{g}_Z^2 + 0.334 \Delta \bar{s}^2 + 0.00043 x_t, \quad (113)$$

where the SM radiative corrections are expressed in terms of the effective couplings $\Delta \bar{g}_Z^2$ and $\Delta \bar{s}^2$ and the top-quark mass dependence of the $Z b_L b_L$ vertex correction in $(g_L^b)_{SM}$ is represented by the parameter x_t

$$x_t \equiv \frac{m_t - 175 \text{ GeV}}{10 \text{ GeV}}. \quad (114)$$

The gauge boson propagator corrections, $\Delta\bar{g}_Z^2$ and $\Delta\bar{s}^2$, are defined as the shift in the effective couplings $\bar{g}_Z^2(m_{Z_1}^2)$ and $\bar{s}^2(m_{Z_1}^2)$ [73] from their SM reference values at $m_t = 175$ GeV and $m_H = 100$ GeV. They can be expressed in terms of the S and T parameters as

$$\Delta\bar{g}_Z^2 = \bar{g}_Z^2(m_{Z_1}^2) - 0.55635 = 0.00412\Delta T + 0.00005 [1 - (100 \text{ GeV}/m_H)^2], \quad (115)$$

$$\Delta\bar{s}^2 = \bar{s}^2(m_{Z_1}^2) - 0.23035 = 0.00360\Delta S - 0.00241\Delta T - 0.00023x_\alpha, \quad (116)$$

where the expansion parameter x_α is introduced to estimate the uncertainty of the hadronic contribution to the QED coupling $1/\bar{\alpha}(m_{Z_1}^2) = 128.75 \pm 0.09$ [77]:

$$x_\alpha \equiv \frac{1/\bar{\alpha}(m_{Z_1}^2) - 128.75}{0.09}. \quad (117)$$

Here, ΔS , ΔT , and ΔU are also measured from their SM reference values and they are given as the sum of the SM and the new physics contributions

$$\begin{aligned} \Delta S &= \Delta S_{SM} + S_{new} \\ \Delta T &= \Delta T_{SM} + T_{new} \\ \Delta U &= \Delta U_{SM} + U_{new} \end{aligned} \quad (118)$$

The SM contributions can be parameterized as [76]

$$\begin{aligned} \Delta S_{SM} &= -0.007x_t + 0.091x_H - 0.010x_h^2, \\ \Delta T_{SM} &= (0.130 - 0.003x_H)x_t + 0.003x_t - 0.079x_H - 0.028x_H^2 + 0.0026x_H^3 \\ \Delta U_{SM} &= 0.022x_t - 0.002x_H, \end{aligned} \quad (119)$$

where x_H is defined as

$$x_H \equiv \log(m_H/100 \text{ GeV}). \quad (120)$$

x_H represents the Higgs mass dependence of the oblique parameters. Using the eight effective couplings g_α^f , the pseudo-observables of the Z-pole experiments are given in the following.

Table 3.2 Numerical values of factors C_{fV} and C_{fA} for quarks and leptons.

	C_{fV}	C_{fA}
u	$3.1166+0.0030x_s$	$3.1351+0.0040x_s$
d=s	$3.1166+0.0030x_s$	$3.0981+0.0021x_s$
c	$3.1167+0.0030x_s$	$3.1343+0.0041x_s$
b	$3.1185+0.0030x_s$	$3.0776+0.0030x_s$
ν	1	1
$e = \mu$	1	1
τ	1	0.9977

The partial width of the Z_1 boson is given by

$$\Gamma_f = \frac{G_F m_{Z_1}^3}{3\sqrt{2}\pi} \left\{ |g_L^f + g_R^f|^2 \frac{C_{fV}}{2} + |g_L^f - g_R^f|^2 \frac{C_{fA}}{2} \right\} \left(1 + \frac{3}{4} Q_f^2 \frac{\bar{\alpha}(m_{Z_1}^2)}{\pi} \right), \quad (121)$$

where the factors C_{fV} and C_{fA} account for the finite mass corrections and the final state QCD corrections for quarks, and their numerical values are listed in Table 3.2. The α_s -dependence in C_{qV} and C_{qA} is parameterized in terms of the parameter x_s

$$x_s \equiv \frac{\alpha_s(m_{Z_1}) - 0.118}{0.003}. \quad (122)$$

The last term proportional to $\bar{\alpha}(m_{Z_1}^2)/\pi$ accounts for the final state QED correction.

The hadronic decay width Γ_h is

$$\Gamma_h = \Gamma_u + \Gamma_d + \Gamma_c + \Gamma_s + \Gamma_b. \quad (123)$$

The total decay width Γ_{Z_1} is given by

$$\Gamma_{Z_1} = 3\Gamma_\nu + \Gamma_e + \Gamma_\mu + \Gamma_\tau + \Gamma_h. \quad (124)$$

The ratios R_l , R_c , R_b and the hadronic peak cross section σ_h^0 are given by

$$R_l = \frac{\Gamma_h}{\Gamma_e}, \quad (125)$$

$$R_c = \frac{\Gamma_c}{\Gamma_h}, \quad (126)$$

$$R_b = \frac{\Gamma_b}{\Gamma_h}, \quad (127)$$

$$\sigma_h^0 = \frac{12\pi}{m_{Z_1}^2} \frac{\Gamma_e \Gamma_h}{\Gamma_{Z_1}^2}. \quad (128)$$

The left-right asymmetry parameter A^f can be written in terms of the effective couplings g_α^f as

$$A^f = \frac{(g_L^f)^2 - (g_R^f)^2}{(g_L^f)^2 + (g_R^f)^2}. \quad (129)$$

The forward-backward(FB) asymmetry $A_{FB}^{0,f}$ and the left-right(LR) asymmetry $A_{LR}^{0,f}$ are then given as follows:

$$A_{FB}^{0,f} = \frac{3}{4} A^e A^f, \quad (130)$$

$$A_{LR}^{0,f} = A^f. \quad (131)$$

3.5.2 W boson mass

The theoretical prediction of m_W can be parametrized as [73, 76]

$$m_W(\text{GeV}) = 80.42 - 0.288\Delta S + 0.418\Delta T + 0.337\Delta U + 0.012x_\alpha \quad (132)$$

3.5.3 Observables in LENC experiments

In this subsection we give the theoretical predictions, which can be found in Ref. [62, 73, 75], for the electroweak observables in the LENC experiments: (i) polarization asymmetry of the charged lepton scattering off a target nucleus, (ii) parity violation in the cesium atom, (iii) inelastic ν -scattering off a nuclear target and (iv) neutrino-electron scattering. Besides the SM contribution, all observables also receive corrections from the new physics: exchange of extra neutral gauge bosons and their mixings with the ordinary Z boson. As the extra neutral gauge bosons are expected to be heavy, the contributions due to exchanges of extra neutral gauge bosons can be described by an effective contact interaction

$$\mathcal{L}_{NC} = \sum_{f,f'} \sum_{\alpha,\beta} \eta_{\alpha\beta}^{f,f'} \bar{\psi}_f \gamma_\mu P_\alpha \psi_f \bar{\psi}_{f'} \gamma^\mu P_\beta \psi_{f'}, \quad (133)$$

where f, f' stands for leptons and quarks, $\alpha, \beta = L, R$ denote their chirality: $P_{L(R)} = (1 \pm \gamma_5)/2$. For a given extra gauge boson, the coefficients $\eta_{\alpha\beta}^{f,f'}$ have the dimension of

(mass)⁻² and are given as

$$\eta_{\alpha\beta}^{f,f'} = -\frac{(g_{\alpha}^f)_E (g_{\beta}^{f'})_E}{m_{Z_E}^2}, \quad (134)$$

where m_{Z_E} is the mass of an extra neutral gauge boson and $(g_{\alpha}^f)_E$ and $(g_{\beta}^{f'})_E$ are the Z_E boson couplings to f_{α} and f'_{β} respectively.

The effective Lagrangian for the lepton-quark four-Fermi interaction can be parametrized as

$$\mathcal{L}_{eff}^{lq} = -\frac{G_F}{\sqrt{2}} \sum_{q=u,d} \{C_{1q} \bar{\psi}_l \gamma^{\mu} \gamma_5 \psi_l \bar{\psi}_q \gamma_{\mu} \psi_q + C_{2q} \bar{\psi}_l \gamma^{\mu} \psi_l \bar{\psi}_q \gamma_{\mu} \gamma_5 \psi_q + C_{3q} \bar{\psi}_l \gamma^{\mu} \gamma_5 \psi_l \bar{\psi}_q \gamma_{\mu} \gamma_5 \psi_q\} \quad (135)$$

where $l = e, \mu, \tau$ and C_{1q}, C_{2q}, C_{3q} are model-independent parameters introduced in Ref. [75, 78]. They can be expressed in terms of the helicity amplitude $M_{\alpha\beta}^{lq}$ of the process $f_{\alpha} f'_{\beta} \rightarrow f_{\alpha} f'_{\beta}$ as below [73]

$$C_{1q} = \frac{1}{2\sqrt{2}G_F} (M_{LL}^{lq} + M_{LR}^{lq} - M_{RL}^{lq} - M_{RR}^{lq}), \quad (136)$$

$$C_{2q} = \frac{1}{2\sqrt{2}G_F} (M_{LL}^{lq} - M_{LR}^{lq} + M_{RL}^{lq} - M_{RR}^{lq}), \quad (137)$$

$$C_{3q} = \frac{1}{2\sqrt{2}G_F} (-M_{LL}^{lq} + M_{LR}^{lq} + M_{RL}^{lq} - M_{RR}^{lq}). \quad (138)$$

In the presence of the mixings and contact terms, the complete helicity amplitude is given by the sum

$$M_{\alpha\beta}^{f,f'}(q^2) = M_{\alpha\beta}^{f,f'}(q^2)^{SM'} + \Delta M_{\alpha\beta}^{f,f'}(q^2) \quad (139)$$

Then the coefficients C_{iq} of the effective lepton-quark interactions can be divided into two pieces correspondingly as

$$C_{iq} = C_{iq}^{SM'} + \Delta C_{iq}. \quad (140)$$

where the first term denotes the contribution from the generic $SU(2)_L \times U(1)_Y$ model. The terms ΔC_{iq} receive contributions from the contact interactions and the mixings. The

former contributions are given as,

$$\Delta C_{1q} = \frac{1}{2\sqrt{2}G_F} (\eta_{LL}^{lq} + \eta_{LR}^{lq} - \eta_{RL}^{lq} - \eta_{RR}^{lq}), \quad (141)$$

$$\Delta C_{2q} = \frac{1}{2\sqrt{2}G_F} (\eta_{LL}^{lq} - \eta_{LR}^{lq} + \eta_{RL}^{lq} - \eta_{RR}^{lq}), \quad (142)$$

$$\Delta C_{3q} = \frac{1}{2\sqrt{2}G_F} (-\eta_{LL}^{lq} + \eta_{LR}^{lq} + \eta_{RL}^{lq} - \eta_{RR}^{lq}). \quad (143)$$

The contributions to ΔC_{iq} from the exchanges of extra neutral gauge bosons are easily to calculated by using Eq. (134) and the above equations. For example, consider the calculation of ΔC_{1u} due to the exchange of the lightest extra neutral gauge boson Z_2 ,

$$\begin{aligned} (g_L^l)_{Z_2} &= g_{Y'} Q_{Y'}^{lL}(\mathbf{U}_1)_{32} + g_I T_{3I}^{lL}(\mathbf{U}_1)_{22}, \\ (g_R^l)_{Z_2} &= g_{Y'} Q_{Y'}^{lR}(\mathbf{U}_1)_{32} + g_I T_{3I}^{lR}(\mathbf{U}_1)_{22}, \\ (g_L^u)_{Z_2} &= g_{Y'} Q_{Y'}^{uL}(\mathbf{U}_1)_{32} + g_I T_{3I}^{uL}(\mathbf{U}_1)_{22}, \\ (g_R^u)_{Z_2} &= g_{Y'} Q_{Y'}^{uR}(\mathbf{U}_1)_{32} + g_I T_{3I}^{uR}(\mathbf{U}_1)_{22}, \end{aligned} \quad (144)$$

and

$$\begin{aligned} \eta_{LL}^{lu} &= -\frac{(g_L^l)_{Z_2} (g_L^u)_{Z_2}}{m_{Z_2}^2}, & \eta_{LR}^{lu} &= -\frac{(g_L^l)_{Z_2} (g_R^u)_{Z_2}}{m_{Z_2}^2}, \\ \eta_{RL}^{lu} &= -\frac{(g_R^l)_{Z_2} (g_L^u)_{Z_2}}{m_{Z_2}^2}, & \eta_{RR}^{lu} &= -\frac{(g_R^l)_{Z_2} (g_R^u)_{Z_2}}{m_{Z_2}^2}, \end{aligned} \quad (145)$$

Combining the above results together, we get

$$\Delta C_{1u} = \frac{1}{2\sqrt{2}G_F} (\eta_{LL}^{lu} + \eta_{LR}^{lu} - \eta_{RL}^{lu} - \eta_{RR}^{lu}). \quad (146)$$

The contributions from other extra neutral gauge bosons should be much smaller because they are heavier, however they can be calculated in the same way and are also included in our analysis.

The contributions due to mixings of the ordinary Z with extra neutral gauge bosons are treated in the similar way. To leading order, we use the mass of the Z_1 boson instead

of $m_{Z_2}^2$ and relevant couplings. Therefore we approximate the mixing effects by contact interactions due to the exchange of the Z_1 boson. This should be reasonable because at low energies one has $|q^2| \ll m_{Z_1}^2$, where q_μ is the typical momentum-transfer in the LENC processes.

3.5.3.1 Polarization asymmetries

There are two types of observables measured in these LENC experiments. First, polarization asymmetry A of charged lepton scattering off the nucleus target

$$A \equiv \frac{d\sigma_R - d\sigma_L}{d\sigma_R + d\sigma_L}, \quad (147)$$

where $d\sigma_{R(L)}$ denotes the differential cross section of the right(left)-handed lepton scattering off the nucleus target. The parameter A has been measured in eD-scattering at SLAC [79, 80], in eC-scattering at Bates [81] and in eBe-scattering at Mainz [82]. The asymmetry has also been measured recently in elastic electron scattering from the proton by SAMPLE [83] and HAPPEX [84], but how the results can constrain new physics remains to be studied further.

Another type of the polarization asymmetry B is

$$B \equiv \frac{d\sigma_L^+ - d\sigma_R^-}{d\sigma_L^+ + d\sigma_R^-}, \quad (148)$$

where $d\sigma_{R(L)}^-$ is the differential cross section of the right(left)-handed negatively charged lepton scattering off the nucleus target, and $d\sigma_{R(L)}^+$ denotes those of positively charged anti-lepton scattering off the nucleus target. The parameter B has been measured in $\mu^\pm C$ scattering at CERN [85]. It has also been measured recently to study the spin structure functions of nucleons by E155 at SLAC [86].

(I) SLAC eD experiment

In SLAC eD experiment longitudinally polarized electrons were scattered deep-inelastically from unpolarized deuterons [79, 80]. This historic experiment still gives non-trivial constraints on new physics. It constrains the parameters $2C_{1u} - C_{1d}$ and $2C_{2u} - C_{2d}$. By the analysis of Ref. [62], the parameter A_{SLAC} has the form

$$\begin{aligned} A_{SLAC} &= 2C_{1u} - C_{1d} + 0.206(2C_{2u} - C_{2d}) \\ &= 0.745 - 0.016\Delta S + 0.016\Delta T \\ &\quad + 2\Delta C_{1u} - \Delta C_{1d} + 0.206(2\Delta C_{2u} - \Delta C_{2d}), \end{aligned} \tag{149}$$

The second line represents mainly contributions from the $SU(2)_L \times U(1)_Y$ model and a bit of contributions from new physics through the oblique parameters which gain small corrections due to the Z - Z' mixings. The third line represents contributions from new physics.

(II) Bates eC experiment

Parity violation in the elastic scattering of polarized electrons from ^{12}C nuclei was measured successfully [81]. It constrains the combination $C_{1u} + C_{1d}$. The analysis of Ref. [62] is quoted as

$$\begin{aligned} A_{Bates} &= C_{1u} + C_{1d} \\ &= -0.1520 - 0.0023\Delta S + 0.0004\Delta T + \Delta C_{1u} + \Delta C_{1d}, \end{aligned} \tag{150}$$

(III) Mainz eBe experiment

In this experiment polarized electrons were scattered quasi-elastically off the 9Be target and the polarization asymmetry was measured [82]. The asymmetry parameter A_{Mainz} can be expressed in the terms of model-independent parameters as below [62]

$$A_{Mainz} = -2.73C_{1u} + 0.65C_{1d} - 2.19C_{2u} + 2.03C_{2d}$$

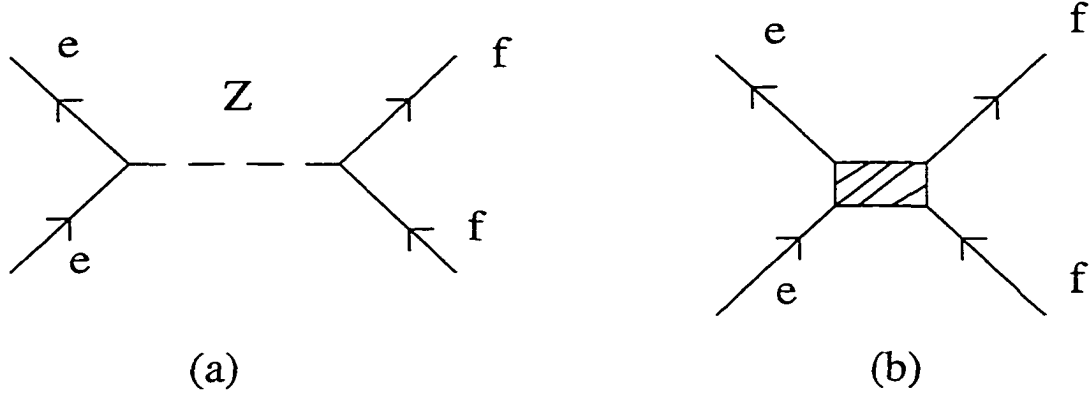


Figure 21: (a) Parity-violating electron-fermion amplitude generated by Z^0 -exchange, (b) Effective four-fermion electron-fermion PV interaction

$$\begin{aligned}
 &= -0.876 + 0.043\Delta S - 0.035\Delta T \\
 &\quad -2.73\Delta C_{1u} + 0.65\Delta C_{1d} - 2.19\Delta C_{2u} + 2.03\Delta C_{2d}, \quad (151)
 \end{aligned}$$

(IV) CERN $\mu^\pm C$ experiment

At CERN SPS the charge and polarization asymmetry of muon deep inelastic scattering off the ^{12}C target were measured [85]. It constrains the combinations of parameters $2C_{2u} - C_{2d}$ and $2C_{3u} - C_{3d}$. The most stringent constraint is found as [62]

$$\begin{aligned}
 A_{CERN} &= 2C_{3u} - C_{3d} + 0.777(2C_{2u} - C_{2d}) \\
 &= -1.42 - 0.016\Delta S + 0.0006\Delta T \\
 &\quad + 2\Delta C_{3u} - \Delta C_{3d} + 0.777(2\Delta C_{2u} - \Delta C_{2d}). \quad (152)
 \end{aligned}$$

3.5.3.2 The weak charges

The weak charge is the weak neutral current counterpart of the electromagnetic charge, Q_{EM} . The Feynman diagrams that give the weak charge are illustrated in Fig. 21. Due to the new physics modification, the weak charge can be written as

$$Q_W = Q_W^0 + \Delta Q_W, \quad (153)$$

where Q_W^0 gives the contribution in the SM while ΔQ_W represents possible contributions from new physics. The new physics can affect Q_W in basically two ways: by physics

which can modify the propagation of the Z^0 from the electron to the other fermion f , and by the exchange of possible new, heavy particles between e and f . The former can be described by corrections to the so-called oblique parameters ΔS , ΔT and ΔU . The latter can be given by the low-energy effective Lagrangian.

$$\mathcal{L} = \mathcal{L}_{SM}^{PV} + \mathcal{L}_{new}^{PV}, \quad (154)$$

where

$$\begin{aligned} \mathcal{L}_{SM}^{PV} &= \frac{G_F}{2\sqrt{2}} g_A^e \bar{e} \gamma^\mu \gamma_5 e \sum_f g_V^f \bar{f} \gamma_\mu f, \\ \mathcal{L}_{new}^{PV} &= \frac{4\pi\kappa^2}{\Lambda} \bar{e} \gamma^\mu \gamma_5 e \sum_f h_V^f \bar{f} \gamma_\mu f. \end{aligned} \quad (155)$$

where \mathcal{L}_{SM}^{PV} gives Q_W^0 with the vector fermion- Z^0 coupling $g_V^f \equiv Q_W^f = 2T_3^f - 4Q_f \sin^2 \theta_W$ and the axial vector fermion- Z^0 coupling $g_A^f = -2T_3^f$ at the tree level in the SM. \mathcal{L}_{new}^{PV} describes the direct new physics contributions to the ΔQ_W . The mass scale of the new physics is represented by Λ and κ^2 sets the coupling strength. The coupling h_V^f characterizes the interaction of the electron axial-vector current with the vector current of fermion f for a given extension of the SM. It is straightforward to write down the corrections to the weak charge, specifically, for the proton and neutron

$$\begin{aligned} \Delta Q_W^P &= \frac{8\sqrt{2}\pi\kappa^2}{\Lambda^2 G_F} (2h_V^u + h_V^d), \\ \Delta Q_W^N &= \frac{8\sqrt{2}\pi\kappa^2}{\Lambda^2 G_F} (h_V^u + 2h_V^d). \end{aligned} \quad (156)$$

In the case of the exchange of a new heavy particle between the electron and the fermion,

$$\begin{aligned} \kappa^2 &= \frac{\tilde{g}^2}{4\pi}, \\ \Lambda^2 &= m_{Z'}^2, \\ h_V^f &= \tilde{g}_A^e \tilde{g}_V^f, \end{aligned} \quad (157)$$

where \bar{g} is the coupling constant of the new interaction, $m_{Z'}$ is the mass of the new heavy particle, and $\bar{g}_A^e(\bar{g}_V^f)$ are the heavy particle axial-vector(vector) couplings to the electron(fermion). The new physics sensitivity of low-energy parity-violating observables is studied in Ref. [87] in detail. In term of the left(right)-handed components,

$$\begin{aligned}\bar{g}_V^f &= \frac{1}{2}(\bar{g}_L^f + \bar{g}_R^f), \\ \bar{g}_A^e &= \frac{1}{2}(\bar{g}_L^e - \bar{g}_R^e),\end{aligned}\tag{158}$$

Then

$$\begin{aligned}h_V^f &= \frac{1}{4}(\bar{g}_L^e \bar{g}_L^f + \bar{g}_L^e \bar{g}_R^f - \bar{g}_R^e \bar{g}_L^f - \bar{g}_R^e \bar{g}_R^f), \\ &\sim \Delta C_{1f},\end{aligned}\tag{159}$$

where C_{1f} is defined in Ref. [62, 75] and has been introduced in the beginning of this section. Correspondingly

$$\begin{aligned}\Delta Q_W^P &= 2(2\Delta C_{1u} + \Delta C_{1d}), \\ \Delta Q_W^N &= 2(\Delta C_{1u} + 2\Delta C_{1d}).\end{aligned}\tag{160}$$

When an electron interacts weakly with a system composed of several elementary fermions, such as an atomic nucleus, the weak charge of that system is just the sum of the weak charges of its constituents. The weak charge $Q_W(A, Z)$ of nuclei is usually used to describe the experimental result of atomic parity violation. The data for the cesium atom $^{133}_{55}\text{Cs}$ [88, 89] is given in Table 3.1. In terms of parameters C_{1q} , the weak charge of a nuclei can be expressed as [62]

$$Q_W(A, Z) = 2ZC_{1p} + 2(A - Z)C_{1n},\tag{161}$$

where

$$\begin{aligned}C_{1p} &= 0.03601 - 0.00681\Delta S + 0.00477\Delta T + 2\Delta C_{1u} + \Delta C_{1d}, \\ C_{1n} &= -0.49376 - 0.00366\Delta T + \Delta C_{1u} + 2\Delta C_{1d}.\end{aligned}\tag{162}$$

Therefore

$$Q_W(^{133}_{55}\text{Cs}) = -73.07 - 0.749\Delta S - 0.046\Delta T + 376\Delta C_{1u} + 422\Delta C_{1d}. \quad (163)$$

In contrast to the weak charge of a heavy atom, the weak charge of the proton, namely Q_W^P , is fortuitously suppressed in the SM. Therefore it is very sensitive to contributions from new physics. Q_W^P is twice as sensitive to new u-quark interactions as it is to new d-quark physics. In our model the right-handed u-quark and d-quark have different isospin content, so it is advantageous to consider the constraints arising from the measurement of Q_W^P . Additionally the interpretation of the experimental result, if the weak charge of the proton is measured, will be free from theoretical uncertainties such as the neutron number density of atomic nuclei. The theoretical prediction for the weak charge of the proton is

$$\begin{aligned} Q_W^P &= 2C_{1p} \\ &= 0.07202 - 0.01362\Delta S + 0.00954\Delta T + 2(2\Delta C_{1u} + \Delta C_{1d}) \end{aligned} \quad (164)$$

3.5.3.3 Neutrino-quark scattering

To describe neutrino-quark scattering experiment, it is conventional to introduce the model-independent parameters, g_α^2 and δ_α^2 ($\alpha = L, R$) [90]

$$g_\alpha^2 = u_\alpha^2 + d_\alpha^2 \quad (165)$$

$$\delta_\alpha^2 = u_\alpha^2 - d_\alpha^2 \quad (166)$$

where u_α and d_α are given by the helicity amplitude [73]

$$\begin{aligned} q_\alpha &= -\frac{1}{2\sqrt{2}G_F} M_{L\alpha}^{\nu_\mu q} \\ &= q_\alpha'^{SM'} + \Delta q_\alpha \quad (q = u, d), \end{aligned} \quad (167)$$

where the Δq_α can get contributions from mixings and the contact terms. They can be calculated in the similar way as described in the first part of this section. The latter

contribution has the form [75]

$$\Delta q_\alpha = -\frac{1}{2\sqrt{2}G_F}\eta_{L\alpha}^{\nu\mu q}. \quad (168)$$

Two independent sets of experimental data are used in our analysis: all the old neutrino-nucleus scattering experiments summarized by Fogli and Haidt [90] and the more recent CCFR measurement [91]. Due to the difference in the typical momentum transfer, the theoretical predictions for the model-independent parameters in the generic $SU(2) \times U(1)_Y$ models are

$$\begin{aligned} u_L'^{SM'} &\approx \begin{pmatrix} 0.3465 \\ 0.3468 \end{pmatrix} - 0.0023\Delta S + 0.0041\Delta T, \\ u_R'^{SM'} &\approx \begin{pmatrix} -0.1549 \\ -0.1549 \end{pmatrix} - 0.0023\Delta S + 0.0004\Delta T, \\ d_L'^{SM'} &\approx \begin{pmatrix} -0.4296 \\ -0.4299 \end{pmatrix} + 0.0012\Delta S - 0.0039\Delta T, \\ d_R'^{SM'} &\approx \begin{pmatrix} 0.0776 \\ 0.0775 \end{pmatrix} + 0.0012\Delta S - 0.0002\Delta T, \end{aligned} \quad (169)$$

where the upper and the lower numbers in the first column are the predictions at $\langle Q^2 \rangle_{FH} = 20 \text{ GeV}^2$ and at $\langle Q^2 \rangle_{CCFR} = 35 \text{ GeV}^2$ respectively. The difference due to the momentum transfer is very small. These two experiments put stringent constraints on the combinations of g_α and δ_α as [62]

$$K_{FH} = g_L^2 + 0.879g_R^2 - 0.010\delta_L^2 - 0.043\delta_R^2, \quad (170)$$

$$K_{CCFR} = 1.7897g_L^2 + 1.1479g_R^2 - 0.0916\delta_L^2 - 0.0782\delta_R^2. \quad (171)$$

3.5.3.4 Neutrino-electron scattering

There are three $\nu - e$ scattering experimental results [92-94]. The combined data [75, 94] are given in Table 3.1. The total cross sections for $\nu_\mu - e$ and $\bar{\nu}_\mu - e$ scatterings can be expressed in terms of the helicity amplitude as [73]

$$\frac{\sigma^{\nu e}}{E_\nu} = \frac{m_e}{4\pi} \left\{ |g_{LL}^{\nu\mu e}(\langle Q^2 \rangle = m_e E_\nu)|^2 + \frac{1}{3} |g_{LR}^{\nu\mu e}(\langle Q^2 \rangle = \frac{m_e E_\nu}{2})|^2 \right\}, \quad (172)$$

$$\frac{\sigma^{\bar{\nu}e}}{E_{\bar{\nu}}} = \frac{m_e}{4\pi} \left\{ \frac{1}{3} |g_{LL}^{\bar{\nu}\mu e}(\langle Q^2 \rangle = \frac{m_e E_{\bar{\nu}}}{2})|^2 + |g_{LR}^{\bar{\nu}\mu e}(\langle Q^2 \rangle = m_e E_{\bar{\nu}})|^2 \right\}, \quad (173)$$

where the helicity amplitude can be parametrized as

$$g_{L\alpha}^{\nu\mu e} = (g_{L\alpha}^{\nu\mu e})'^{SM'} + \Delta g_{L\alpha}^{\nu\mu e} \quad (174)$$

For the generic $SU(2) \times U(1)_Y$ model, the theoretical predictions are [62]

$$(g_{LL}^{\nu\mu e})'^{SM'} = -0.273 + 0.0033\Delta S - 0.0042\Delta T, \quad (175)$$

$$(g_{LR}^{\nu\mu e})'^{SM'} = 0.233 + 0.0033\Delta S - 0.0006\Delta T. \quad (176)$$

and the contribution from the contact terms is [75]

$$\Delta g_{L\alpha}^{\nu\mu e} = \eta_{L\alpha}^{\nu\mu e}. \quad (177)$$

This is straightforward to calculate and the contribution due to the mixings can also be treated similarly as described before.

3.6 Constraints on extra neutral gauge bosons

Using the electroweak precision data, constraints on the parameters T_{new} , mixing angles and masses of extra neutral gauge bosons can be obtained from the standard χ^2 analysis. But here we are mainly concerned with constraints on the parameter spaces between mixing angles and the masses of extra neutral gauge bosons, we will not try to give the fit for T_{new} parameter. For our specific model, we just go through reasonably possible parameter spaces and find the acceptable physically parameter spaces by fitting the predictions of our model with various experimental results. For simplicity, S_{new} and U_{new} will be set zero because they are very small. Through our analysis, we will use

$$\begin{aligned} m_{Z_1} &= 91.1867 \pm 0.0020 \text{ GeV [74]}, \\ G_f &= 1.16637(1) \times 10^{-5} \text{ GeV}^{-2} [31], \\ 1/\bar{\alpha}(m_{Z_1}^2) &= 128.75 \pm 0.09 [77], \end{aligned} \quad (178)$$

as inputs and

$$\begin{aligned} m_t &= 175.6 \pm 5.5 \text{ GeV}, \\ \alpha_s &= 0.118 \pm 0.003 \end{aligned} \tag{179}$$

as constraints on the SM parameters which were used in Ref. [62]. The Higgs mass dependence of the results are parameterized by x_H and we just set $x_H = 0$ for simplicity. We first obtain the constraints from Z-pole experiments and m_W measurement only, and then we combine the LENC experiments with them to get further constraints. Finally we will study the constraint which would arise from measuring the weak charge of the proton.

3.6.1 Constraints from Z-pole and m_W data

From the previous section, it is found that the Z-pole experiments are related to mixings and the T-parameter, while m_W is only relevant for the T-parameter. From these data the number of degrees of freedom is 14. If we set all mixing angles and T_{new} equal to zero, it will give the fit for the SM, which can be found in Ref. [31, 62]. There is a small difference between them because different experimental data were used. It serves as a reference because the SM fits the experiments very well. Defining $\Delta\chi^2 = \chi^2 - \chi_{SM}^2$, by requiring acceptable $\Delta\chi^2$ we can get constraints on the mixings and the masses of extra neutral gauge bosons at different confidence levels. The result for $\Delta\chi^2 = 1.0$ is illustrated in Fig. 22. The lower mass limits for Z_2 , Z_3 and Z_4 bosons are about 330 GeV, 1000 GeV and 1.5 TeV respectively. It seems that the model allows for the existence of a comparatively light extra neutral gauge bosons. But we will find in the following that this is not true when LENC experiments are included. The mixing angles are found to be very small, namely $|\theta| \leq 0.005$. Although the lower mass limits are largely different for Z_2 , Z_3 and Z_4 bosons, the ranges of the mixing angles are all almost the same.

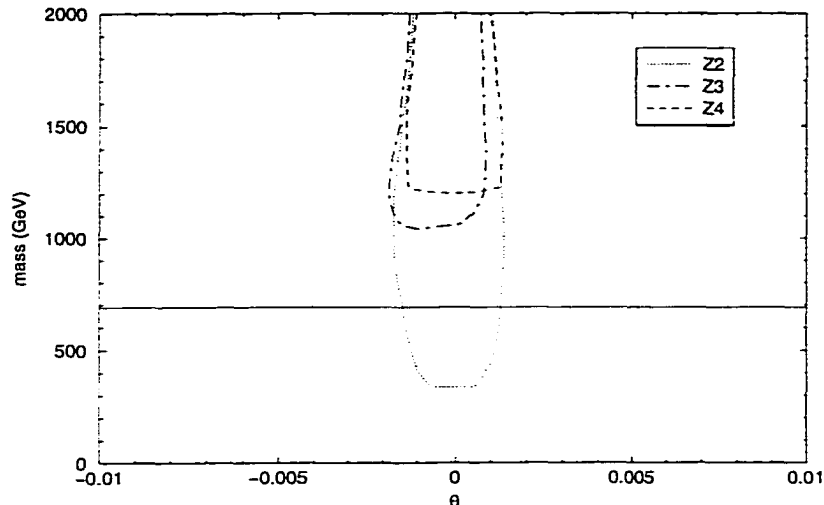


Figure 22: The contours of $\Delta\chi^2 = \chi^2 - \chi_{SM}^2 = 1.0$ for extra neutral gauge bosons. The constraints are obtained by use of Z-pole experiments [74] and m_W measurement [74]. As a reference the lower direct production limit from CDF [58] for the sequential Z_{SM} is also shown (solid line).

The Z-pole experiments have been updated [31] and slightly more stringent constraints can be found. It is found that the lower mass bound of the lightest extra neutral gauge boson is about 380 GeV with little change of the mixing angle.

The sequential Z_{SM} boson [95] is defined to have the same couplings to fermions as the SM Z boson. Such a boson is not expected in the context of gauge theories. However, it serves as a useful reference case when comparing constraints from various sources. The direct production limit for the sequential Z_{SM} boson from Ref. [58] is 690 GeV. It is assumed that all exotic decay channels are forbidden, and have to be relaxed by about 100 to 150 GeV when all exotic decays (including channels involving superparticles) are kinetically allowed. It was found that, at this time, the lower mass limit for the lightest extra neutral gauge boson, Z_2 is much lower than the direct production limit for the sequential Z_{SM} boson.

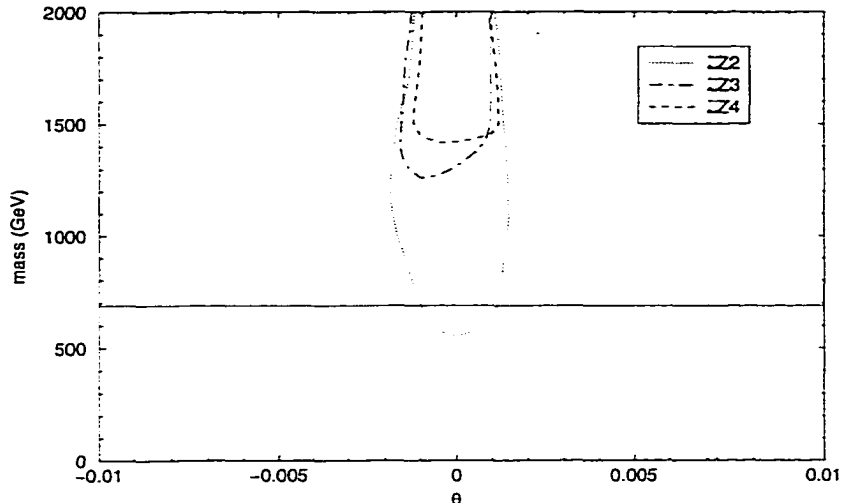


Figure 23: The contours of $\Delta\chi^2 = \chi^2 - \chi_{SM}^2 = 1.0$ for extra neutral gauge bosons. The constraints are obtained by use of Z-pole experiments [74], m_{EW} measurement [74] and LENC experiments [75]. As a reference the lower direct production limit from CDF [58] for the sequential Z_{SM} is also shown (solid line).

3.6.2 Constrains from Z-pole + m_W + LENC data

The LENC experiments can get contributions from the exchanges of extra neutral gauge bosons, which can be approximated by the contact interactions. The contact interaction is inversely-proportional to the mass of the extra gauge bosons exchanged in the processes. So the LENC experiments can put stringent constraints on the masses of extra neutral gauge bosons. The fitting results of Z-pole experiments, m_W measurement and LENC experiments are shown in Fig. 23. It is remarkable that the lower mass limits for the extra neutral gauge bosons are raised much higher than those without LENC experiments. The lower mass bound for the lightest extra gauge boson is about 560 GeV. This is comparative with the direct production limit for the sequential Z_{SM} boson.

In Ref. [61], similar constraints on various possible extra Z' bosons were studied. In all cases the mixing angles are severely constrained ($\sin\theta < 0.01$), and the lower mass limit are generally of the order of several hundred GeV, depending on the specific models considered.

In the model considered here, from the appendices, $m_{W_I^3}^2 \sim m_B^2$ assuming that $g_I = g_L$ and $g_{Y'} = g_Y$. It is apparent that $m_{W_I^\pm}$ is degenerate with $m_{W_I^3}$ without mixing. Generally the lightest extra neutral gauge boson mainly consists of W_I^3 , or Z_I . It is noted that Z_I corresponds to $Z'(\theta = -\arcsin\sqrt{5/8})$ and is orthogonal to Z_η . There is no mass limit on Z_I from electroweak precision data available in the literature. From constraints on Z_ψ , Z_χ and Z_η [61], it could be inferred that the mass limit on Z_I would be about 430 GeV at 95% CL. In Ref. [58] the lower mass limit of 565 GeV for Z_I was set by direct search for heavy neutral gauge bosons with the Collider Detector at Fermilab. Although Z_I mixes with other neutral gauge bosons in the model, our results are compatible with previous limits in the literature.

It should be pointed out that an updated value for $Q_W(Cs) = -72.06(28)_{\text{expt}}(34)_{\text{theor}}$ has been reported [96]. The experimental precision was improved and indicated a 2.5σ deviation from the prediction of the SM. The possibility that the discrepancy is due to contributions from new physics has been suggested. In Ref. [97, 98] it was shown that the contribution from the exchange of an extra U(1) boson could explain the data without $Z - Z'$ mixing. Some models which would give negative contributions to $Q_W(Cs)$, such as Z_{SM} and Z_η , were excluded at 99% CL. The existence of Z_I with a central value of about 760 GeV could explain the deviation.

Of course, a 2.5σ discrepancy is insufficient to claim a discovery, so we will use the data to determine the lower mass bound of additional neutral gauge bosons. The discrepancy can easily be reached by the contributions due to exchange of extra neutral gauge bosons in the model considered here without affecting the fit with the other experimental data significantly. As mentioned above, the lightest extra neutral gauge boson in the model mainly consists of Z_I . We use the updated value for $Q_W(Cs)$ to put a lower mass bound for the lightest extra neutral gauge boson of 700 GeV with a small mixing. As the mixing increases the masses of extra neutral gauge bosons, its contribution to the weak charge

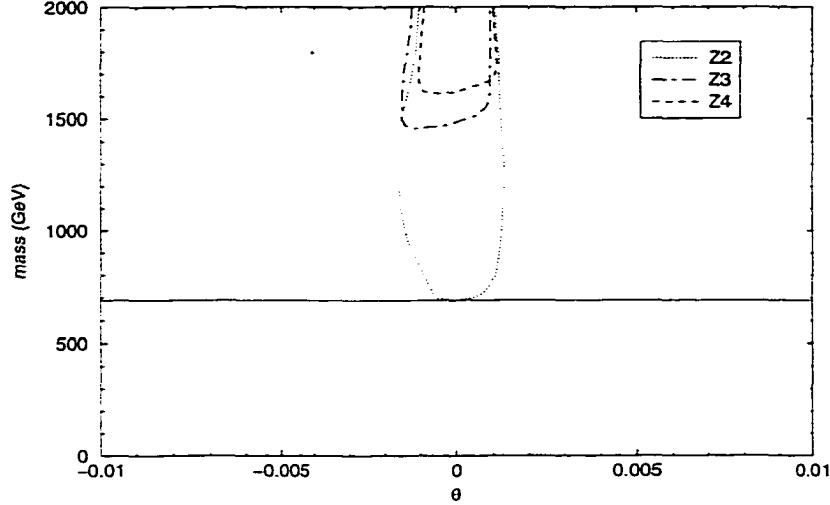


Figure 24: The contours of $\Delta\chi^2 = \chi^2 - \chi^2_{SM} = 1.0$ for extra neutral gauge bosons. The constraints are obtained by use of Z-pole experiments [74], m_W measurement [74], LENC experiments [75] and a proposed measurement of Q_W^P . As a reference the lower direct production limit from CDF [58] for the sequential Z_{SM} is also shown (solid line).

will be lowered compared with the case without mixing, so the lower mass bound on extra neutral gauge bosons will also be a little lowered in order that the contributions are large enough to explain the data.

From Ref. [59] the typical bounds achievable on extra neutral or charged gauge bosons $m_{Z'(W')}$ at the coming colliders such as Tevatron, DiTevatron, LHC, 500 GeV NLC and 1 TeV NLC are approximately 1 TeV, 2 TeV, 4 TeV, 1-3 TeV and 2-6 TeV correspondingly. Therefore the extra neutral gauge bosons in our model can be expected to be studied well in the coming colliding experiments.

3.6.3 Constrains from Z-pole + m_W + LENC data + Q_W^P

In Ref. [99], it is proposed to measure the weak charge of the proton, Q_W^P , with parity-violating ep scattering at $Q^2 = 0.03(\text{GeV}/c)^2$ at Jefferson Lab. A high statistical accuracy is expected to be achieved with the current facility. Specifically $\Delta Q_W^P / Q_W^{0P} \sim 4\%$, even better, is promising. Fig.24 illustrates the constraints on the lightest extra

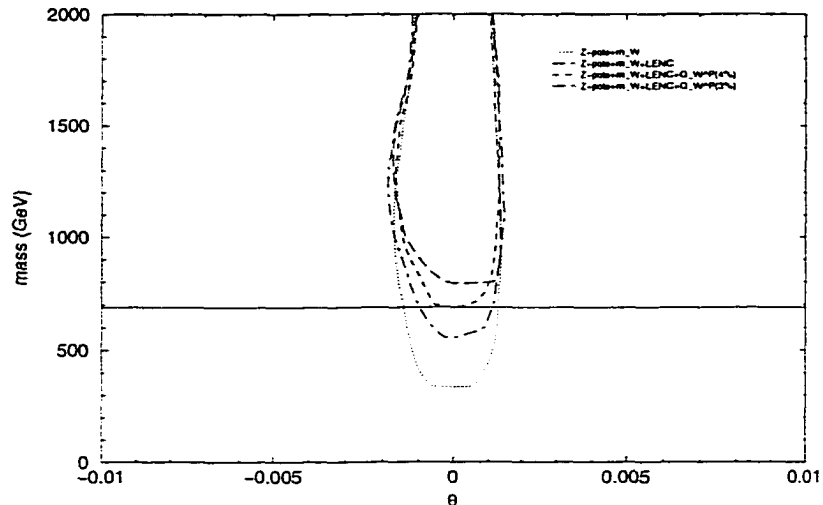


Figure 25: Constraints on the lightest extra neutral gauge boson, Z_2 , with the data of Z-pole experiments [74], m_W measurement [74], LENC experiments [75] and a proposed measurement of Q_W^P (4% and 3%). As a reference the lower direct production limit from CDF [58] for the sequential Z_{SM} is also shown (solid line).

neutral gauge boson including the Q_W^P with different precision levels. It can be found that the lower bounds of the masses of the extra neutral gauge bosons would be raised significantly. With $\Delta Q_W^P/Q_W^{0P} = 4\%$, the lower mass bound for the lightest extra gauge boson is already slightly above the direct search limit for the sequential Z_{SM} boson. With $\Delta Q_W^P/Q_W^{0P} = 3\%$, the bound is about 800 GeV which is much higher than the direct search limit of the sequential Z_{SM} boson. If the experiment were carried out and there were no deviation from the SM observed, the parameter space for the new physics to exist would be highly reduced.

In Ref. [100], the new physics sensitivity of a variety of low-energy parity-violating observables was analyzed. Taken as an example, present and prospective mass limits on an additional gauge boson, Z_χ , were given. Were the precision of measuring the weak charge of the proton 10%(3%), the lower bound could be 585(1100) GeV. This is compatible with our result.

Chapter 4 Fermion sector

4.1 Introduction

Many extensions of the SM, such as grand unified theories, contain exotic fermions. Although the minimal SU(5) only contain the fermions of the SM, a right-handed neutrino is at least needed in the SO(10) model. And many additional fermions appear in E_6 model. There include non-chiral color singlets—N and E leptons, color triplet—h quark, and so on(See Table 1.3). So far there is no experimental indication of exotic fermions. If any one of the exotic fermions is discovered experimentally, it would pinpoint E_6 as the underlying unification group because they are the true hallmark of E_6 .

Strongly interacting exotics, such as heavy quarks, can be produced in abundance at the Tevatron or the LHC. However, particles which are not strongly interacting, such as heavy charged leptons, can best be produced at an electron-positron collider. In general, studies of heavy charged leptons at such colliders focus on s-channel production, through a γ , Z , Z' , etc. The phenomenology of exotic particles in E_6 models has been considered widely [26, 101-107]. A good summary can be found in Ref. [22].

In this chapter, we will first give the Lagrangians relevant to all fermions, discuss briefly masses and mixings of exotic fermions. We will study pair productions of heavy charged leptons. A t-channel contribution due to W_T -boson exchange, which is unsuppressed by mixing angles, is quite important. We calculate the cross section, the left-right and forward-backward asymmetries, and discuss how to differentiate different models. Pair production of the h-quark is also discussed briefly.

4.2 Lagrangians

Lagrangians relevant to fermions contain the kinetic terms for all the fermions, the interactions between gauge bosons and matter multiplets induced through the covariant

derivatives and Yukawa couplings which give interactions between fermions and Higgs bosons and masses to fermions after the spontaneous symmetry breaking.

$$\begin{aligned}
& \sim \bar{h}_L \gamma^\mu [\partial_\mu - \frac{i}{2} g_Y (-\frac{2}{3}) A_\mu - \frac{i}{2} g_{Y'} (-\frac{4}{3}) B_\mu] h_L \\
& + \bar{e}_R \gamma^\mu [\partial_\mu - \frac{i}{2} g_Y (-2) A_\mu - \frac{i}{2} g_{Y'} (-\frac{2}{3}) B_\mu] e_R \\
& + \bar{u}_R \gamma^\mu [\partial_\mu - \frac{i}{2} g_Y (\frac{4}{3}) A_\mu - \frac{i}{2} g_{Y'} (-\frac{2}{3}) B_\mu] u_R \\
& + \left(\begin{array}{c} \bar{\nu} \\ \bar{S} \end{array} \right)_R \gamma^\mu [\partial_\mu - \frac{i}{2} g_I \vec{\tau} \cdot \vec{W}_\mu^I - \frac{i}{2} g_{Y'} (-\frac{5}{3}) B_\mu] \left(\begin{array}{c} \nu \\ S \end{array} \right)_R \\
& + \left(\begin{array}{c} \bar{d} \\ \bar{h} \end{array} \right)_R \gamma^\mu [\partial_\mu - \frac{i}{2} g_I \vec{\tau} \cdot \vec{W}_\mu^I - \frac{i}{2} g_Y (-\frac{2}{3}) A_\mu - \frac{i}{2} g_{Y'} (\frac{1}{3}) B_\mu] \left(\begin{array}{c} d \\ h \end{array} \right)_R \\
& + \left(\begin{array}{c} \bar{u} \\ \bar{d} \end{array} \right)_L \gamma^\mu [\partial_\mu - \frac{i}{2} g_L \vec{\sigma} \cdot \vec{W}_\mu^L - \frac{i}{2} g_Y (\frac{1}{3}) A_\mu - \frac{i}{2} g_{Y'} (\frac{2}{3}) B_\mu] \left(\begin{array}{c} u \\ d \end{array} \right)_L \\
& + \left(\begin{array}{c} \bar{N} \\ \bar{E} \end{array} \right)_R \gamma^\mu [\partial_\mu - \frac{i}{2} g_L \vec{\sigma} \cdot \vec{W}_\mu^L - \frac{i}{2} g_Y (-1) A_\mu - \frac{i}{2} g_{Y'} (\frac{4}{3}) B_\mu] \left(\begin{array}{c} N \\ E \end{array} \right)_R \\
& + Tr \left\{ \left(\begin{array}{c} \bar{\nu} \\ \bar{N} \\ \bar{E} \end{array} \right)_L \gamma^\mu [\partial_\mu - \frac{i}{2} g_L \vec{\sigma} \cdot \vec{W}_\mu^L - \frac{i}{2} g_Y (-1) A_\mu - \frac{i}{2} g_{Y'} (-\frac{1}{3}) B_\mu] \left(\begin{array}{cc} \nu & N \\ e & E \end{array} \right)_L \right. \\
& + \left. \left(\begin{array}{c} \bar{\nu} \\ \bar{e} \end{array} \right)_L \gamma^\mu (-\frac{i}{2} g_I \vec{\tau} \cdot \vec{W}_\mu^I) \left(\begin{array}{cc} \nu & e \\ N & E \end{array} \right)_L \right\} \\
& - f_{ij}^u \bar{u}_{iR} \tilde{H}_2^\dagger \left(\begin{array}{c} u_j \\ d_j \end{array} \right)_L + H.c. \\
& - f_{ij}^h \bar{h}_{iL} N^\dagger \left(\begin{array}{c} d_j \\ h_j \end{array} \right)_R + H.c. \\
& - f_{ij}^{h'} \bar{h}_{iL} N'^\dagger \left(\begin{array}{c} d_j \\ h_j \end{array} \right)_R + H.c. \\
& - f_{ij}^d (\bar{d}_{iR} \tilde{\nu} d_{jL} - \bar{d}_{iR} \tilde{e} u_{jL} - \bar{h}_{iR} H_1^0 d_{jL} + \bar{h}_{iR} H_1^- u_{jL} + H.c. \\
& - f_{ij}^e \bar{e}_{iR} (H_1^0 E_{jL} - \tilde{\nu} e_{jL} - H_1^- N_{jL} + \tilde{e} \nu_{jL}) + H.c. \\
& - f_{ij}^E (\bar{N}_{iR} N_1 N_{jL} - \bar{N}_{iR} N_2 \nu_{jL} - \bar{E}_{iR} N_1 E_{jL} + \bar{E}_{iR} N_2 e_{jL}) + H.c. \\
& - f_{ij}^\nu (\bar{S}_{iR} H_2^+ e_{jL} - \bar{\nu}_{iR} H_2^+ E_{jL} - \bar{S}_{iR} H_2^0 \nu_{jL} + \bar{\nu}_{iR} H_2^0 N_{jL}) + H.c. \tag{180}
\end{aligned}$$

where i, j are generation indices.

4.3 Masses and mixing

After spontaneous symmetry breaking, fermions get masses through the Yukawa couplings. From the most general mass matrix possible in this model, the SM fermions can be mixed with additional fermions. But there is no mixing for u-typed quarks, therefore weak universality restricts the mixing be small. For simplicity the intergenerational mixing will be ignored if it is not necessarily needed.

4.3.1 d-h quark mixing

The most general mass matrix for d-h quarks can be written as

$$\left(\bar{d} \quad \bar{h} \right)_R M^{(dh)} \begin{pmatrix} d \\ h \end{pmatrix}_L + H.c. \quad (181)$$

where $M^{(dh)}$ is a 2×2 matrix. Generally the mass matrix is Hermitian, but it can also be non-Hermitian. To get the mass eigenstates, mixing angles $\theta_L^{(dh)}$ and $\theta_R^{(dh)}$ are introduced through

$$\begin{aligned} d'_L &= \cos \theta_L^{(dh)} d_L + \sin \theta_L^{(dh)} h_L \\ h'_L &= -\sin \theta_L^{(dh)} d_L + \cos \theta_L^{(dh)} h_L \end{aligned} \quad (182)$$

and

$$\begin{aligned} d'_R &= \cos \theta_R^{(dh)} d_R + \sin \theta_R^{(dh)} h_R \\ h'_R &= -\sin \theta_R^{(dh)} d_R + \cos \theta_R^{(dh)} h_R \end{aligned} \quad (183)$$

Then $M^{(dh)}$ become diagonal

$$\begin{pmatrix} m_d & 0 \\ 0 & m_h \end{pmatrix}$$

with

$$m_d = M_{11}^{(dh)} \cos \theta_R^{(dh)} \cos \theta_L^{(dh)} + M_{12}^{(dh)} \cos \theta_R^{(dh)} \sin \theta_L^{(dh)}$$

$$\begin{aligned}
& + M_{21}^{(dh)} \sin \theta_R^{(dh)} \cos \theta_L^{(dh)} + M_{22}^{(dh)} \sin \theta_R^{(dh)} \sin \theta_L^{(dh)} \\
m_h & = M_{11}^{(dh)} \sin \theta_R^{(dh)} \sin \theta_L^{(dh)} - M_{12}^{(dh)} \sin \theta_R^{(dh)} \cos \theta_L^{(dh)} \\
& - M_{21}^{(dh)} \cos \theta_R^{(dh)} \sin \theta_L^{(dh)} + M_{22}^{(dh)} \cos \theta_R^{(dh)} \cos \theta_L^{(dh)}
\end{aligned} \tag{184}$$

and

$$\begin{aligned}
\tan(\theta_R^{(dh)} + \theta_L^{(dh)}) & = \frac{M_{12}^{(dh)} + M_{21}^{(dh)}}{M_{11}^{(dh)} - M_{22}^{(dh)}} \\
\tan(\theta_R^{(dh)} - \theta_L^{(dh)}) & = \frac{M_{21}^{(dh)} - M_{12}^{(dh)}}{M_{11}^{(dh)} + M_{22}^{(dh)}}
\end{aligned} \tag{185}$$

when $M_{12}^{(dh)} = M_{21}^{(dh)}$, that is to say the mass matrix is Hermitian, $\theta_L^{(dh)} = \theta_R^{(dh)}$.

In our model the mass matrix $M^{(dh)}$ has the form

$$\frac{f^d}{\sqrt{2}} \begin{pmatrix} v_3 & 0 \\ -v_1 & 0 \end{pmatrix} + \frac{f^h}{\sqrt{2}} \begin{pmatrix} 0 & n_2 \\ 0 & n_1 \end{pmatrix} + \frac{f'^h}{\sqrt{2}} \begin{pmatrix} 0 & n'_2 \\ 0 & n'_1 \end{pmatrix}, \tag{186}$$

where all the vacuum expectation values and Yukawa coupling constants are unspecified parameters, and there is no experimental values for exotic fermions, so the the mixing angle seem to be arbitrary. Generally the vacuum expectation values n_i and n'_i are much larger than v_i , and the mass of the d-quark is small, so the mass matrix $M^{(dh)}$ can be written as

$$\begin{pmatrix} m & M' \\ m' & M \end{pmatrix},$$

If $M \gg m, m', M'$, then $m_d \simeq m$, $m_h \simeq M$ and $\theta_L^{(dh)} \simeq M'/M$, $\theta_R^{(dh)} \simeq m'/M$. Implications and constraints on quarks, such as h-quark in our model, whose left- and right-handed chiral components are both singlets with respect to the weak-isospin gauge group $SU(2)_L$ were discussed in Ref. [108].

4.3.2 e-E lepton mixing

In our model the mass matrix of e-E leptons has the form

$$\left(\bar{e} \quad \bar{E} \right)_R M^{(eE)} \begin{pmatrix} e \\ E \end{pmatrix}_L + H.c. \tag{187}$$

with

$$M^{(eE)} = \frac{f^e}{\sqrt{2}} \begin{pmatrix} -v_3 & v_1 \\ 0 & 0 \end{pmatrix} + \frac{f^E}{\sqrt{2}} \begin{pmatrix} 0 & 0 \\ n_2 & n_1 \end{pmatrix} + \frac{f'^E}{\sqrt{2}} \begin{pmatrix} 0 & 0 \\ n'_2 & n'_1 \end{pmatrix} \quad (188)$$

Similarly mixing angles $\theta_L^{(eE)}$ and $\theta_R^{(eE)}$ are needed to get mass eigenstates.

$$\begin{aligned} e'_L &= \cos \theta_L^{(eE)} e_L + \sin \theta_L^{(eE)} E_L \\ E'_L &= -\sin \theta_L^{(eE)} e_L + \cos \theta_L^{(eE)} E_L \end{aligned} \quad (189)$$

and

$$\begin{aligned} e'_R &= \cos \theta_R^{(eE)} e_R + \sin \theta_R^{(eE)} E_R \\ E'_R &= -\sin \theta_R^{(eE)} e_R + \cos \theta_R^{(eE)} E_R \end{aligned} \quad (190)$$

4.3.3 Constraints on masses and mixings

Masses and mixing appear to be arbitrary as we don't know the vacuum expectation values and Yukawa coupling constants appearing in the mass matrices. This is even the case in the SM. The details of the observed mass spectrum, from 0.51 MeV of the electron mass to 175 GeV the top quark mass, still remain a mystery in the SM, although masses and mixing angles can somehow be accommodated in the SM. We don't understand the mass spectrum of fermions observed so far, although there have many theoretical attempts ranging from flavor symmetries to relationships in grand unification models. In the case of additional fermions, mass and mixing angles also are arbitrary. A direct bounds can be found that masses of additional fermions should be bounded from below by $M_Z/2$ because they cannot contribute too much to the decay width of the Z boson. But that's not enough. Further constraints on masses and mixing angles can be obtained (in)directly from search for exotic fermions, electroweak precision measurements and theoretical requirements that the SM vacuum is stable and the perturbation is valid up to a large scale [14].

In Ref. [109] a search for unstable heavy fermions with DELPHI at LEP was reported. A mass limits in the region between 70 GeV and 90 GeV was established by the search for pair productions of new leptons at the 95% CL, depending on the channel.

Various considerations on masses and mixings of exotic fermions can be found in the literature mentioned before.

4.4 Pair production of heavy charged leptons

In this subsection, we will study the pair production of heavy charged leptons and study the forward-backward and left-right asymmetries at linear colliders [110]. For simplicity, we neglect the mixing between extra particles (bosons or fermions) and the normal particles of the SM, since such mixing angles are generally small as shown above.

4.4.1 Cross section and asymmetries

The relevant interactions for the process $e^+e^- \rightarrow E^+E^-$ are

$$\begin{aligned}
\mathcal{L} = & \sum_{f=e,E} Q_f \bar{f}_\alpha \gamma^\mu f_\alpha A_\mu + \frac{g_L}{\cos \theta_W} \bar{e}_\alpha \gamma^\mu (T_{e_\alpha}^3 - Q_e \sin^2 \theta_W) e_\alpha Z_\mu \\
& + \frac{g_L}{2 \cos \theta_W} \bar{E}_\alpha \gamma^\mu (1 - 2 \sin^2 \theta_W) E_\alpha Z_\mu \\
& + \frac{g_I}{2\sqrt{2}} \bar{e} \gamma^\mu (1 - \gamma_5) E W_{I\mu} + H.c. \\
& + \frac{g_I}{4} (\bar{E} \gamma^\mu (1 - \gamma_5) E - \bar{e} \gamma^\mu (1 - \gamma_5) e) Z_{I\mu} \\
& + \sum_{f=e,E} g_{Y'} \frac{Y'_{f_\alpha}}{2} \bar{f}_\alpha \gamma^\mu f_\alpha Z'_\mu
\end{aligned} \tag{191}$$

where $\alpha = L$ or R . g_L , g_I and $g_{Y'}$ are coupling constants and θ_W is the electroweak mixing angle. For simplicity, we will assume that $g_I = g_L$ and $g_{Y'} = g_Y$ in our numerical results, it is straightforward to relax this assumption. The first two lines are couplings between fermions and standard γ and Z . The rest are couplings with extra neutral gauge bosons. The $e^+e^- \rightarrow E^+E^-$ process can proceed via s-channel exchange of a γ , Z , Z' or Z_I , and can also proceed via t-channel exchange of a W_I . The Feynman diagrams are

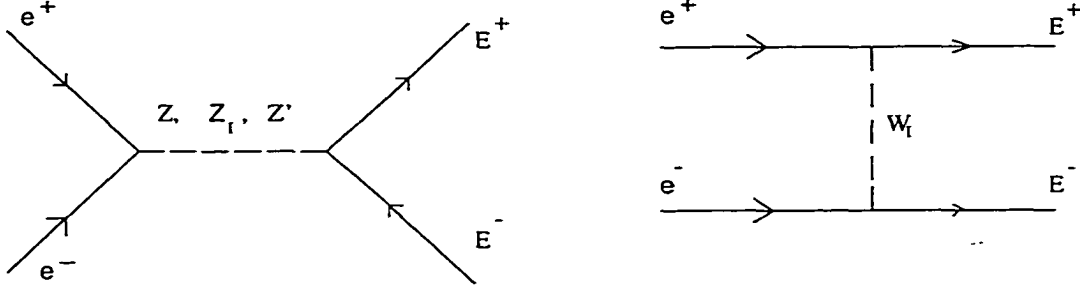


Figure 26: Feynman diagram responsible for $e^+e^- \rightarrow E^+E^-$

listed in Fig. 26. Each amplitude can be written as the form of

$$C_i \bar{v}_e \gamma^\mu (1 - a_i \gamma_5) u_e \bar{u}_E \gamma_\mu (1 - b_i \gamma_5) v_E. \quad (192)$$

Note that the W_t leads to a t-channel process unsuppressed by small mixing angles. This is unique to this model. Note that if one considered production of the heavy charged leptons which form an $SU(2)_I$ doublet with the muon or the tau, then the diagrams would be identical except that the t-channel diagram would be absent.

The differential cross section for this process is given by

$$\frac{d\sigma}{d\cos\theta} = \frac{1}{8\pi s} \sqrt{\frac{1}{4} - \frac{m_E^2}{s}} \{D_1(m_E^2 - u)^2 + D_2(m_E^2 - t)^2 + 2D_3 m_E^2 s\} \quad (193)$$

s , t and u are the Mandelstam variables, and with

$$\begin{aligned} D_1 &= \sum_{i,j=1}^5 C_i C_j \{(1 + a_i a_j)(1 + b_i b_j) + (a_i + a_j)(b_i + b_j)\} \\ D_2 &= \sum_{i,j=1}^5 C_i C_j \{(1 + a_i a_j)(1 + b_i b_j) - (a_i + a_j)(b_i + b_j)\} \\ D_3 &= \sum_{i,j=1}^5 C_i C_j \{(1 + a_i a_j)(1 - b_i b_j)\} \end{aligned} \quad (194)$$

where the C_i , a_i and b_i are given in Table 4.1.

The forward-back asymmetry is defined by

$$A_{FB} = \frac{\int_0^1 \frac{d\sigma}{d\cos\theta} d\cos\theta - \int_{-1}^0 \frac{d\sigma}{d\cos\theta} d\cos\theta}{\int_{-1}^1 \frac{d\sigma}{d\cos\theta} d\cos\theta} \quad (195)$$

Table 4.1 Coefficients appearing in Eq. 194

i	C_i	a_i	b_i
1	$\frac{e^2}{s}$	0	0
2	$\frac{g^2(1-4\sin^2\theta_W)(1-2\sin^2\theta_W)}{8\cos^2\theta_W(s-m_Z^2)}$	$\frac{1}{1-4\sin^2\theta_W}$	0
3	$\frac{-g_I^2}{16(s-m_{Z_I}^2)}$	1	1
4	$\frac{-9g_{Y'}^2}{144(s-m_{Z'}^2)}$	$-\frac{1}{3}$	$-\frac{1}{5}$
5	$\frac{g_I^2}{8(t-m_{W_I}^2)}$	1	1

The left-right asymmetry is defined by

$$A_{LR} = \frac{\sigma_L - \sigma_R}{\sigma_L + \sigma_R}, \quad (196)$$

Note that the C_i , a_i and b_i will be somewhat different for σ_L and σ_R due to the insertion of the projection operator in Eq. (192). They are listed in table 4.2 and Table 4.3. Both A_{FB} and A_{LR} at e^+e^- colliders were studied in Ref. [111, 112], but only s-channel contributions were considered.

4.4.2 Results

The electroweak part $SU(2)_L \times U(1)_Y$ has been measured precisely. Let us first consider the rank 5 case. Setting $g_{Y'} = 0$, we have two gauge boson mass parameters m_{W_I} and m_{Z_I} . We will assume that these masses are equal and thus there is only one mass parameter remaining, which we choose to be near the experimental lower bound for direct production, $m_{Z_I} = 650$ GeV. This is basically the same as assuming that the gauge bosons do not substantially mix with each other. The numerical results for cross section, forward-backward and left-right asymmetries are shown in Fig. 28-30. We have plotted the results for E^+E^- and M^+M^- production, where M is the $SU(2)_I$ partner of the muon or tau (the only difference will be due to the t-channel process). For comparison, we also include the standard model result for both a vectorlike heavy lepton and a chiral heavy lepton. Although we have assumed that the Z_I mass (E, M mass) is 650 GeV (200

Table 4.2 Coefficients appearing in Eq. (194) for calculating σ_L

i	C_i	a_i	b_i
1	$\frac{e^2}{2s}$	1	0
2	$\frac{g^2(1-2\sin^2\theta_W)^2}{8\cos^2\theta_W(s-m_Z^2)}$	1	0
3	$\frac{-g_I^2}{16(s-m_{Z'}^2)}$	1	1
4	$\frac{-3g_{Y'}^2}{144(s-m_{Z'}^2)}$	1	$\frac{5}{3}$
5	$\frac{g_I^2}{8(t-m_{W'}^2)}$	1	1

GeV), it is easy to see how the figures will be qualitatively modified if these assumptions are relaxed.

In the rank 6 model, one has an additional mass scale and additional coupling. If we assume that the $g_{Y'}$ coupling is the same as g_Y , and that the mass of the Z' is $\frac{5g_Y}{3g_I} M_{Z'}$, then one can recalculate the cross section, forward-backward and left-right asymmetries. We find that there is not a substantial difference from the rank 5 case, except in the immediate vicinity of the Z' mass(See Fig. 31-33).

How does one detect these leptons? The main decay modes depend sensitively on the masses and mixing angles. Since the E and its isodoublet partner N are degenerate in the limit of no mixing, one expects the $E \rightarrow NW^*$ to be into a virtual W , leading to a three-body decay. Since the allowed three-body phase space is very small, this decay will be negligible unless the mixing with the lighter generations is extremely small. In the more natural case, in which such mixing is not very small, the two-body decays $E \rightarrow \nu_e W$ and $E \rightarrow eZ$ would dominate. A detailed analysis of the lifetimes and the decay modes can be found in Ref. [14]. There, it was shown that the ratio of $\Gamma(E \rightarrow eZ)$ to $\Gamma(E \rightarrow \nu_e W)$ is given by the ratio of $|U_{Ee}|^2$ to $|U_{E\nu_e}|^2$. This is very model-dependent.

Certainly, the signature for $E \rightarrow eZ$ would be quite dramatic. Even if the Z decays hadronically or invisibly, the monochromatic electron, plus the invariant mass of the Z decay products, would allow for virtually background-free detection. The signature for

Table 4.3 Coefficients appearing in Eq. (194) for calculating σ_R

i	C_i	a_i	b_i
1	$\frac{e^2}{2s}$	-1	0
2	$\frac{-g^2(1-2\sin^2\theta_W)\sin^2\theta_W}{4\cos^2\theta_W(s-m_Z^2)}$	-1	0
3	$\frac{-g_I^2}{16(s-m_{Z_I}^2)}$	0	0
4	$\frac{-6g_{V_I}^2}{144(s-m_{Z_I}^2)}$	-1	$-\frac{5}{3}$
5	$\frac{g_I^2}{8(t-m_{W_I}^2)}$	0	0

$E \rightarrow \nu_e W$ is less dramatic, but would lead to W^+W^- plus missing transverse momentum. As discussed in Ref. [107], requiring that the W 's decay leptonically gives a signal of l^+l^- , where $l = (e, \mu)$. The backgrounds, due to $e^+e^- \rightarrow \tau^+\tau^-$, W^+W^- and ZZ , can be eliminated by calculating the invariant mass of the charged fermion pair. The signal would be striking since it would consist of a pair of l^+l^- with approximately the same invariant mass.

Suppose these leptons are found. One would first learn the cross section. Unless one is in the vicinity of the Z_I resonance, the cross section in this model would be somewhat higher than the standard model. For example, at an NLC of $\sqrt{s} = 500$ GeV and luminosity of 6×10^4 pb $^{-1}$ /yr and for a heavy lepton of 200 GeV, one expects approximately 2×10^4 SM vectorlike fermion pairs produced per year, whereas one has 3×10^4 E^+E^- pairs and 5×10^4 M^+M^- pairs (note that the t-channel process destructively interferes). In the vicinity of the resonance, of course, the cross section can be much larger. As discussed in the previous paragraph, if the main decay is into νW , then a very clear signature arises if both W 's decay into $e\nu_e$ or $\mu\nu_\mu$. This will occur approximately 5% of the time, giving a few thousand such events per year. Necessary cuts on the transverse missing energy will reduce the number of usable events, but it should still be several hundred per year, with very low background. If the main decay is into eZ or μZ , then the signature is even more dramatic.

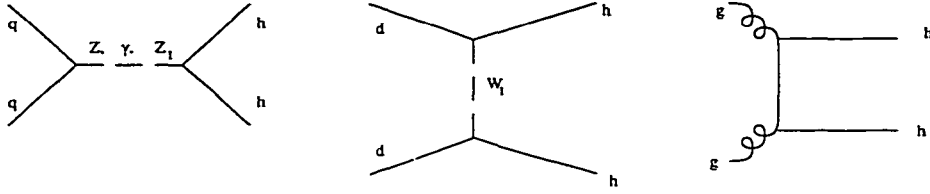


Figure 27: Feynman diagrams at the parton level for pair production of h quark in $pp(\bar{p})$ collisions

There is no forward-backward asymmetry for the pair production of SM vectorlike fermions, while the polarization asymmetry for heavy SM chiral fermions is very small. Therefore, combining A_{FB} with A_{LR} would make it very straightforward to distinguish E^+E^- and M^+M^- pairs from SM fermions. The behavior of the asymmetries for each of these is very different at high \sqrt{s} .

An important point is to note that the statistical uncertainty, $\left(\frac{1-A^2}{N}\right)^{1/2}$, is very small for this model. With the approximate number of reconstructed events being between several hundred and several thousand, this gives a statistical uncertainty of between 1 and 10 percent. This will be even smaller in the vicinity of the resonance. From the figures, it is clear that this uncertainty is small enough that the various models can be distinguished, even off-resonance.

4.5 Pair production of h-quark

The production of h-quark had been studied in great details [26, 102, 113]. Here we mainly consider the W_I contribution of h-quark production in $pp(\bar{p})$ colliders. The diagrams are listed in Fig. 27. Generally the gluon fusion process, $gg \rightarrow h\bar{h}$, dominates over the quark annihilation process, $q\bar{q} \rightarrow h\bar{h}$. It was noted[22] that W_I t-channel exchange contribution is negligible compared to the gluon fusion mechanism.

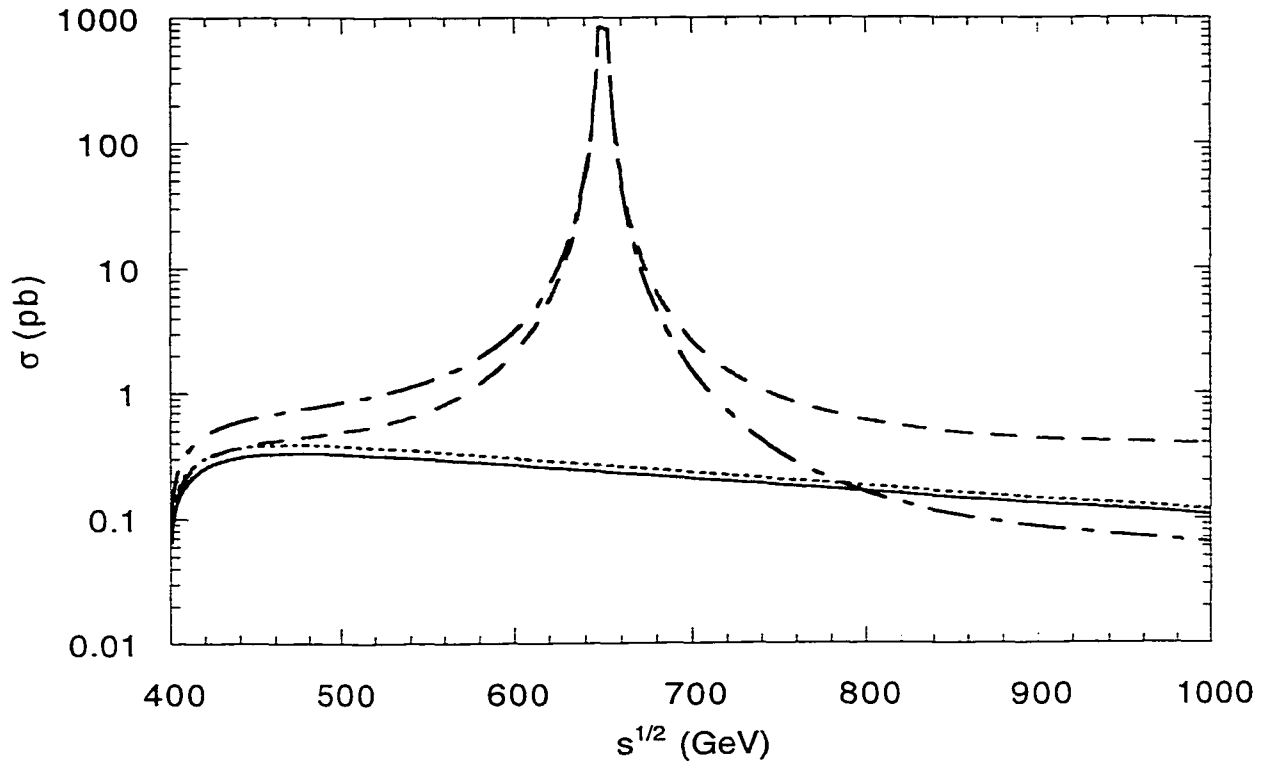


Figure 28: Total cross section for the process $e^+e^- \rightarrow L^+L^-$ as a function of \sqrt{s} , for a heavy lepton of 200 GeV in the rank-5 model. The solid and dotted lines correspond to Standard Model production of chiral and vectorlike fermions, respectively. The dashed and dot-dashed lines correspond to $L = E$ and $L = M$ in the $SU(2)_I$ model, respectively, where E and M are the $SU(2)_I$ partners of the electron and muon.

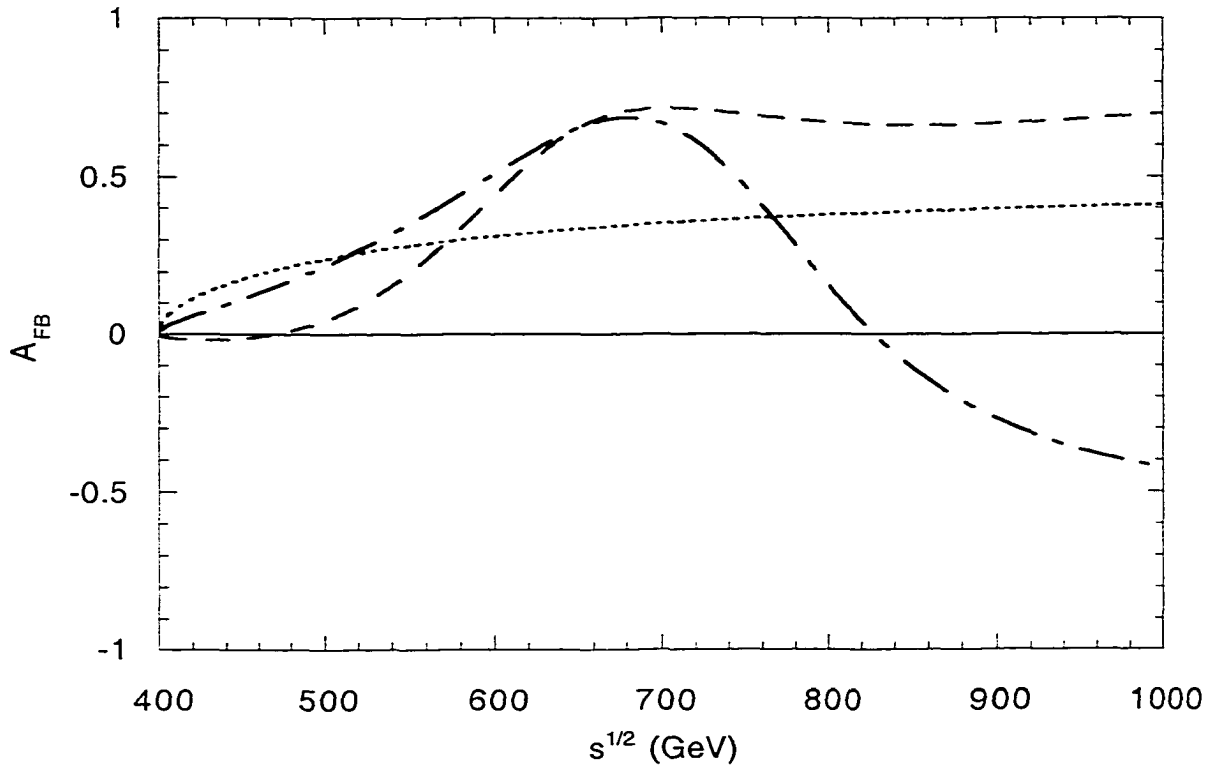


Figure 29: A_{FB} , the forward-backward asymmetry, for the process $e^+e^- \rightarrow L^+L^-$ as a function of \sqrt{s} , for a heavy lepton of 200 GeV in the rank-5 model. The solid and dotted lines correspond to Standard Model production of chiral and vectorlike fermions, respectively. The dashed and dot-dashed lines correspond to $L = E$ and $L = M$ in the $SU(2)_I$ model, respectively, where E and M are the $SU(2)_I$ partners of the electron and muon.

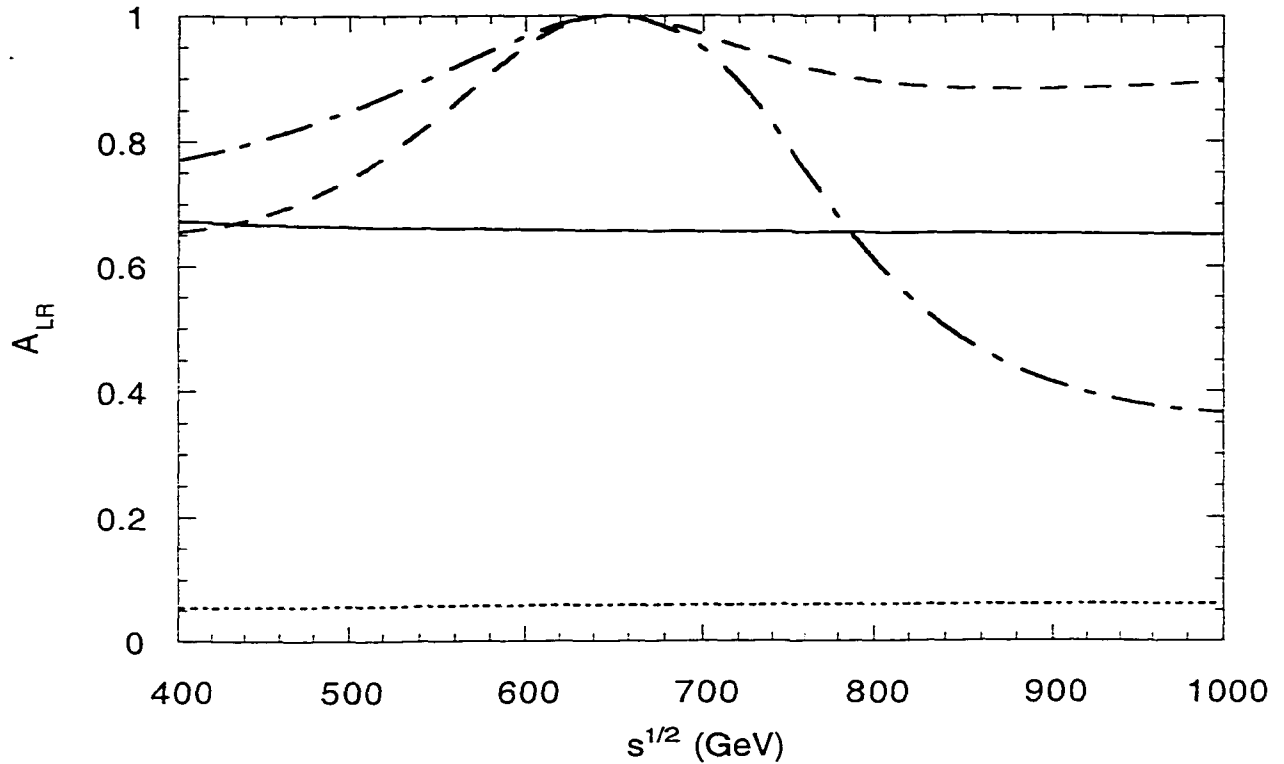


Figure 30: A_{LR} , the left-right asymmetry, for the process $e^+e^- \rightarrow L^+L^-$ as a function of \sqrt{s} , for a heavy lepton of 200 GeV in the rank-5 model. The solid and dotted lines correspond to Standard Model production of chiral and vectorlike fermions, respectively. The dashed and dot-dashed lines correspond to $L = E$ and $L = M$ in the $SU(2)_I$ model, respectively, where E and M are the $SU(2)_I$ partners of the electron and muon.

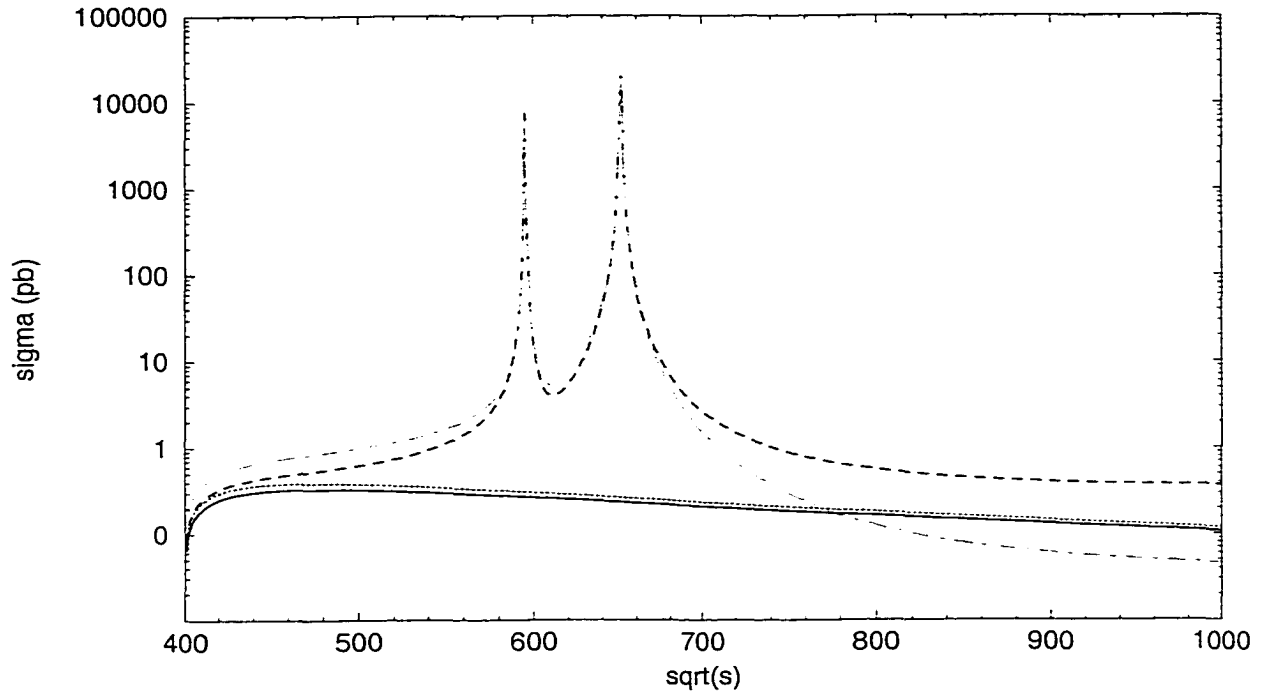


Figure 31: Total cross section for the process $e^+e^- \rightarrow L^+L^-$ as a function of \sqrt{s} , for a heavy lepton of 200 GeV in the rank-6 model. The solid and dotted lines correspond to Standard Model production of chiral and vectorlike fermions, respectively. The dashed and dot-dashed lines correspond to $L = E$ and $L = M$ in the $SU(2)_I$ model, respectively, where E and M are the $SU(2)_I$ partners of the electron and muon.

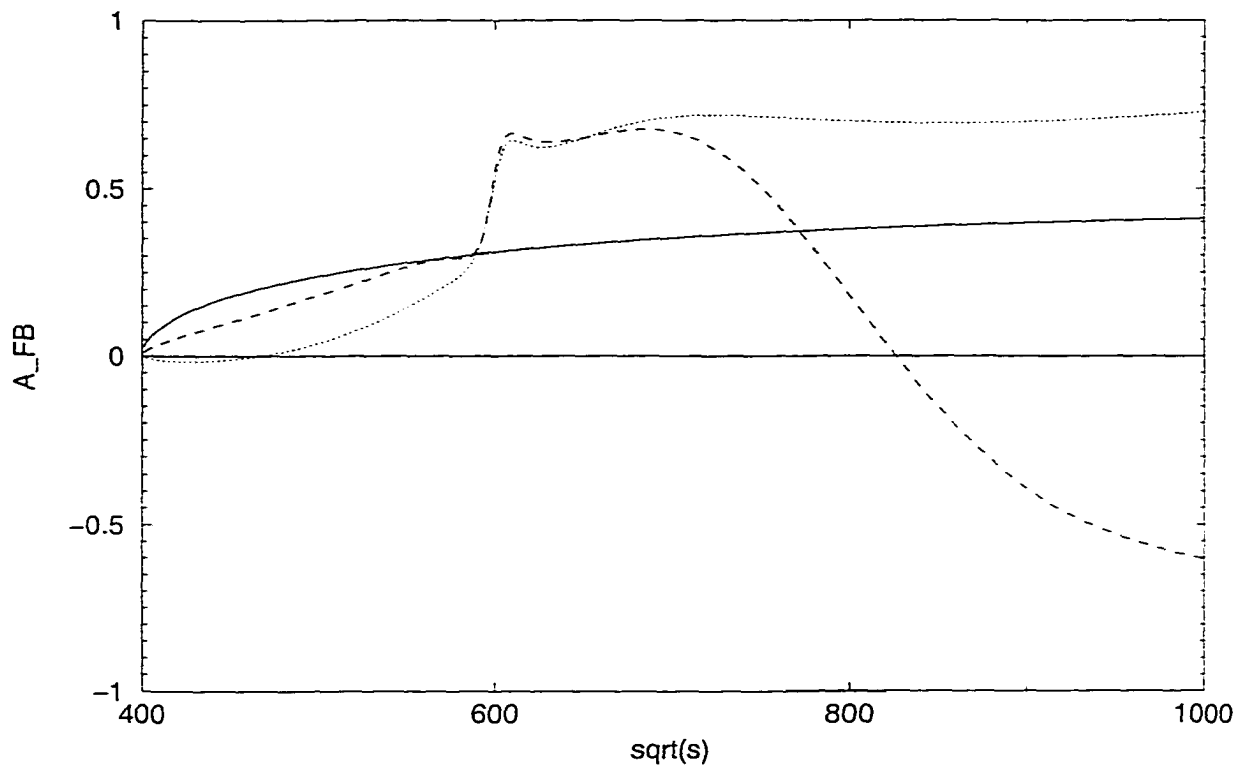


Figure 32: A_{FB} , the forward-backward asymmetry, for the process $e^+e^- \rightarrow L^+L^-$ as a function of \sqrt{s} , for a heavy lepton of 200 GeV in the rank-6 model. The solid and dotted lines correspond to Standard Model production of chiral and vectorlike fermions, respectively. The dashed and dot-dashed lines correspond to $L = E$ and $L = M$ in the $SU(2)_I$ model, respectively, where E and M are the $SU(2)_I$ partners of the electron and muon.

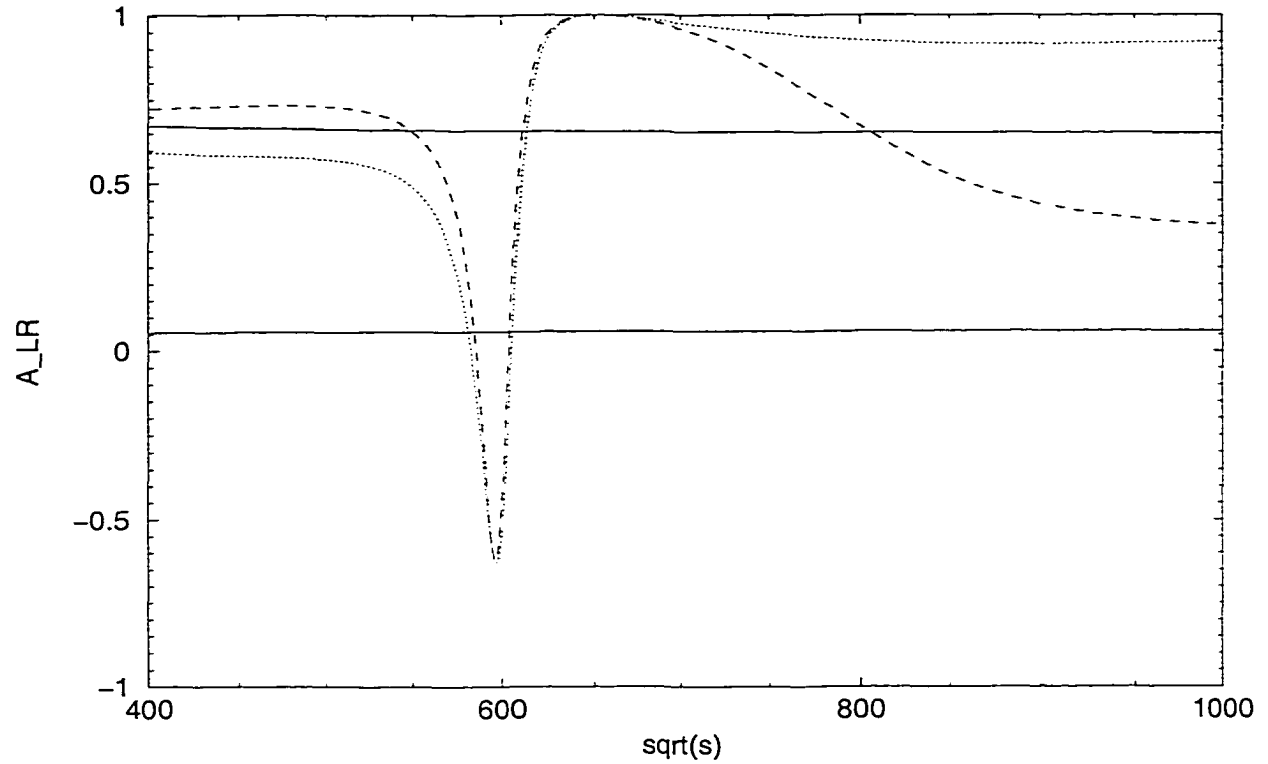


Figure 33: A_{LR} , the left-right asymmetry, for the process $e^+e^- \rightarrow L^+L^-$ as a function of \sqrt{s} , for a heavy lepton of 200 GeV in the rank-6 model. The solid and dotted lines correspond to Standard Model production of chiral and vectorlike fermions, respectively. The dashed and dot-dashed lines correspond to $L = E$ and $L = M$ in the $SU(2)_I$ model, respectively, where E and M are the $SU(2)_I$ partners of the electron and muon.

Chapter 5 Conclusions

We have studied the effective low-energy supersymmetric $SU(2)_L \times SU(2)_I \times U(1)_Y \times U(1)_{Y'}$ model, which is based on the E_6 grand unification theory. $SU(2)_I$ is a subgroup of $SU(3)_R$ and its corresponding gauge bosons are neutral. The Higgs boson sector, gauge boson sector and fermion sector of the model were considered.

A specific Higgs structure was introduced. The scalar potential is highly constrained in the supersymmetric version of the model. An upper bound of about 150 GeV to the lightest neutral Higgs scalar was found. Other Higgs-boson mass relationships were also discussed. Failure to find a Higgs boson with a mass near or below 150 GeV would therefore rule out this supersymmetric E_6 -based model.

Electroweak precision experiments, including Z-pole experiments, m_W measurements and low-energy neutral current experiments were used to put indirect constraints on masses of the extra neutral gauge bosons and the mixings between them and the ordinary Z boson. We also considered the possible constraint from a proposed measurement of the proton's weak charge at Jefferson Lab. It was found that the mixing angles are very small, namely $|\theta| \leq 0.005$. The lower bound for the mass of the lightest extra neutral gauge boson was found to be about 560–800 GeV, which is comparable with the current direct search limit. low-energy neutral current experiments give the strongest bounds on the lightest extra neutral gauge boson. The precise measurement of the weak charge of the proton is anticipated to reduce the parameter space for new physics strongly.

We also studied the pair production of heavy charged exotic leptons at e^+e^- colliders in this model. In addition to the standard γ and Z boson contributions, we also included the contributions from extra neutral gauge bosons. A t-channel contribution due to W_I -boson exchange, which is unsuppressed by mixing angles, is quite important. We calculated the left-right and forward-backward asymmetries, and discussed how to differentiate different models. Pair production of the h-quark was also discussed briefly.

There are many new(exotic) particles, such as various Higgs bosons, extra neutra gauge bosons and additional fermions in this model. There is not any experimental signal for their existence to date. It is anticipated that future experiments, such as Tevatron, LHC, NLC and precise low-energy measurements, may discover them or prove the model is or is not the right model to describe the nature. At the same time more theoretical work is needed to put stricter constraints based on current experimental results, and give more clear guidance where to find new physics beyond the SM.

Appendix

A Various Higgs Boson Mass Squared Matrices

The Higgs-boson mass squared matrix is obtained from

$$M_{ij}^2 = \frac{\partial^2 V}{\partial \phi_i \partial \phi_j} \Big|_{\text{minimum}}. \quad (197)$$

A.1 Scalar Higgs Boson Mass Squared Matrix

The mass-squared matrix for scalar Higgs bosons is a 7×7 symmetric matrix S . The expressions for the matrix elements are listed below.

$$\begin{aligned} S_{11} &= (\lambda n_1 + \lambda' n'_1)^2 + (\lambda^2 + \lambda'^2)v_2^2 + \frac{1}{2}(g_L^2 + g_Y^2 + g_I^2 + \frac{1}{9}g_{Y'}^2)v_1^2 \\ &\quad + \frac{1}{4}g_L^2(v_1^2 - v_2^2 + v_3^2) + \frac{1}{4}g_Y^2(v_1^2 - v_2^2 + v_3^2) + \frac{1}{4}g_I^2(v_1^2 + v_3^2 + n_2^2 - n_1^2 + n_2'^2 - n_1'^2) \\ &\quad + \frac{1}{36}g_{Y'}^2(v_1^2 + 4v_2^2 + v_3^2 - 5(n_1^2 + n_2^2 + n_1'^2 + n_2'^2)) + m_{\mathcal{H}}^2 \\ S_{12} &= 2(\lambda^2 + \lambda'^2)v_1v_2 - \frac{1}{2}(g_L^2 + g_Y^2 - \frac{4}{9}g_{Y'}^2)v_1v_2 + \lambda A n_1 + \lambda' A' n'_1 \\ S_{13} &= -(\lambda n_1 + \lambda' n'_1)(\lambda n_2 + \lambda' n'_2) + \frac{1}{2}(g_L^2 + g_Y^2 + g_I^2 + \frac{1}{9}g_{Y'}^2)v_1v_3 + \frac{1}{2}g_I^2(n_1n_2 + n_1'n_2') \\ S_{14} &= -\lambda v_3(\lambda n_1 + \lambda' n'_1) + \frac{1}{2}g_I^2(v_1n_2 + v_3n_1) - \frac{5}{18}g_{Y'}^2v_1n_2 \\ S_{15} &= 2\lambda v_1(\lambda n_1 + \lambda' n'_1) - \lambda v_3(\lambda n_2 + \lambda' n'_2) + \frac{1}{2}g_I^2(v_3n_2 - v_1n_1) - \frac{5}{18}g_{Y'}^2v_1n_1 + \lambda A v_2 \\ S_{16} &= -\lambda' v_3(\lambda n_1 + \lambda' n'_1) + \frac{1}{2}g_I^2(v_1n_2' + v_3n_1') - \frac{5}{18}g_{Y'}^2v_1n_2' \\ S_{17} &= \lambda' v_1(\lambda n_1 + \lambda' n'_1) + \lambda'[(\lambda n_1 + \lambda' n'_1)v_1 - (\lambda n_2 + \lambda' n'_2)v_3] \\ &\quad + \frac{1}{2}g_I^2(v_3n_2' - v_1n_1') - \frac{5}{18}g_{Y'}^2v_1n_1' + \lambda' A' v_2 \\ S_{22} &= (\lambda n_1 + \lambda' n'_1)^2 + (\lambda n_2 + \lambda' n'_2)^2 + (\lambda^2 + \lambda'^2)(v_1^2 + v_3^2) + \frac{1}{2}(g_L^2 + g_Y^2 + \frac{16}{9}g_{Y'}^2)v_2^2 \\ &\quad - \frac{1}{4}g_L^2(v_1^2 - v_2^2 + v_3^2) + \frac{1}{4}g_Y^2(v_1^2 - v_2^2 + v_3^2) \\ &\quad + \frac{1}{9}g_{Y'}^2(v_1^2 + 4v_2^2 + v_3^2 - 5(n_1^2 + n_2^2 + n_1'^2 + n_2'^2)) + m_{\mathcal{H}_2}^2 \\ S_{23} &= 2(\lambda^2 + \lambda'^2)v_2v_3 - \frac{1}{2}(g_L^2 + g_Y^2 - \frac{4}{9}g_{Y'}^2)v_2v_3 - \lambda A n_2 - \lambda' A' n_2' \end{aligned}$$

$$\begin{aligned}
S_{24} &= 2\lambda v_2(\lambda n_2 + \lambda' n'_2) - \frac{10}{9}g_{Y'}^2 v_2 n_2 - \lambda A v_3 \\
S_{25} &= 2\lambda v_2(\lambda n_1 + \lambda' n'_1) - \frac{10}{9}g_{Y'}^2 v_2 n_1 + \lambda A v_1 \\
S_{26} &= 2\lambda' v_2(\lambda n_2 + \lambda' n'_2) - \frac{10}{9}g_{Y'}^2 v_2 n'_2 - \lambda' A' v_3 \\
S_{27} &= 2\lambda' v_2(\lambda n_1 + \lambda' n'_1) - \frac{10}{9}g_{Y'}^2 v_2 n'_1 + \lambda' A' v_1 \\
S_{33} &= (\lambda n_2 + \lambda' n'_2)^2 + (\lambda^2 + \lambda'^2)v_2^2 + \frac{1}{2}(g_L^2 + g_Y^2 + g_I^2 + \frac{1}{9}g_{Y'}^2)v_3^2 \\
&\quad + \frac{1}{4}g_L^2(v_1^2 - v_2^2 + v_3^2) + \frac{1}{4}g_Y^2(v_1^2 - v_2^2 + v_3^2) + \frac{1}{4}g_I^2(v_1^2 + v_3^2 + n_1^2 - n_2^2 + n_1'^2 - n_2'^2) \\
&\quad + \frac{1}{36}g_{Y'}^2(v_1^2 + 4v_2^2 + v_3^2 - 5(n_1^2 + n_2^2 + n_1'^2 + n_2'^2)) + m_H^2 \\
S_{34} &= 2(\lambda n_2 + \lambda' n'_2)\lambda v_3 - (\lambda n_1 + \lambda' n'_1)\lambda v_1 + \frac{1}{2}g_I^2(v_1 n_1 - v_3 n_2) - \frac{5}{18}g_{Y'}^2 v_3 n_2 - \lambda A v_2 \\
S_{35} &= -(\lambda n_2 + \lambda' n'_2)\lambda v_1 + \frac{1}{2}g_I^2(v_1 n_2 + v_3 n_1) - \frac{5}{18}g_{Y'}^2 v_3 n_1 \\
S_{36} &= 2(\lambda n_2 + \lambda' n'_2)\lambda' v_3 - (\lambda n_1 + \lambda' n'_1)\lambda' v_1 + \frac{1}{2}g_I^2(v_1 n'_1 - v_3 n'_2) - \frac{5}{18}g_{Y'}^2 v_3 n'_2 - \lambda' A' v_2 \\
S_{37} &= -(\lambda n_2 + \lambda' n'_2)\lambda' v_1 + \frac{1}{2}g_I^2(v_1 n'_2 + v_3 n'_1) - \frac{5}{18}g_{Y'}^2 v_3 n'_1 \\
S_{44} &= \lambda^2(v_2^2 + v_3^2) + \frac{1}{2}(g_I^2 + \frac{25}{9}g_{Y'}^2)n_2^2 + \frac{1}{4}g_I^2(v_1^2 - v_3^2 + n_1^2 + n_2^2 - n_1'^2 + n_2'^2) \\
&\quad - \frac{5}{36}g_{Y'}^2(v_1^2 + 4v_2^2 + v_3^2 - 5(n_1^2 + n_2^2 + n_1'^2 + n_2'^2)) + m_N^2 \\
S_{45} &= -\lambda^2 v_1 v_3 + \frac{1}{2}g_I^2(v_1 v_3 + n_1 n_2 + n_1' n_2') + \frac{25}{18}g_{Y'}^2 n_1 n_2 \\
S_{46} &= \lambda\lambda'(v_2^2 + v_3^2) + \frac{1}{2}g_I^2(n_1 n_1' + n_2 n_2') + \frac{25}{18}g_{Y'}^2 n_2 n_2' - m_3^2 \\
S_{47} &= -\lambda\lambda' v_1 v_3 + \frac{1}{2}g_I^2(n_1 n_2' - n_2 n_1') + \frac{25}{18}g_{Y'}^2 n_2 n_1' \\
S_{55} &= \lambda^2(v_1^2 + v_2^2) + \frac{1}{2}(g_I^2 + \frac{25}{9}g_{Y'}^2)n_1^2 + \frac{1}{4}g_I^2(v_3^2 - v_1^2 + n_1^2 + n_2^2 + n_1'^2 - n_2'^2) \\
&\quad - \frac{5}{36}g_{Y'}^2(v_1^2 + 4v_2^2 + v_3^2 - 5(n_1^2 + n_2^2 + n_1'^2 + n_2'^2)) + m_N^2 \\
S_{56} &= -\lambda^2 v_1 v_3 + \frac{1}{2}g_I^2(n_2 n_1' - n_1 n_2') + \frac{25}{18}g_{Y'}^2 n_1 n_2' \\
S_{57} &= \lambda\lambda'(v_1^2 + v_2^2) + \frac{1}{2}g_I^2(n_1 n_1' + n_2 n_2') + \frac{25}{18}g_{Y'}^2 n_1 n_1' - m_3^2 \\
S_{66} &= \lambda'^2(v_2^2 + v_3^2) + \frac{1}{2}(g_I^2 + \frac{25}{9}g_{Y'}^2)n_2'^2 + \frac{1}{4}g_I^2(v_1^2 - v_3^2 + n_1'^2 + n_2'^2 - n_1^2 + n_2^2) \\
&\quad - \frac{5}{36}g_{Y'}^2(v_1^2 + 4v_2^2 + v_3^2 - 5(n_1^2 + n_2^2 + n_1'^2 + n_2'^2)) + m_N^2
\end{aligned}$$

$$\begin{aligned}
S_{67} &= -\lambda'^2 v_1 v_3 + \frac{1}{2} g_I^2 (v_1 v_3 + n_1 n_2 + n'_1 n'_2) + \frac{25}{18} g_Y^2 n'_1 n'_2 \\
S_{77} &= \lambda'^2 (v_1^2 + v_2^2) + \frac{1}{2} (g_I^2 + \frac{25}{9} g_Y^2) n_1'^2 + \frac{1}{4} g_I^2 (v_3^2 - v_1^2 + n_1'^2 + n_2'^2 + n_1^2 - n_2^2) \\
&\quad - \frac{5}{36} g_Y^2 (v_1^2 + 4v_2^2 + v_3^2 - 5(n_1^2 + n_2^2 + n_1'^2 + n_2'^2)) + m_{N'}^2
\end{aligned} \tag{198}$$

A.2 Pseudocalar Higgs Boson Mass Squared Matrix

The mass-squared matrix for pseudoscalar Higgs bosons is also a 7×7 symmetric matrix

P . The expressions for the matrix elements are listed below.

$$\begin{aligned}
P_{11} &= (\lambda n_1 + \lambda' n'_1)^2 + (\lambda^2 + \lambda'^2) v_2^2 + \frac{1}{4} g_L^2 (v_1^2 - v_2^2 + v_3^2) \\
&\quad + \frac{1}{4} g_Y^2 (v_1^2 - v_2^2 + v_3^2) + \frac{1}{4} g_I^2 (v_1^2 + v_3^2 + n_2^2 - n_1^2 + n_2'^2 - n_1'^2) \\
&\quad + \frac{1}{36} g_Y^2 (v_1^2 + 4v_2^2 + v_3^2 - 5(n_1^2 + n_2^2 + n_1'^2 + n_2'^2)) + m_{\mathcal{H}}^2 \\
P_{12} &= \lambda A n_1 + \lambda' A' n'_1 \\
P_{13} &= -(\lambda n_1 + \lambda' n'_1)(\lambda n_2 + \lambda' n'_2) + \frac{1}{2} g_I^2 (n_1 n_2 + n'_1 n'_2) \\
P_{14} &= \lambda v_3 (\lambda n_1 + \lambda' n'_1) - \frac{1}{2} g_I^2 v_3 n_1 \\
P_{15} &= -\lambda v_3 (\lambda n_2 + \lambda' n'_2) + \frac{1}{2} g_I^2 v_3 n_2 + \lambda A v_2 \\
P_{16} &= \lambda' v_3 (\lambda n_1 + \lambda' n'_1) - \frac{1}{2} g_I^2 v_3 n'_1 \\
P_{17} &= -\lambda' v_3 (\lambda n_2 + \lambda' n'_2) + \frac{1}{2} g_I^2 v_3 n'_2 + \lambda' A' v_2 \\
P_{22} &= (\lambda n_1 + \lambda' n'_1)^2 + (\lambda n_2 + \lambda' n'_2)^2 + (\lambda^2 + \lambda'^2) (v_1^2 + v_3^2) - \frac{1}{4} g_L^2 (v_1^2 - v_2^2 + v_3^2) \\
&\quad + \frac{1}{4} g_Y^2 (v_1^2 - v_2^2 + v_3^2) + \frac{1}{9} g_Y^2 (v_1^2 + 4v_2^2 + v_3^2 - 5(n_1^2 + n_2^2 + n_1'^2 + n_2'^2)) + m_{H_2}^2 \\
P_{23} &= -\lambda A n_2 - \lambda' A' n'_2 \\
P_{24} &= \lambda A v_3 \\
P_{25} &= -\lambda A v_1 \\
P_{26} &= \lambda' A' v_3 \\
P_{27} &= -\lambda' A' v_1
\end{aligned}$$

$$\begin{aligned}
P_{33} &= (\lambda n_2 + \lambda' n'_2)^2 + (\lambda^2 + \lambda'^2) v_2^2 + \frac{1}{4} g_L^2 (v_1^2 - v_2^2 + v_3^2) \\
&\quad + \frac{1}{4} g_Y^2 (v_1^2 - v_2^2 + v_3^2) + \frac{1}{4} g_I^2 (v_1^2 + v_3^2 + n_1^2 - n_2^2 + n_1'^2 - n_2'^2) \\
&\quad + \frac{1}{36} g_{Y'}^2 (v_1^2 + 4v_2^2 + v_3^2 - 5(n_1^2 + n_2^2 + n_1'^2 + n_2'^2)) + m_{\mathcal{H}}^2 \\
P_{34} &= -(\lambda n_1 + \lambda' n'_1) \lambda v_1 + \frac{1}{2} g_I^2 v_1 n_1 - \lambda A v_2 \\
P_{35} &= (\lambda n_2 + \lambda' n'_2) \lambda v_1 - \frac{1}{2} g_I^2 v_1 n_2 \\
P_{36} &= -(\lambda n_1 + \lambda' n'_1) \lambda' v_1 + \frac{1}{2} g_I^2 v_1 n'_1 - \lambda' A' v_2 \\
P_{37} &= (\lambda n_2 + \lambda' n'_2) \lambda' v_1 - \frac{1}{2} g_I^2 v_1 n'_2 \\
P_{44} &= \lambda^2 (v_2^2 + v_3^2) + \frac{1}{4} g_I^2 (v_1^2 - v_3^2 + n_1^2 + n_2^2 - n_1'^2 + n_2'^2) \\
&\quad - \frac{5}{36} g_{Y'}^2 (v_1^2 + 4v_2^2 + v_3^2 - 5(n_1^2 + n_2^2 + n_1'^2 + n_2'^2)) + m_N^2 \\
P_{45} &= -\lambda^2 v_1 v_3 + \frac{1}{2} g_I^2 (v_1 v_3 + n_1' n'_2) \\
P_{46} &= \lambda \lambda' (v_2^2 + v_3^2) + \frac{1}{2} g_I^2 n_1 n'_1 - m_3^2 \\
P_{47} &= -\lambda \lambda' v_1 v_3 - \frac{1}{2} g_I^2 n_1 n'_2 \\
P_{55} &= \lambda'^2 (v_1^2 + v_2^2) + \frac{1}{4} g_I^2 (v_3^2 - v_1^2 + n_1^2 + n_2^2 + n_1'^2 - n_2'^2) \\
&\quad - \frac{5}{36} g_{Y'}^2 (v_1^2 + 4v_2^2 + v_3^2 - 5(n_1^2 + n_2^2 + n_1'^2 + n_2'^2)) + m_N^2 \\
P_{56} &= -\lambda^2 v_1 v_3 - \frac{1}{2} g_I^2 n_2 n'_1 \\
P_{57} &= \lambda \lambda' (v_1^2 + v_2^2) + \frac{1}{2} g_I^2 n_2 n'_2 - m_3^2 \\
P_{66} &= \lambda'^2 (v_2^2 + v_3^2) + \frac{1}{4} g_I^2 (v_1^2 - v_3^2 + n_1'^2 + n_2'^2 - n_1^2 + n_2^2) \\
&\quad - \frac{5}{36} g_{Y'}^2 (v_1^2 + 4v_2^2 + v_3^2 - 5(n_1^2 + n_2^2 + n_1'^2 + n_2'^2)) + m_N^2 \\
P_{67} &= -\lambda'^2 v_1 v_3 + \frac{1}{2} g_I^2 (v_1 v_3 + n_1 n_2) \\
P_{77} &= \lambda'^2 (v_1^2 + v_2^2) + \frac{1}{4} g_I^2 (v_3^2 - v_1^2 + n_1'^2 + n_2'^2 + n_1^2 - n_2^2) \\
&\quad - \frac{5}{36} g_{Y'}^2 (v_1^2 + 4v_2^2 + v_3^2 - 5(n_1^2 + n_2^2 + n_1'^2 + n_2'^2)) + m_N^2
\end{aligned} \tag{199}$$

A.3 Charged Higgs Boson Mass Squared Matrix

The mass-squared matrix for charged Higgs bosons is a 3×3 symmetric matrix C . The expressions for the matrix elements are listed below.

$$\begin{aligned}
C_{11} &= (\lambda n_1 + \lambda' n'_1)^2 + \frac{1}{4} g_L^2 (v_1^2 - v_2^2 + v_3^2) + \frac{1}{4} g_I^2 (v_1^2 + v_3^2 + n_2^2 - n_1^2 + n_2'^2 - n_1'^2) \\
&\quad + \frac{1}{4} g_Y^2 (v_1^2 - v_2^2 + v_3^2) + \frac{1}{36} g_{Y'}^2 (v_1^2 + 4v_2^2 + v_3^2 - 5(n_1^2 + n_2^2 + n_1'^2 + n_2'^2)) + m_{\mathcal{H}}^2 \\
C_{12} &= (\lambda^2 + \lambda'^2) v_1 v_2 - \frac{1}{2} g_L^2 v_1 v_2 + \lambda A n_1 + \lambda' A' n'_1 \\
C_{13} &= -(\lambda n_1 + \lambda' n'_1)(\lambda n_2 + \lambda' n'_2) + \frac{1}{2} g_L^2 v_1 v_3 + \frac{1}{2} g_I^2 (v_1 v_3 n_1 n_2 + n_1' n_2') \\
C_{22} &= (\lambda n_1 + \lambda' n'_1)^2 + (\lambda n_2 + \lambda' n'_2)^2 + \frac{1}{4} g_L^2 (v_1^2 + v_2^2 + v_3^2) \\
&\quad - \frac{1}{4} g_Y^2 (v_1^2 - v_2^2 + v_3^2) + \frac{1}{9} g_{Y'}^2 (v_1^2 + 4v_2^2 + v_3^2 - 5(n_1^2 + n_2^2 + n_1'^2 + n_2'^2)) + m_{\mathcal{H}_2}^2 \\
C_{23} &= (\lambda^2 + \lambda'^2) v_2 v_3 - \frac{1}{2} g_L^2 v_2 v_3 - \lambda A n_2 - \lambda' A' n'_2 \\
C_{33} &= (\lambda n_2 + \lambda' n'_2)^2 + \frac{1}{4} g_L^2 (-v_1^2 + v_2^2 + v_3^2) + \frac{1}{4} g_I^2 (v_1^2 + v_3^2 + n_1^2 - n_2^2 + n_1'^2 - n_2'^2) \\
&\quad + \frac{1}{4} g_Y^2 (v_1^2 - v_2^2 + v_3^2) + \frac{1}{36} g_{Y'}^2 (v_1^2 + 4v_2^2 + v_3^2 - 5(n_1^2 + n_2^2 + n_1'^2 + n_2'^2)) + m_{\mathcal{H}}^2
\end{aligned} \tag{200}$$

References

- [1] S. L. Glashow, Nucl. Phys. **22**, 579 (1961);
A. Salam and J. C. Ward, Phys. Lett. **13**, 168 (1964);
S. Weinberg, Phys. Rev. Lett. **19**, 1264 (1967).
- [2] P. Langacker, Phys. Rep. **72**, 185 (1981);
S. M. Bilenky and J. Hosek, Phys. Rep. **90**, 73 (1982);
H. Fritzsch and P. Minkowski, Phys. Rep. **73**, 67 (1981).
- [3] F. Abe *et al.* (CDF Collaboration) Phys. Rev. Lett. **74**, 2626 (1995);
S. Abachi *et al.* (D0 Collaboration) Phys. Rev. Lett. **74**, 2632 (1995);
C. Campagnari and M. Franklin, Rev. Mod. Phys. **69**, 137 (1997).
- [4] DONUT Collaboration, Nucl. Phys. Proc. Suppl. **77**, 259 (1999).
- [5] The L3 Collaboration, M. Acciarri *et al.*, Phys. Lett. **B495**, 18 (2000).
- [6] The ALEPH Collaboration, R. Barate *et al.*, Phys. Lett. **B495**, 1 (2000).
- [7] The OPAL Collaboration, G. Abbiendi *et al.*, Phys. Lett. **B499**, 38 (2001).
- [8] The DELPHI Collaboration, P. Abreu *et al.*, Phys. Lett. **B499**, 23 (2001).
- [9] J. Erler, P. Langacker, *Physics beyond the Standard Model* (WEIN 98), ed. P. Herczeg *et al.*, World Scientific, 1999, hep-ph/9809352;
G. Bhattacharyya, J. Phys. **A72**, 469 (1998);
D. Karlen, High energy physics, Vol. 1, P47, Vancouver 1998, ed. A. Astbury *et al.*, World Scientific, 1999.
- [10] Y. Fukuda *et al.*, Phys. Rev. Lett. **82**, 1810 (1999);
For a review, see J. M. Conrad, Proceedings of 29th International Conference on

High-Energy Physics (ICHEP98), Vancouver, Canada, ed. A. Astbury *et al.*, World Scientific, 1999, hep-ex/9811009.

- [11] R. N. Mohapatra, *Unification and Supersymmetry* (Springer, New York, 1986) and references therein.
- [12] The LEP Collaboration and the LEP Electroweak Working Group, J. Mnich, International Europhysics Conference, Tampere, Finland (July 1999), ed. K. Huitu *et al.*, UK, IOP, 2000.
- [13] L3: M. Acciarri *et al.*, Phys. Lett. **B431**, 199 (1998);
DELPHI: P. Abreu *et al.*, Z. Phys. **C74**, 577 (1997);
OPAL: R. Akers *et al.*, Z. Phys. **C65**, 47 (1995);
ALEPH: D. Buskulic *et al.*, Phys. Lett. **B313**, 520 (1993).
- [14] P. H. Frampton, P. Q. Hung and M. Sher, Phys. Rep. **330**, 263 (2000).
- [15] M. Kaku, *Introduction to Superstrings and M-Theory*, Springer 1998.
- [16] J. C. Pati and A. Salam, Phys. Rev. Lett. **31**, 661 (1973); Phys. Rev. **D8**, 1240 (1973).
- [17] H. Georgi and S. L. Glashow, Phys. Rev. Lett. **32**, 438 (1980).
- [18] H. Georgi, H. Quinn and S. Weinberg, Phys. Rev. Lett. **33**, 451 (1974).
- [19] H. Georgi, in: Proc. APS Division of Particle and Fields Meeting (Williamsburg, VA) ed. C. E. Carlson (AIP, New York, 1975) p.575;
H. Fritsch and P. Minkowski, Ann. Phys. (NY) **93**, 193 (1975);
R. N. Mohapatra and J. C. Pati, Phys. Rev. **D11**, 566 (1975);
G. Senjanovic and R. N. Mohapatra, Phys. Rev. **D12**, 1502 (1975);

- A. DeRújula, H. Georgi and S. L. Glashow, *Ann. Phys. (NY)* **109**, 242 (1977);
 R. Marshak and R. N. Mohapatra, *Phys. Lett.* **B91**, 222 (1980).
- [20] M. B. Green and J. H. Schwarz, *Phys. Lett.* **B149**, 117 (1984).
- [21] D. Gross, J. Harvey, E. Martinec and R. Rohm, *Phys. Rev. Lett.* **54**, 502 (1985);
Nucl. Phys. **B256**, 253(1985); **B267**, 75(1986);
 P. Candelas, G. Horowitz, A. Strominger and E. Witten, *Nucl. Phys.* **B258**, 519
 (1985);
 E. Witten, *Nucl. Phys.* **B258**, 75 (1985); *Phys. Lett.* **B149**, 351 (1984).
- [22] J. L. Hewett and T. G. Rizzo, *Phys. Rep.* **183**, 193 (1989).
- [23] H. Georgi, *Lie algebras in particle physics : from isospin to unified theories*, Benjamin/Cummings Pub. Co., 1982.
- [24] R. Slansky, *Phys. Rep.* **79**, 1 (1981).
- [25] T. G. Rizzo, Ames Lab Report IS-J-2823, IS-J-2821(1987); *Phys. Rev.* **D38**, 71
 (1988); *Phys. Rev.* **D39**, 3490 (1989).
- [26] S. Godfrey, *Phys. Lett.* **B195**, 78 (1987).
- [27] P. Langacker, *Phys. Rep.* **72**, 185 (1981).
- [28] M. Sher, *Phys. Rep.* **179**, 273 (1989).
- [29] M. Sher, *Phys. Lett.* **B317**, 159 (1993) ; J. A. Casas, J. R. Espinosa and M. Quiros, *Phys. Lett.* **B324**, 171 (1995) and *Phys. Lett.* **B382**, 374 (1996) ; J. R. Espinosa and M. Quiros, *Phys. Lett.* **B353**, 257 (1995) .

- [30] K. Riesselmann, *Limitations of a Standard Model Higgs Boson*, The 35th Course of the International School of Subnuclear Physics: "Highlights: 50 Years Later", Erice, Italy, Aug. 1997, ed. A. Zichichi, World Scientific, 1999, hep-ph/9711456.
- [31] D. E. Groom *et al.* (Particle Data Group), *Eur. Phys. Jour.* **C15**, 1 (2000).
- [32] LEP Electroweak Working Group, <http://lepewwg.web.cern.ch/LEPEWWG/>.
- [33] S. L. Glashow and S. Weinberg, *Phys. Rev.* **D15**, 1958 (1977).
- [34] M. Sher, *Perspectives in Higgs Physics I*, G. Kane, ed. (World Scientific, 1994).
- [35] T. P. Cheng and M. Sher, *Phys. Rev.* **D35**, 3484 (1987).
- [36] A. Antaramian, L. J. Hall and A. Rasin, *Phys. Rev. Lett.* **69**, 1871 (1992) .
- [37] L. J. Hall and S. Weinberg, *Phys. Rev.* **D48**, R979 (1993).
- [38] M. J. Savage, *Phys. Lett.* **B266**, 135 (1991) .
- [39] M. Luke and M.J. Savage, *Phys. Lett.* **B307**, 387 (1993) .
- [40] W. S. Hou, *Phys. Lett.* **B296**, 179 (1992) .
- [41] D. Atwood, L. Reina and A. Soni, *Phys. Rev.* **D53**, 1199 (1996)
- [42] D. Atwood, L. Reina and A. Soni, *Phys. Rev. Lett.* **75**, 3800 (1995) .
- [43] D. Atwood, L. Reina and A. Soni, *Phys. Rev.* **D55**, 3156 (1997).
- [44] E821 Collaboration, preliminary result announced at APS Meeting, Columbus, OH, April 1998.
- [45] M. Sher and Y. Yuan, *Phys. Rev.* **D44**, 1461 (1991).

- [46] S. Nie and M. Sher, *Phys. Rev.* **D58**, 097701 (1998).
- [47] V. W. Hughes, in *Frontiers of High Energy Spin Physics* edited by T. Hasegawa, *et al.* (Universal Academy Press, Tokyo, 1992), pp. 717-722.
- [48] Muon $g-2$ Collaboration, H. N. Brown, *et al.*, *Phys. Rev. Lett.* **86**, 2227 (2001).
- [49] S. Nie and M. Sher, *Phys. Lett.* **B449**, 89 (1999).
- [50] F. M. Borzumati and C. Grueb, hep-ph/9810240, Proc. of XXIX Int'l Conference on High Energy Physics, Vancouver, BC, Canada, July 1998, ed. A. Astbury *et al.*, World Scientific, 1999.
- [51] T. M. Aliev and E. O. Iltan, *J. Phys.* **G25**, 989 (1999).
- [52] H. E. Haber and M. Sher, *Phys. Rev.* **D35**, 2206 (1987).
- [53] L3 Collaboration, M. Acciarri *et al.*, *Phys. Lett.* **B471**, 321 (1999).
- [54] UA1 Collab., C. Albajar *et al.*, *Phys. Lett.* **B198**, 271 (1987).
- [55] UA2 Collab., R. Ansari *et al.*, *Phys. Lett.* **B195**, 613 (1987).
- [56] V. Barger, N. G. Deshpande, J. L. Rosner and K. Whisnant, *Phys. Rev.* **D35**, 2893 (1987).
- [57] J. Ellis, P. J. Franzini and F. Zwirner, *Phys. Lett.* **B202**, 417 (1988).
- [58] F. Abe, *et al.*, *Phys. Rev. Lett.*, Vol. **79**, 2192 (1997).
- [59] M. Cvetič and S. Godfrey, Summary of the Working Subgroup on Extra Gauge Bosons of the DPF Long-Range Planning Study, in *Electroweak Symmetry Breaking and Beyond the Standard Model*, (ed). T. Barklow, S. Dawson, H. Haber, and J. Seigrüst, World Scientific (1995) hep-ph/9504216.

- [60] P. Langacker and M. Luo, Phys. Rev. **D45**, 278 (1992).
- [61] J. Erler and P. Langacker, Phys. Lett. **B456**, 68 (1999); Phys. Rev. Lett. **84**, 212 (2000).
- [62] G.-C. Cho, K. Hagiwara and Y. Umeda, Nucl. Phys. **B531**, 65(1998); Erratum-ibid. **B555**, 651 (1999).
- [63] G.-C. Cho, Mod. Phys. Lett. **A15**, 311 (2000).
- [64] A. Leike, Phys. Rep. **317**, 143 (1999).
- [65] F. Aversa, S. Bellucci, M. Greco and P. Chiappetta, Phys. Lett. **B254**, 478 (1991).
- [66] D. London and J. L. Rosner, Phys. Rev. **D34**, 1530 (1986).
- [67] P. Langacker, Phys. Rev. **D30**, 2008 (1984).
- [68] V. Barger, N. G. Deshpande and K. Whisnant, Phys. Rev. **D35**, 1005 (1987).
- [69] Y. Umeda, G.-C. Cho and K. Hagiwara, Phys.Rev. **D58**, 115008 (1998).
- [70] B. Holdom, Phys. Lett. **B166**, 196 (1986).
- [71] K. S. Babu, C. Kolda and J. March-Russell, Phys. Rev. **D57**, 6788 (1998).
- [72] M. E. Peskin and T. Takeuchi, Phys. Rev. Lett. **65** , 964 (1990); Phys. Rev. **D46**, 381 (1992).
- [73] K. Hagiwara, D. Haidt, C. S. Kim and S. Matsumoto, Z. Phys. **C64**, 559 (1994); **C68**, 352 (1995)(E).
- [74] The LEP Collaborations ALEPH, DELPHI, L3, OPAL, the LEP Electroweak Working Group and the SLD Heavy Flavor Group, CERN-PPE/97-154.

- [75] G.-C. Cho, K. Hagiwara and S. Matsumoto, Eur. Phys. J. **C5**, 155 (1998).
- [76] K. Hagiwara, D. Haidt and S. Matsumoto, Eur. Phys. J. **C2**, 95 (1998).
- [77] S. Eidelman and F. Jegerlehner, Z. Phys. **C67**, 585 (1995).
- [78] J. E. Kim, P. Langacker, M. Levine and H. H. Williams, Rev. Mod. Phys. **53**, 211 (1981).
- [79] C. Y. Prescott *et al.*, Phys. Lett. **B77**, 347 (1978).
- [80] C. Y. Prescott *et al.*, Phys. Lett. **B84**, 524 (1979).
- [81] P. A. Souder *et al.*, Phys. Rev. Lett. **65**, 694 (1990).
- [82] W. Heil *et al.*, Nucl. Phys. **B327**, 1 (1989).
- [83] SAMPLE Collaboration, B. Mueller *et al.*, Phys. Rev. Lett. **78**, 3824 (1997); **84**, 1106 (2000).
- [84] HAPPEX Collaboration, K. A. Aniol *et al.*, Phys. Rev. Lett. **82**, 1096 (1999).
- [85] A. Argento *et al.*, Phys. Lett. **B120**, 245 (1983).
- [86] E155 Collaboration, P. L. Anthony *et al.*, Phys. Lett. **B463**, 339 (1999); **B493**, 19 (2000).
- [87] M. J. Ramsey-Musolf, *Sensitivity of low-energy parity violation to new physics*, Proceedings of Parity-Violation in Electron Hadron Electroweak Interactions (PAVI97), edited by B. Frois and M. A. Bouchiat, Singapore, World Scientific, 1999.
- [88] M. C. Noecker, B. P. Masterson and C. E. Wieman, Phys. Rev. Lett. **61**, 310 (1988).

- [89] C. S. Wood *et al.*, *Science* **275**, 1759 (1997).
- [90] G. L. Fogli and D. Haidt, *Z. Phys.* **C40**, 379 (1988).
- [91] K. McFarland *et al.*, *Eur. Phys. J.* **C1**, 509 (1998).
- [92] CHARM collaboration, J. Dorenbosch *et al.*, *Z. Phys.* **C41**, 567 (1989).
- [93] L. A. Ahrens *et al.*, *Phys. Rev.* **D41**, 3297 (1990).
- [94] CHARM-II collaboration, P. Vilain *et al.*, *Phys. Lett.* **B281**, 159 (1992).
- [95] V. Barger, W. Y. Keung and Ernest Ma, *Phys. Lett.* **B94**, 377 (1980).
- [96] S. C. Bennett and C. E. Wieman, *Phys. Rev. Lett.* **82**, 2484 (1999).
- [97] J. L. Rosner, *Phys. Rev. D* **61**, 01600 (2000).
- [98] R. Casalbuoni *et al.*, *Phys. Lett. B* **460**, 135 (1999).
- [99] R. Carlini, J. M. Finn and M. J. Ramsey-Musolf, *Search for new physics at the TeV scale via a measurement of the proton's weak charge*, A Letter of Intent to Jlab, private communication.
- [100] M. J. Ramsey-Musolf, *Phys. Rev.* **C60**, 015501 (1999).
- [101] R. W. Robinett, *Phys. Rev.* **D33**, 1908 (1986).
- [102] V. Barger, N. G. Deshpande, R. J. N. Phillips and K. Whisnant, *Phys. Rev.* **D33**, 1912 (1986).
- [103] T. G. Rizzo, *Phys. Rev.* **D33**, 3329 (1986).
- [104] T. G. Rizzo, *Phys. Rev.* **D34**, 1438 (1986).

- [105] P. Langacker and D. London, Phys. Rev. **D38**, 886 (1988).
- [106] M. M. Boyce and M. A. Doncheski, Phys. Rev. **D55**, 68 (1997).
- [107] J. E. Cieza Montalvo, Phys. Rev. **D59**, 095007 (1999).
- [108] V. Barger, M. S. Berger and R. J. N. Phillips, Phys. Rev. **D52**, 1663 (1995).
- [109] DELPHI Collaboration, P. Abreu *et al.*, Eur. Phys. J. **C8**, 41 (1999).
- [110] S. Nie and M. Sher, Phys. Rev. **D63**, 053001 (2001).
- [111] T. G. Rizzo, Phys. Rev. **D34**, 2699 (1986).
- [112] J. L. Hewett and T. G. Rizzo, Phys. Rev. **D36**, 209 (1987).
- [113] JoAnne L. Hewett, Phys. Lett. **B196**, 223 (1987); T. G. Rizzo, Phys. Rev. **D40**, 754 (1989); F. M. L. Almeida *et al.*, Phys. Rev. **D50**, 5627 (1994).

Vita

Shuquan Nie

Born in Sichuan, P. R. China, July 28, 1970. Graduated from Chongqing University, Chongqing, P. R. China, with B.S. in Applied Physics, July 1993. Received M.S. in Physics at Tsinghua University, Beijing, China, July 1996. Ph. D. candidate, College of William and Mary, 1997-2001, with a concentration on theoretical particle physics.